Aptamers as enhancers of oncolytic virus therapy

by

Darija Muharemagic

Thesis submitted to the
Faculty of Graduate and Postdoctoral Studies
In partial fulfillment of the requirements
For the Ph.D. degree in
Chemistry

Department of Chemistry
Faculty of Science
University of Ottawa

Abstract

Oncolytic viruses promise to significantly improve current cancer treatments through their tumour-selective replication and multimodal attack against cancer cells. However, one of the biggest setbacks for oncolytic virus therapies is the intravenous delivery of the virus, as it can be cleared by neutralizing antibodies (nAbs) from the bloodstream before it reaches the tumour cells. In our group, we have succeeded in developing aptamers to vesicular stomatitis virus (VSV), as well as to rabbit anti-VSV polyclonal neutralizing antibodies (nAbs). We tested these aptamers' biological activity with a cell-based plaque forming assay and found that the aptamers prevented in vitro neutralization of VSV by nAbs and increased the virus infection rate of transformed cells up to 77%.

In line with this approach, we enhanced the delivery of oncolytic viruses by selecting aptamers to the CT26 colon carcinoma cell line. The binding of aptamer pools has been tested on flow cytometry and the best pools were subjected to high throughput sequencing. Selected aptamers were linked to anti-VSV aptamers and applied for target delivery of the virus to cancer cells. Development of this aptamer-based technology aims to improve viral anti-cancer therapies, with a potential to be applied as treatment for patients affected with cancer.

Finally, in collaboration with a group from Erlangen University, we performed an aptamer selection using capillary electrophoresis and cell-SELEX. The target, the extracellular domain of human CD83, is a maturation marker for dendritic cells and is involved in the regulation of the immune system. Selected aptamer sequences bound selectively to mature dendritic cells, in comparison to immature dendritic cells, and thus hold promise to be applied for further studies leading to a better understanding of CD83's mechanism of action.

Acknowledgements

First and foremost, I would like to thank my supervisor, Dr. Maxim Berezovski, for giving me the opportunity to complete my studies in his laboratory. I am grateful for his support and his positive attitude, especially when experiments did not go as expected.

I would like to thank Afnan Azizi for his friendship and the endless number of hours he spent editing my drafts, listening to my presentations and discussing my experiments. I want to thank Ana Gargaun for her companionship and encouragement to pursue graduate school. However, I am mostly grateful to her for always making sure that our goodies drawer was well stocked with treats. I have been fortunate to have had Nasrin Khan with me from the very beginning of our degree, from our initial capillary electrophoresis troubleshooting to the final thesis writing, five years later. I would like to thank Mohamed Wehbe and will miss our summers of lively discussions and Starbucks ice coffee. I appreciate having had the opportunity to work with Dr. Anna Zamay, Dr. Pavel Milman and Shahrokh Ghobadloo, a group of experienced researchers, from whom I have learned many important lessons. I would like to thank all of the Berezovski lab members as well as other colleagues, past and present, Nadia, Thao, Mahmoud, Gleb, Alexey, Christine, Tabussom, Andrea, Nadia, Joanne, Jennifer, Siu-Yan, Jenny, Kaylee, Greg, Marko, Laura, Alex, Suzy, Noreen, Nadine, Victor, Danny, Ali, Oguzcan, Rebecca and Di, who have all contributed towards making my time in the lab a memorable experience.

I would like to thank our collaborators without whom my projects would not have been possible. Dr. John C. Bell, whose expertise and helpfulness have been much appreciated. His great team of students and researchers, notably Laura Evgin, Dominic Roy and Theresa Falls, were always there to help us with our experiments. Dr. Matthias Lechmann, who kindly agreed to allow me to visit his laboratory in my first year of studies. I would like to extend my gratitude to all of his lab members who made sure that my stay in Germany was a pleasant one, particularly Dr. Simon Kreiser and Dr. Jenny Eckhardt.

Most importantly, I want to thank all my friends and family, for their encouragement. More specifically, my mom and dad, for their support throughout my studies, as well as the countless walks they had to go on with Lea when I was working late in the lab. The new addition to our family, little baby Viktor, who has brightened up my spirit during the thesis writing period. And finally, my sister Maja, without whom I never would have made it through this endeavour.

To my mother and father

Bosa and Safet Muharemagic

Table of Contents

List of Tables

List of Figures

List of Abbreviations

Symbol	Description
6-FAM	6-carboxyfluorescein
AptaVIP	Aptamer-Facilitated Virus Protection
AuNP	gold nanoparticles
bp	base pair
CE-LIF	capillary electrophoresis-laser-induced fluorescence
CTC	circulating tumour cell
DC	dendritic cell
DMEM	Dulbecco's modified Eagle medium
DPBS	Dulbecco's Phosphate Buffered Saline
dsDNA	double stranded DNA
FBS	fetal bovine serum
Fluc	firefly (*Photinus pyralis*) luciferase
FP	forward primer
G	glycoprotein
hCD83ext	extracellular human CD83 domain
HIV	human immunodeficiency virus
HTS	high throughput sequencing
iDC	immature dendritic cell
IDT	Integrated DNA Technologies
IFN	interferon
Ig	immunoglobulin
LIF	laser-induced fluorescence
LNA	locked nucleic acid
M	matrix protein
MB	magnetic beads

Symbol	Description
mDC	mature dendritic cell
MEME	Multiple Em for Motif Elicitation
MHC	major histocompatibility complex
N	nucleocapsid
nAbs	neutralizing antibodies
NECEEM	nonequilibrium capillary electrophoresis of equilibrium mixtures
nt	nucleotide
OV	oncolytic virus
PEG	polyethlyene glycol
PFU	plaque forming unit
PS	phosphatidylserine
qPCR	real-time polymerase chain reaction
RFP	red fluorescent protein
PSMA	prostate specific membrane antigen
RCA	rolling circle amplification
RP	reverse primer
SELEX	systematic evolution of ligands by exponential enrichment
ssDNA	single stranded DNA
VSV	vesicular stomatitis virus
YFP	yellow fluorescent protein

Chapter 1

Introduction

The term "aptamer" is a merge of two words: from Latin *aptus*, to fit, and Greek *meros*, parts. Aptamers can be made of short single stranded oligonucleotides or short polypeptides that can be selected to bind a specific target from a large library.

Oncolytic viruses are a class of modified pathogens that have been engineered to selectively replicate in cancerous cells with minimal damage to healthy cells.

This introduction aims to detail relevant scientific background in oncolytic virus and aptamer biochemistry.

1.1 Aptamer selection

The concept of nucleic acid ligands as potential protein response modulators first emerged in the 1980's, where research on human immunodeficiency virus (HIV) and adenovirus revealed RNAs that evolved to bind to viral proteins to regulate gene and protein expressions [1, 2]. Sullenger et al. explored the notion further by taking advantage of the tat-TAR system, a protein-RNA pair. Tat is a regulatory protein (*trans*-activation response element), whose interaction with a specific RNA sequence results in an upregulation of vi-

ral transcription. The Sullinger group showed that overexpression of the TAR sequence in mammalian cells resulted in its binding to tat, and thus inhibited it from binding to the actual TAR region on the mRNA [3].

Interestingly, in the same year, two publications described selection of aptamers. The first one, published by Tuerk and Gold, reported the selection of an RNA ligand to a bacteriophage T4 DNA ligase using systematic evolution of ligands by exponential enrichment (SELEX) – a term coined by Gold. SELEX is a protocol used to identify nucleic acid binders consisting of four main steps: (1) incubation of the ligand library with the target, (2) removal of poor binders, (3) amplification of good binders and (4) re-selection [4]. The oligonucleotide library used for the first aptamer selection was significantly less diverse than the one that is generally used today, as the authors randomized a single 8-nucleotide-long region originating from a hairpin loop, resulting in 65,536 different sequences [5]. The selection was performed on a known target of the hairpin loop and the binding of selected DNA sequences was compared. Even though the number of variable sequences was not as large, the analysis showed that the affinities of selected oligonucleotides were comparable to the wild type. Less than a month later, a similar publication emerged, this time with a more diverse library, which contained approximately 10^{13} unique sequences [6]. The Szostak group presented and defined, for the first time, the term aptamer. Both of these works opened the door to possibilities of discovering and developing novel ribozymes, targeting and delivering agents, as well as biosensors.

To date, pegaptanib (Macugen) is the only aptamer drug commercially available. It originates from a modified RNA inhibitor to vascular endothelial growth factor and is used for the treatment of age-related macular degeneration [7]. Nevertheless, pegaptanib is not the only success story for targeting this disease; E10030 and ARC1905 aptamers also reached clinical trials, phase I and III, respectively. Aptamers for a number of other targets and treatments are also undergoing clinical tests. Among them is an aptamer used for the treatment of von Willebrands disease, a bleeding disorder. It works by binding to the

von Willebrand factor in blood and thus induces an antithrombotic effect. An interesting feature of this effect is that it can be reversed, simply by adding an oligonucleotide with a complementary sequence [8]. Other conditions that have the potential for being treated by these oligonucleotides include carcinomas [9], diabetes [10], and hemophilia [11].

1.1.1 Design of DNA libraries

There have been many aptamers selected for a wide array of targets, ranging from small molecules, proteins, bacteria and viruses. To select an oligonucleotide with the ability to bind specifically and with a high affinity to targets, it is important to have a library constituted from a diverse range of sequences and tertiary structures. Single-stranded aptamers adopt three-dimensional shapes, which allow them to bind or to fit into a certain pocket. There are four main structural shapes that these oligonucleotides maintain: hairpin stem, symmetric and asymmetric bulges flanked by helical regions, pseudoknots, and G quartets (Figure 1.1) [4].

As it has been previously mentioned, one of the first aptamer libraries, developed by Ellington et al., consisted of 100 bases of randomized oligonucleotides [6]. The number of these randomized nucleotides in a library used for aptamer selection varies; however, the majority of researchers use libraries between 40 and 70 nucleotides, due to their ease of synthesis and facile manipulation [12]. In line with the library developed by Tuerk et al., where they varied a stem-loop region [5], the Liu group designed a 100-nucleotide long DNA library using a statistical approach. Based on the probability of having Watson-Crick base-pairing, and thus a formation of stem-loops, they designed a RYRYRY pattern – where R is A/G (ratio of 50:50) and Y is T/C (ratio of 50:50) [13]. The chance of obtaining a 6-bp stem with this design increases by 32-fold, compared to an NNNNNN sequence. Using the RYRYRY pattern, and aiming to obtain a larger diversity of secondary structures, the group incorporated randomized nucleotides between the patterns. Finally,

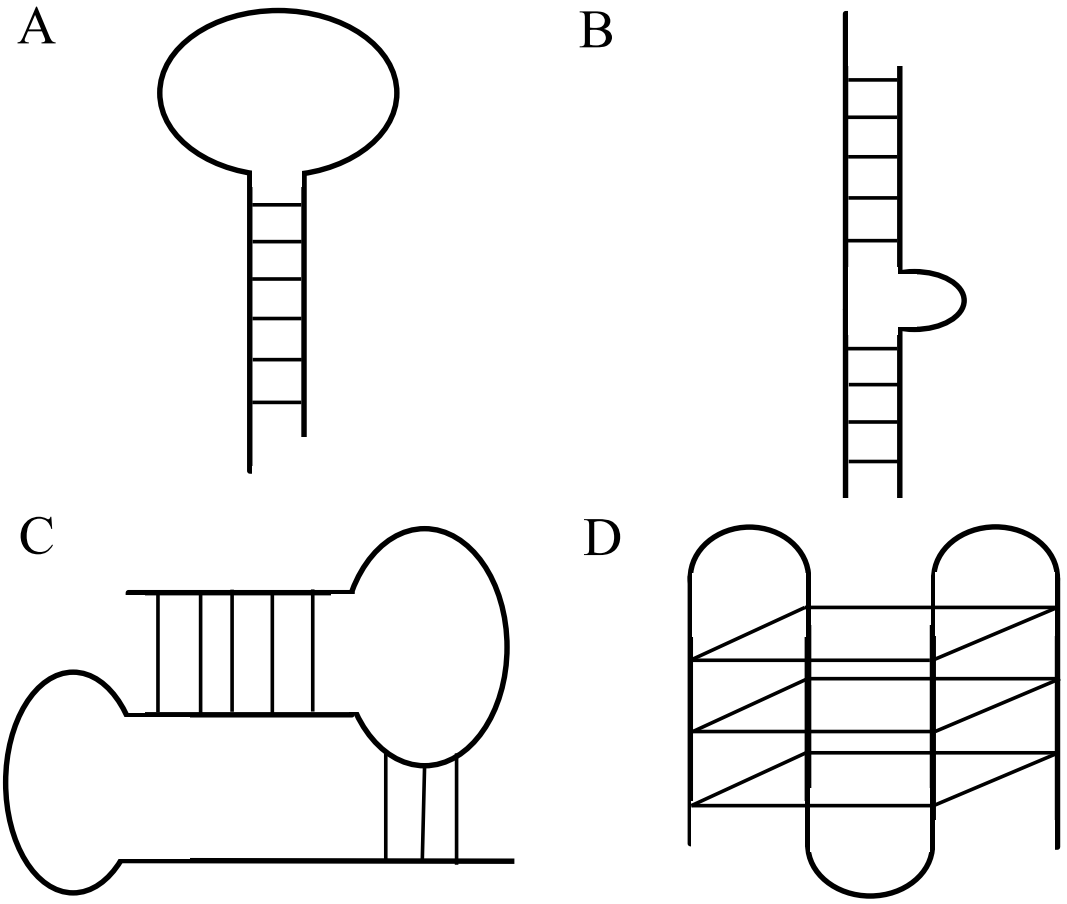

Figure 1.1: Four main structural shapes that single-stranded oligonucleotides can maintain: (A) hairpin stem, (B) symmetric and asymmetric bulges flanked by helical regions, (C) pseudoknots, and (D) G quartets.

they hypothesized that some structures would require a nucleotide that is not purely R or Y, which is why they incorporated a small amount of the other two nucleotides and changed the ratio of R and Y to (5:45)(5:45); this library was called R*Y*. The two patterned libraries (RY and R*Y*), as well as the randomized one (N_{60}), were then synthesized with 60 randomized nucleotides (with or without the patterns), flanked by 20-nucleotide primers and used for three different proof-of-concept aptamer selections [13]. The results showed that the R*Y* library was significantly better for two out of three selections and equal to the N_{60} library for the third selection.

1.1.2 Sequencing of DNA pools

Once the aptamer selection is completed, it is necessary to identify sequences that are present in aptamer pools. The initial work, published by the Szostak group, and the ones that followed it, relied on molecular cloning procedure [6], consisting of aptamer ligation into plasmid vectors and their transformation into bacteria. This well-established procedure has the advantage of being relatively rapid and simple, as cloning kits are commercially available and sequencing of short inserts is available at a low cost. The sequencing platform that is usually used for this application is Sanger dideoxy sequencing, which consists of incorporation of chain-terminating dideoxynucleotides by a DNA polymerase, where each of the four modified nucleotides correspond to a different colour. Amplified oligonucleotides of different sizes are separated by capillary gel electrophoresis and the fluorochromes are detected and identified with their corresponding lasers. However, this approach has its disadvantages, since bacterial colonies must be identified, inoculated, and confirmed individually, which limits the number of sequences analyzed. On average, researchers isolate and sequence approximately 50 colonies (i.e. clones), assuming that the ones that are more statistically abundant will have a higher probability of being picked.

More recently, next generation sequencing (i.e. high throughput sequencing) has become

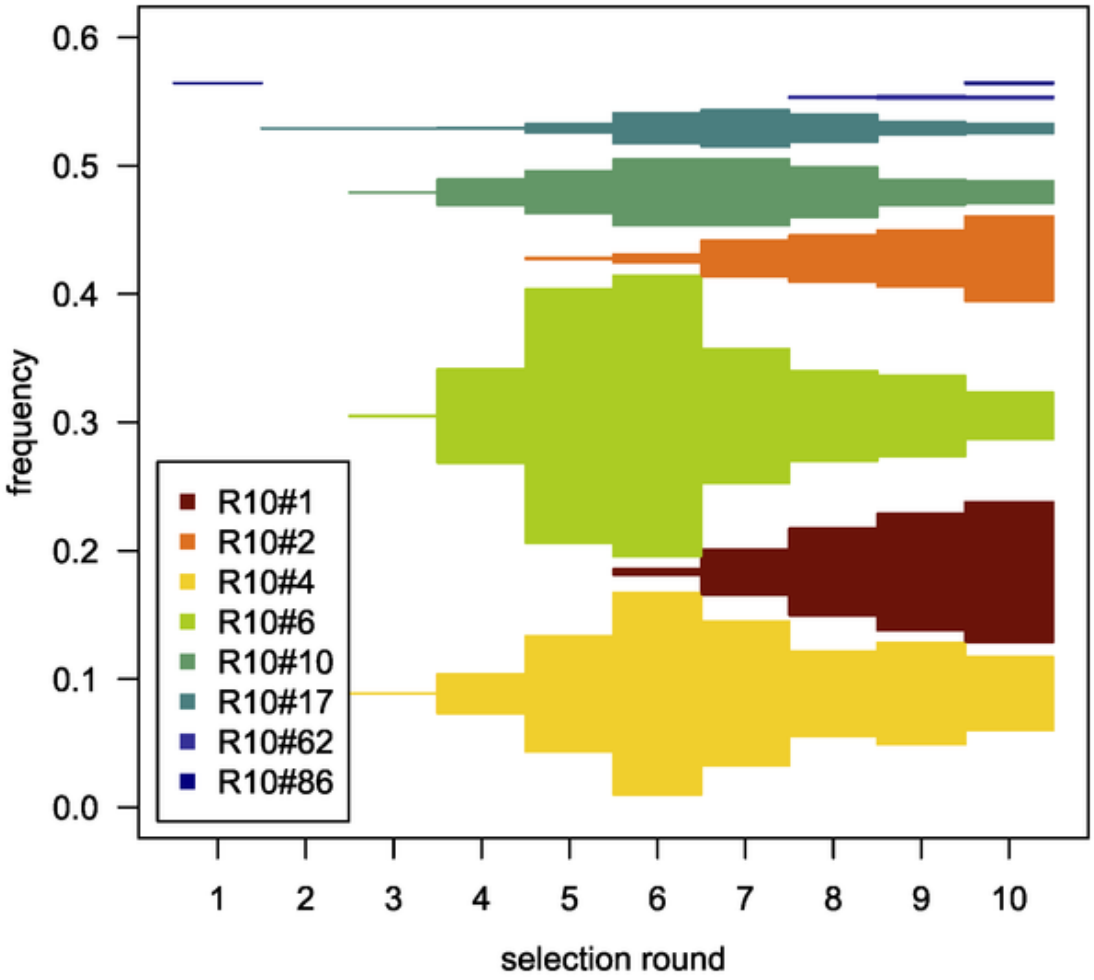

Figure 1.2: Individual sequences identified in first ten rounds of aptamer selection and their relative frequencies evaluated by next generation sequencing. The sequences' binding affinity was evaluated by fluorescent dye-linked aptamer assay (FLAA) and surface plasmon resonance (SPR) and the best results were obtained for R10#17 and R10#86. Adapted from PLoS ONE 69120: e29604, 2011 freely available under the terms of the Creative Commons Attributions License.

prevalent, facilitating a clearer and more elaborate picture of these oligonucleotide pools. This method enables the identification of all, or the majority, of sequences that are present in a pool. The technology, initially developed by 454 Life Technologies, and later acquired by Roche, quickly became a highly demanded method and gave rise to development of many different platforms [14]. One of those platforms, developed by Solexa and later purchased by Illumina, consists of preparing the pool by adding nucleic acid barcodes (i.e. adaptors), either by PCR or ligation, which will then be used to anneal the DNA on a flow cell. The fragments are then amplified with their specific primers, thus forming clusters—each cluster corresponding to a unique sequence. Consequently, complementary sequences are removed and fluorescent nucleotides are added. The nucleotides are finally excited with lasers, their emission is registered and the cycle is repeated.

Once the clones have been sequenced, it is important to differentiate high affinity aptamers from PCR artifacts. Different properties could be considered in order to identify desirable sequences, including repeating motifs [15], copy number [16] or enrichment fold [17]. Finding a region of homology (repeating motifs) allows the identification of nucleotides that are identical throughout different sequences and that may have good binding properties. On the other hand, identification of a copy number or enrichment fold permits the quantification of sequences that are either highly abundant in a pool or are enriched throughout different rounds. In 2011, Shutze et al. used high throughput sequencing to analyze ten rounds of selection, starting from the initial round, by attempting to correlate their binding to their copy number (Figure 1.2). With their work, they were able to show that it is possible to identify sequences with good affinities to their respective targets as early as in round three, even if the pool itself does not exhibit a significant increase in binding affinity [18].

1.1.3 Improvement of aptamers

Even though aptamers are not immunogenic, their biggest setbacks for *in vivo* use is their susceptibility to degradation by nucleolytic agents. The half-life of RNA oligonucleotides in plasma is a few seconds, whereas for DNA oligonucleotides it can range from 20 to 60 minutes [19]. To develop DNA and RNA aptamers more applicable for therapeutic use, a number of strategies have been used to attempt to increase their stability, as well as to improve their binding to the target. These mostly include chemical modifications at the 3' and 5' positions, as well as modifications at the 2' position of the ribose moiety on RNA molecules [19].

An example of such modification is the incorporation of locked nucleic acids (LNAs), consisting of an additional bond to connect the 2' oxygen to the 4' carbon of the ribose moiety [20, 21]. The resulting oligonucleotide's properties, including increased stability in serum, increased melting temperature, and improved selectivity, have been attributed to increased base stacking interactions and, thus, a better organization of the phosphate backbone [22–24]. The Erdmann group has successfully shown that by incorporating LNAs into previously-selected aptamers, they can improve the oligomer's properties [25]. For this work, they used an anti-Tenascin-C aptamer, a protein involved in tumorigenesis and wound healing [26] and found that the modification not only conserved the aptamer's binding to its target and improved its stability in serum, but also resulted in a higher tumour uptake [25].

Another type of oligonucleotide modification is the use of spiegelmers, which are DNA or RNA ligands in their non-natural L-enantiomeric form. Due to their mirror-image property, these molecules are not susceptible to degradation by nucleases [27]. The selection is based on the fact that if a ligand is selected to bind to a specific target, then a mirror-image of this ligand will bind to a mirror-image of its target [28]. This has been applied to aptamer selection, where naturally-occurring aptamers can be selected for enantiomeric images of

the desired target. To date, these have been selected for a variety of molecules, including adenosine, arginine, migraine-associated calcitonin gene-related peptide and staphylococcal enterotoxin B [27, 29–31].

Finally, instead of chemically modifying aptamers, the structure of nucleic acids can be modified in order to improve their affinity or stability. One way is to make a circular form of the aptamer, thus making it less bioavailable to exonucleases and improving its affinity [32]. Furthermore, non-circular multivalent aptamers were introduced by the Gilboa group, where they annealed four anti-cytotoxic T cell antigen (CTLA) aptamers in order to increase the oligonucleotide's binding affinity to the target [33]. In line with this approach, they also conjugated a bivalent 4-1BB-targeting aptamer to an aptamer targeting prostate specific membrane antigen (PSMA) [34]. With this bi-specific conjugate they showed the application of these aptamers for therapeutic use and demonstrated the potential of applying this construct for targeted delivery.

1.2 Aptamers as delivery vehicles

1.2.1 Drug delivery by DNA nanostructures

Advancements in computational chemistry have enabled the prediction of oligonucleotides' unique secondary and tertiary structures, based on their primary sequences. Therefore, oligomers can be self-assembled in solution with precise architecture and high efficiency. Many researchers have taken advantage of these properties to make an array of different structures, also known as DNA origami, ranging from rectangular, triangular and circular shapes, to smiley faces [35, 36]. Several works have also demonstrated that compact three-dimensional nucleic acids are more readily internalized within cells, possibly by the anionic ligand-binding receptor (ALBR) pathway or by scavenger receptors [37–39]. Charoenphol et al. targeted a well-characterized DNA-based nanostructure that self-assembles into

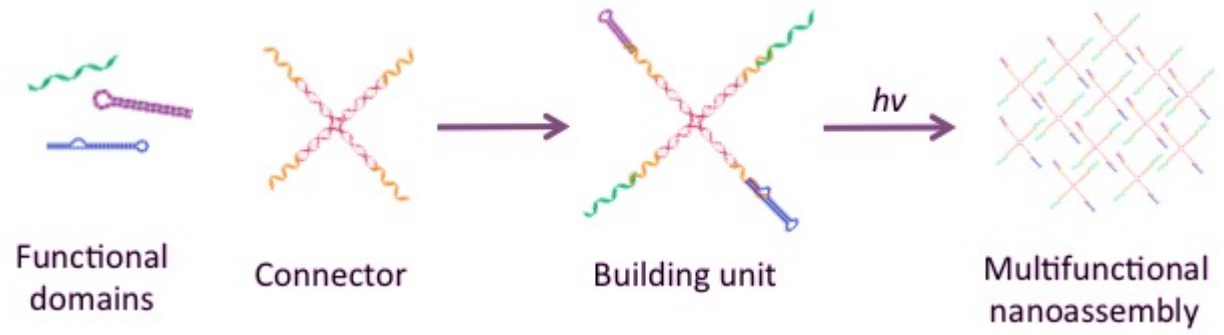

Figure 1.3: A schematic of a multifunctional self-assembled nanostructure consisting of functional groups, such as aptamers or antisense oligonucleotides, a connector and building units. Once assembled, these are photo-cross-linked into a nanostructure.

a pyramidal cage using AS1411, an aptamer that binds to a glycoprotein upregulated in several cancer types [38]. Their experiments showed that uptake of the pyramidal structure was increased when the aptamer was incorporated, suggesting that the uptake was mediated by the aptamer-cell specific interaction [39].

The major benefit of these designs is that different molecular loads, such as small drugs [40], proteins [41], and nanoparticles [42], can be incorporated and entrapped inside. Furthermore, in order to allow a controlled release of the carried load, aptamers have recently been combined with these structures. Wu et al. demonstrated the concept of these multifunctional molecules by building a nucleic acid nano-assembly, consisting of "connectors" and "building units". Each building unit had three functional groups, such as targeting aptamers, a DNA-intercalating anticancer drug, or therapeutic antisense oligonucleotides (Figure 1.3). By incorporating a CCRF-CEM cancer cell-targeting aptamer, they observed selective cell-type specific toxicity [43].

In order to design a three-dimensional DNA-based structure, researchers have to rely on Watson-Crick base-pairing rules to anneal small building blocks. However, the Tan group has proposed an alternative. They were able to obtain spherical structures, termed nanoflowers, which can be generated from long nucleic acid strands and self-assembled

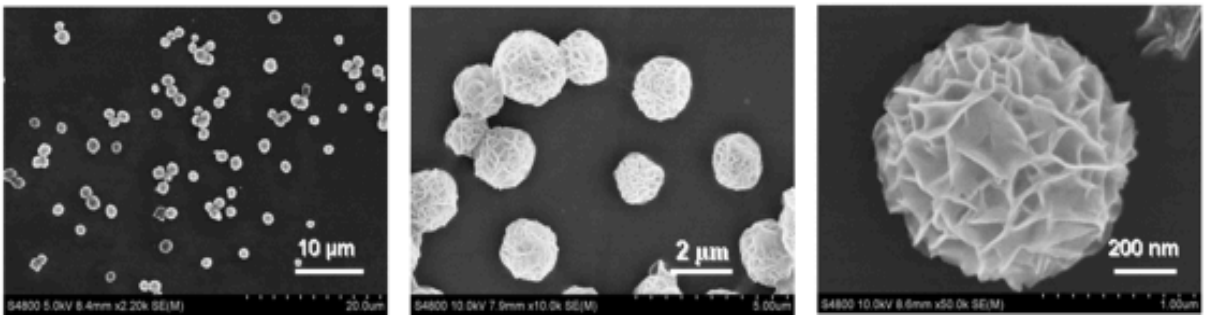

Figure 1.4: Scanning electron microscopy images of DNA nanoflowers obtained from rolling circle amplification (RCA). Reproduced from John Wiley and Sons: Angewandte Chemie International Edition 53:5821, copyright 2014.

through liquid crystallization (Figure 1.4). These strands are formed by rolling circle amplification (RCA), a unidirectional replication of oligonucleotides, where a template and primers are used to make concatemeric DNA, containing multiple copies of the same sequence [44]. Furthermore, during RCA, chemically modified deoxynucleotides were incorporated to obtain multicoloured nucleic acids, which facilitated the tracking of these molecules when bound to target cells. Nanoflower structures offer a number of advantages as delivery vehicles: their size is tunable by amplifying different lengths of DNA strands, compacted moieties present a reduced amount of potential nick sites, making these oligonucleotides less susceptible to nuclease degradation [45], and cancer cell specific aptamers can be seamlessly integrated into the sequence of these long concatemers [46]. The efficacy of this technique was tested through delivery of doxorubicin-treated nanoflowers to different cancer cell types; only cells targeted by the incorporated aptamers exhibited dose-dependent cytotoxicity [47].

1.2.2 Aptamer-siRNA chimera

Short interfering RNA (siRNA) and micro RNA (miRNA) have been recently described as important gene regulators of most eukaryotic lineages, including fungi, plants and animals. RNA molecules regulate gene expression through multiple routes, including guided cleavage

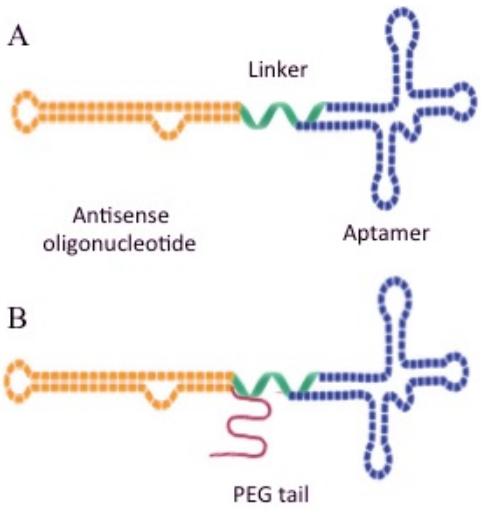

Figure 1.5: A general schematic of (A) an aptamer-siRNA/miRNA chimera linked by an oligonucleotide linker; (B) a modified version of the chimera including a 20 kDa polyethylene glycol (PEG) tail.

of mRNA, inhibition of protein translation, or chromatin modifications [48]. This regulatory function of RNA interference (RNAi) has a tremendous potential in therapeutics, as it allows the control of cellular protein expression. However, when exogenous siRNA is administered, it needs to be uptaken by targeted cells, avoid those cells' endosomes, and become incorporated into their RNA-induced silencing complex (RISC); here lie the biggest setbacks of RNAi therapeutics [49].

The Giangrande group was the first to report successful use of a covalent aptamer-siRNA chimera for cell-type specific delivery [50]. For this purpose, they used an aptamer developed to bind the prostate-specific membrane antigen. This aptamer was linked to the sense strand of a 21-mer siRNA (Figure 1.5 A), which targets polo-like kinase 1 (PLK1) and B-cell lymphoma 2 (BCL2), two survival genes overexpressed in most tumors. Application of this construct, with a double stranded siRNA part, both *in vitro* and with intratumoral administration, resulted in decreased proliferation and increased apoptosis of cells expressing PSMA [50]. Several other aptamer-siRNA chimeras ensued using a similar approach [51–53].

Giangrande and colleagues set out to improve their previously developed chimera in order to make it more apt for systemic administration. To this end, three years later, the group modified the construct in a variety of ways, including shortening the aptamer to make its large-scale synthesis more affordable, addition of a 20 kDa polyethylene glycol (PEG) moiety (Figure 1.5 B) to increase the half-life of the construct from less than 35 min to more than 30 hours, and, finally, alteration of the siRNA duplex to favour RISC processing of the correct siRNA guide strand. When injected intraperitoneally, the new generation of the construct was tolerated better and showed less toxicity [54].

Unlike siRNAs, which target and inhibit one specific gene, miRNAs have the ability to produce a more global effect on many different genes. Recently, the de Franciscis group has shown the efficacy of *in vivo* delivery of miRNA-aptamer chimera [55]. For this proof-of-principle study, they used the GL21.T aptamer as a delivery carrier, previously selected and characterized in their laboratory [56]. This aptamer has been found to inhibit Axl tyrosine kinase activity and to interfere with target cell growth and motility [56, 57]. The let-7g miRNA, an inhibitor of high mobility group AT-hook 2 (HMGA2) [58] and N-Ras, was used as the gene-silencing part of the chimera [59]. When conjugated, the addition of GL21.T-let construct to Axl-positive cells resulted in a more pronounced silencing of let-7g targets. Finally, for the *in vivo* evaluation of the conjugate effect, Esposito et al. used immunodeficient mice bearing Axl-positive and Axl-negative tumors. When treated with a single intravenous injection of GL21.T-let, they observed an increase of let-7g miRNA in Axl-positive cells only, followed by a significant reduction in the targeted tumours after a two-week administration of the treatment. Therefore, these two studies have shown that aptamers can be used for a safe and targeted delivery of RNAi *in vitro* and *in vivo*.

1.2.3 Nanoparticle-aptamer conjugates

Nanomaterials became widely used due to their ease of synthesis, as well as their easily tunable size. However, because of their lack of specificity, they often need to be conjugated with other agents that will make their delivery more efficient. A number of research groups have investigated coupling aptamers with such nanomaterials as liposomes [60, 61], micelles [62, 63], single-walled carbon nanotubes [64, 65], and quantum dots [66, 67], for a number of applications, including detection of small molecules, drug delivery to cells, or imaging of cancer cells. Gold nanoparticles (AuNPs), in particular, have shown great promise for many applications due to their ease of synthesis and stability.

Nanoparticle-aptamer conjugates have been widely explored for targeted drug delivery and imaging, both *in vitro* and *in vivo* [68–70]. The nanoparticles used for this purpose can be made from a variety of different materials, such as polymeric micelles, liposomes and dendrimers. These particles could potentially be loaded with drugs [71], or they could themselves have imaging properties [69]; specificity is obtained once they are conjugated with aptamers that bind to a target of interest (e.g. a biomarker on a cell). The Tan group successfully demonstrated that nanoparticles can get internalized inside targeted cells, even if the aptamer itself does not have internalizing properties, using an aptamer-micelle construct. Furthermore, they showed that this type of construct had a good affinity and specificity in flow channel systems, demonstrating the potential of applying this system *in vivo* [63].

Another promising area of aptamer-AuNP conjugates is in the detection of early circulating tumour cells (CTCs). CTCs are cells that have detached from a primary tumour and are circulating in the bloodstream. It has been recognized, as early as in the 19th century, that CTCs are responsible for cancer metastasis and the formation of multiple tumours in a single host [72, 73]. The period from the detachment of the cells before the tumour metastasis is of utmost importance. Recently, there has been an emergence of

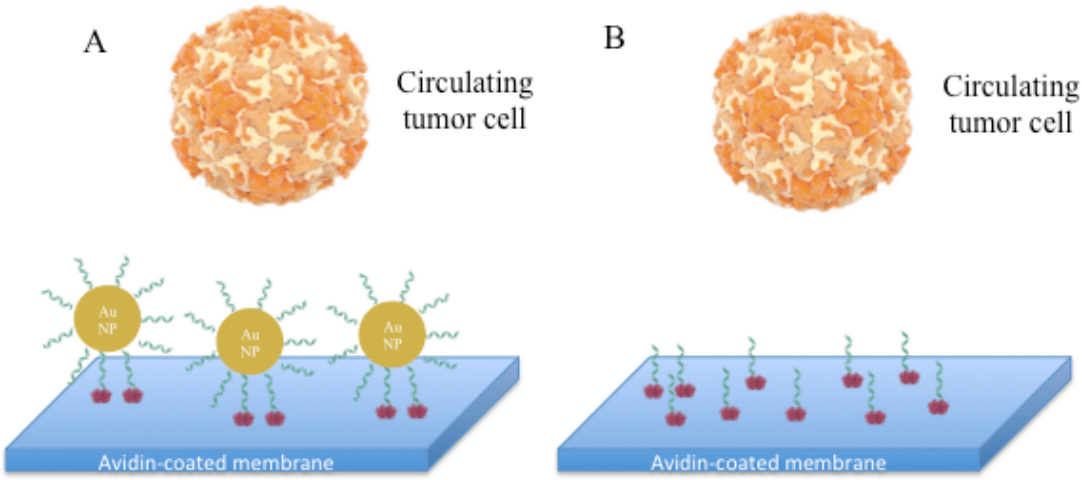

Figure 1.6: A schematic of circulating tumor cells (CTCs) captured using a combination of gold nanoparticles (AuNP) and aptamers in a microfluidic device. (A) The use of AuNPs allowed a higher capture efficiency of CTCs when compared to (B) the use of aptamers alone.

several instruments designed to detect these cells. The majority of these platforms rely on the capture of CTCs based on their biomarkers or their morphology. For instance, the only currently FDA-approved platform is the CellSearch Assay, which uses antibody-coated magnetic particles to isolate these CTCs. However, the capture efficiency of this assay is not optimal, and many circulating cancer cells go undetected. Therefore, there is a need for an instrument that possesses high specificity and a low limit of detection that will be able to identify these rare circulating cells [74].

The Fan research group proposed a technique for detection and isolation of these circulating tumour cells by combining the technology of gold nanoparticles and aptamers (Figure 1.6). The use of these particles allowed them to attach up to 95 aptamers onto each AuNP, which greatly increased their binding affinity to cancer cells. Moreover, they employed a herringbone groove-based micromixer device to achieve a capture efficiency of more than 90% by processing 1 ml of whole blood, with samples containing as little as 100 cells. This proof-of-principle opened the door for many others to combine nanoparticles and aptamers for the isolation of CTCs [75].

1.3 Aptamers for infectious agents

1.3.1 Aptamers for inhibition of infectious agents

Other than binding their respective targets, aptamers can have other properties, such as modifying their target's function. Viruses are a diverse type of infectious agents, with more than 2,400 identified viral species. Their DNA or RNA genomes are usually packaged in a protein shell, which also carries them to the host organism. Once the host is infected, the virus produces its ubiquitous progeny, leaving the host tissue damaged [76]. To date, aptamers have been selected for an array of different viruses, including HIV [77], rabies virus [78], hepatitis C [79], vaccinia virus [80] and ebola [81]. Several of these aptamers bind to viruses and prevent their attachment to the cellular membrane, thus inhibiting their infectivity. Jeon et al. have reported one such example where the selected aptamer was able to block the binding of the influenza virus to target cell receptors. The binding inhibition was observed *in vitro* in tissue cultures, where cells treated with the aptamer survived in presence of the virus. Moreover, intranasal administration of this aptamer treatment in mice resulted in decreased weight loss, as well as a lower amount of virus in their lungs [82].

Furthermore, similar to antibodies, high specificity and affinity of aptamers makes them ideal candidates for their use in detection systems. This method has been applied to various types of bacterial pathogens, such as *Escherichia coli* [83], *Staphylococci* [84], and *Salmonella* [85], for their detection in foods and the environment. Moreover, the Zamay group, in collaboration with our research team, has demonstrated that aptamers originally developed for detection of two *Salmonella* species possessed bacteriostatic effect, paving the way for a new application of aptamer technology. The aptamers inhibited the formation of bacterial colonies by depolarizing the bacterial membrane [86].

1.3.2 Oncolytic viruses

The effect of oncolytic viruses was first reported in the early 1900s when George Dock reported the case of a woman suffering from leukemia who contracted the influenza virus and went into remission for a year, before succumbing to the disease [87]. Even though the treatment did not last for a long time, the case did help make a link between cancer regression and viral infections, which increasingly led to an interest in oncolytic viruses since the 1950s. These viruses are attractive due to their ability to propagate and selectively destroy tumour tissue without having detrimental consequences for normal non-cancerous cells [88]. When non-cancerous cells are infected with a virus, they downmodulate their metabolism or undergo apoptosis in order to prevent propagation of the pathogen. However, cancer cells have evolved to resist apoptosis and translational suppression, making them naturally more prone to the majority of viral infections [89].

One of the recognized mechanisms for this selection involves the interferon pathway. Interferons (IFNs) are a family of proteins that are involved in cellular growth, immune activation, as well as antiviral defence [90]. There are two types of interferons, I and II, which have different roles in cellular function, even though they can both stimulate an antiviral response. Type I, which consists of $IFN-\alpha$ and $IFN-\beta$, are activated directly following a viral infection, whereas type II ($IFN-\gamma$) is induced in response to the recognition elements of viral elements, such as natural killer (NK) cells and T lymphocytes [91]. Furthermore, both of these can slow the rate of cellular growth or induce apoptosis. Therefore, in order to proliferate, cancerous cells have evolved to suppress interferons; about 70% of cancerous cells have a defective interferon pathway [92].

With this in mind, researchers have genetically engineered viruses to form systems that would not be able to replicate in normal cells and would thus be more selective towards tumours. Among these are viruses such as measles, adenovirus, vesicular stomatitis virus, vaccinia virus, and herpes simplex virus. In 2011, the Bell lab reported a clinical

trial involving JX-594, an oncolytic virus developed from a Wyeth strain derived from a poxvirus. Phase I trials, involving 23 patients, consisted of intratumoral injection of JX-594 into their liver tumors, which was well tolerated and able to replicate in cancer tissue while not affecting normal cells [93].

Vesicular stomatitis virus is an attractive oncotherapeutic agent for several reasons. First and foremost, its ubiquity and its rapid life cycle make it an ideal candidate for studying oncolytic viruses and their effects, both *in vivo* and *in vitro*. Furthermore, since humans have not been exposed to this virus, we do not have a developed immunity, which means that VSV could be used in human trials as well. Finally, there is a very low chance of recombination of its genome, as it is an RNA virus that replicates in the cellular cytoplasm, and not in the nucleus [92, 94].

In 2003, Stojdl et al. explored the idea to produce a generation of viruses that are more selective for tumour cells [95, 96]. They hypothesized that the best way to do this would be to generate a virus that both induces the production of interferons and is susceptible to its antiviral effects. Therefore, they selected two naturally-occurring VSVs and a mimetic, AV1 (M51R) and AV2 (V221F/S226R or $M\Delta51$). These mutated variants were not able to block the production of interferons in infected cells, and thus showed a significant decrease of infection in normal tissue [96]. Due to their improved selectivity, these variants continue to be used in research laboratories to study the effects of oncolytic viruses and their mechanism of action [97–99].

Vesicular stomatitis virus (VSV) is a negative-stranded RNA virus, known to infect mammals and insects, but is generally rare in humans. Infection in cattle, horses and swine is marked by the formation of vesicular lesions around the mouth, hooves, and teeth [100]. Virions have a bullet shape and their typical dimensions are 180×75 nm. The genome of VSV encodes for five structural proteins: the nucleocapsid (N), the polymerase proteins (P and L), the matrix protein (M), and the surface glycoprotein (G). The viral RNA is wrapped tightly within the N, P and L proteins, to which binds the matrix protein.

Finally, the G protein forms trimers, which enfold the virion upon its budding from the cell (Figure 1.7) [92].

Due to VSV's broad tropism, there have been difficulties in identifying the viral binding receptor. Initially, it has been hypothesized that phosphatidylserine (PS) was the cell surface receptor [101, 102]; however, this hypothesis was disproved in 2004 by the Miller group as they did not find a correlation between PS levels and viral infection [103]. More recently, it has been proposed that the low density lipoprotein (LDL) receptor serves as the cellular receptor which enables the ubiquity of VSV host tissue [104, 105]. Once the virus binds to the target cell, the G protein is rearranged in order to fuse to the membrane and release the nucleoprotein core [106]. The viral genes are then transcribed, and once all the proteins are accumulated, the virion is assembled, and the cycle is repeated. Expression of viral proteins lasts a few hours and ends with cytotoxicity, marked by cell rounding and detachment, mostly due to the M protein which causes depolarization of actin, tubulin, and vimentin [101, 107].

1.3.3 Immune system

When a pathogen is introduced into an individual's system, the first line of defence is the innate immune system, such as physical barriers (e.g. mucosal surfaces, enzymes and stomach acid), or macrophages and neutrophils once the foreign molecule has passed through these barriers. Even though the innate system is much faster, the adaptive immune system is more efficient in eliminating infections due to its specific recognition of pathogens with antibodies and T cells [108].

T cells play an important role in fighting intracellular pathogens by binding to peptides expressed on cellular surfaces. Cellular proteins regularly undergo degradation and peptidic products are expressed on cell's surface by class I major histocompatibility complexes (MHCs). These class I molecules are presented by nearly all nucleated cells; however, it

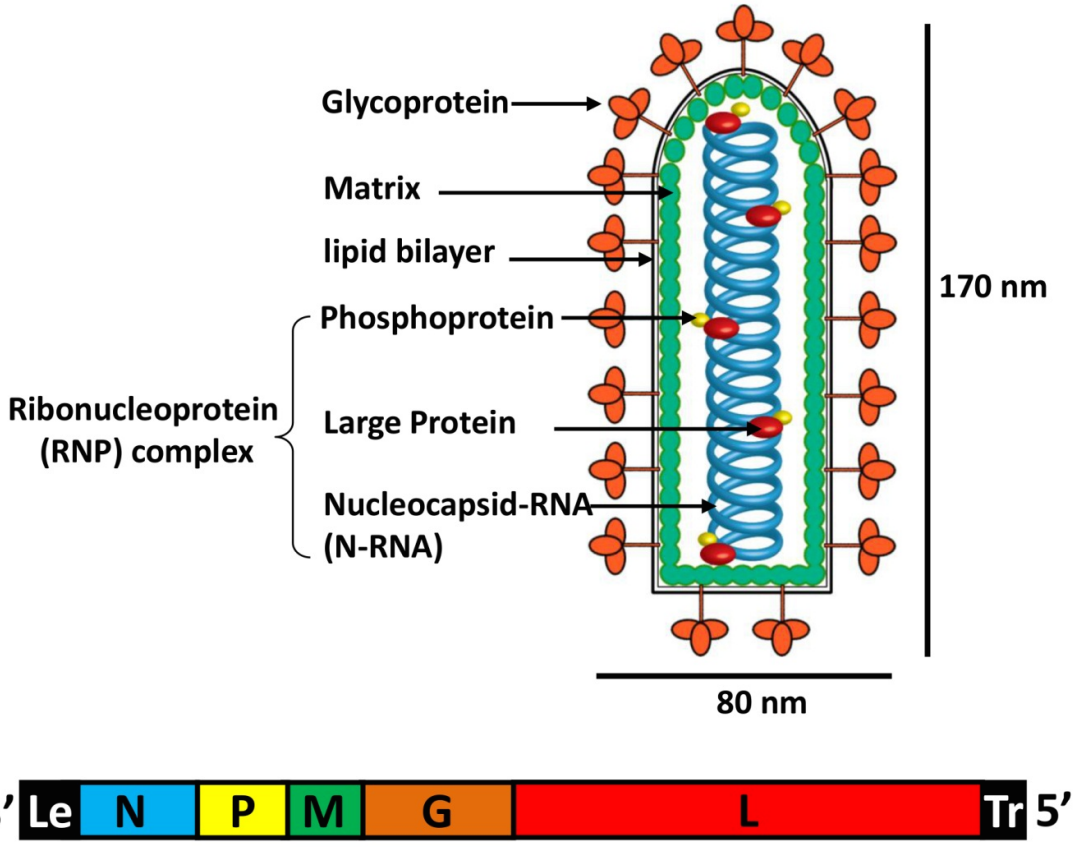

Figure 1.7: A schematic for the structure of vesicular stomatitis virus (VSV) and its genome. Genome of VSV encodes for five structural proteins: the nucleocapsid (N), the polymerase proteins (P and L), the matrix protein (M), and the surface glycoprotein (G), and is flanked by 3' and 5' untranslated leader and trailer sequences. Reproduced from InTech: Methylation - From DNA, RNA and Histones to Diseases and Treatment, 2012 freely available under the terms of the Creative Commons Attribution License.

has recently become clear that tumour cells have a way of inhibiting this T cell signalling and can thus evade their detection and elimination [109, 110]. Second class of MHCs is categorized into peptides originating from proteins that have been uptaken by phagocytosis or endocytosis and are presented by antigen presenting cells (APCs), such as macrophages, B cells and dendritic cells (DCs) [109, 111].

Dendritic cells are one of the most important antigen presenting cells. In their immature state, they sample different tissues in order to detect foreign bodies present in the system. Their activation is induced by maturation signals (e.g. bacterial lipopolysaccharides), which leads to the presentation of internalized and degraded antigen to be presented to T or B cells [109, 112]. The maturation of dendritic cells is marked by a number of surface biomarkers, the most important and best known being CD83, a membrane-bound glycoprotein [112–114]. It has been recognized that this molecule, aside from being a marker, might possess immunoregulatory properties as well [115]; both *in vitro* and *in vivo* studies have suggested that the soluble form of CD83, which can be released by DCs, has an inhibitory effect on the maturation of these cells [116].

Since there is a large variety of peptides that are presented on cellular surface, which might be highly similar, antigen receptors expressed on lymphocytes (B cells and T cells) need to be highly specific in order to recognize the targeted pathogen. Therefore, there will also be a large variety of antigen-specific receptors. These are generated from three sets of genes – V, D and J segments – which can be arranged using different combinations and may also contain mutations in order to increase the diversity [117]. Finally, T and B cells expressing antigen receptors will be released into circulation—each cell expressing a different receptor. Once this cell encounters a corresponding antigen, it will replicate and thus generate a multitude of its clones [111]. Following an infection, a fraction of these induced lymphocytes remains in the system, which accelerates the immune response in case of a reoccurrence. It has been reported that this protective immune memory can last as long as 75 years, even in the absence of re-exposure to the pathogen [118, 119]. However,

chronic exposure does remain the most effective way of maintaining a high level of specific antibodies [118].

One of the main functions of B cells is to make antibodies, which can also be expressed on the cell's surface. Once a B cell recognizes a pathogen that binds to the B cell receptor, the same pathogen is internalized and degraded inside the lymphocyte. Peptides from degraded proteins are presented on the cell's surface, and are presented to a helper T cell, which has previously been primed by antigen presenting cells. Consequently, this interaction sends signals to the B cell to commence the production of antibodies specific to the detected pathogen [108].

There are five main classes, or isotypes, of antibodies, differentiated by their heavy chain: IgA, IgG, IgD, IgE and IgM (Table 1.1). Each of these isotypes of antibodies has constant and variable regions within their light and heavy chains — antigen-binding domains are embedded within the variable region. Approximately 75% of immunoglobulins in serum belong to the IgG class, which is the most versatile class and is mostly responsible for opsonization and neutralization of pathogens [108,111]. Immunoglobulin G is Y-shaped and is composed of two heavy chains and two light chains, which are linked with disulfide bonds (Figure 1.8) [120].

Antibodies can interact in different ways with a pathogen that will lead to its elimination or inhibition. The first one is by signalling for the activation of proteins involved with the complement system. The complement proteins can make pores in the pathogen, leading to its lysis, or can recruit phagocytic cells [108]. This recruitment of phagocytic cells can also be executed by antibodies themselves, through opsonization: as the antibody binds to the pathogen with its variable regions, the constant heavy chain (Fc domain) will interact with an Fc receptor on a phagocyte. However, the most efficient way of eliminating the pathogen is with neutralizing antibodies, which will bind the foreign body and prevent it from entering cells [108, 121].

Table 1.1: Different isotypes of immunoglobulins and their main function.

Isotype	Function	Abundance
IgA	Prevents attachment of microbes.	Saliva, tears, respiratory, intestinal and genital
IgG	Secreted during secondary response Promotes opsonization and neutralization	Blood, intestine and lymph
IgD	Function unknown	Plasma membrane and blood serum
IgM	Secreted during primary response Functions as B cell receptor	Serum
IgE	Triggers allergic reactions.	Mucous membrane, skin and lungs

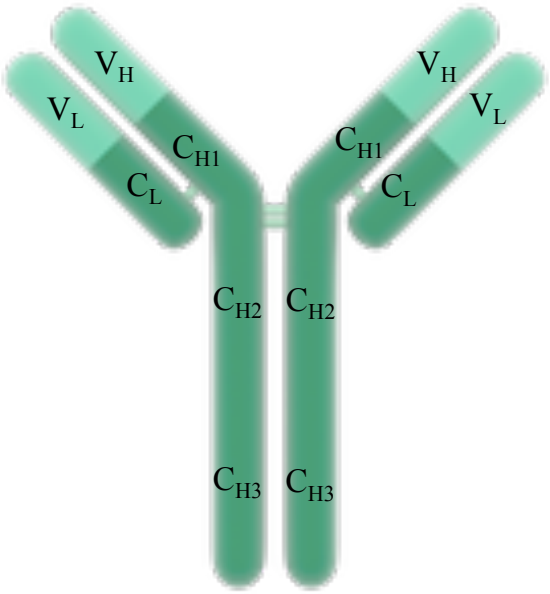

Figure 1.8: A schematic for the structure of an IgG antibody, which is composed of two light chains (L) and two heavy chains, connected with disulfide bridges. Both of these are composed of constant (C_L, C_{H1}, C_{H2} and C_{H3}) and variable (V_L and V_H) regions.

1.3.4 Delivery of oncolytic viruses

Vesicular stomatitis virus is a well studied virus, and even though its application has not mounted to clinical trials, it has been used as a proof-of-principle agent. However, VSV, as well as other oncolytic viruses, do have an important drawback, which is their sensitivity to the immune system. These viruses can be cleared or inactivated in the bloodstream by the complement system [122, 123] or the reticuloendothelial system [124, 125]. Before clearance, the particles are coated with signalling antibodies, complement proteins, coagulation factors, or other serum proteins that promote their recognition by splenic macrophages and hepatic Kupffer cells, resulting in a rapid elimination of the virus from circulation [89]. Nonetheless, the most restrictive barrier to effective treatment is the acquired immunity with neutralizing antibodies (nAbs) [94,121,126]. This is specifically an issue after repeated infections, which is usually required when administering a treatment with oncolytic viruses [127].

To overcome or reduce the negative impact of the immune system, several approaches have been developed, mostly consisting of viral modifications. In 1977, Davis et al. used bovine serum albumin and showed that the otherwise immunogenic protein had non-immunogenic properties once coupled to polyethylene glycol [128]. This method proved to be also useful in case of viral particles to prolong their circulation time and reduce off target toxicity using polymers such as PEG and N-[2-hydroxypropyl]-methacrylamide [129–131]. In case of VSV, PEGylation of its pseudotyped lentiviral vectors prevented viral inactivation in serum and increased its circulation half-life by a factor of five [132]. Furthermore, use of immunosuppressive drugs such as cyclophosphamide in combination with oncolytic viruses can significantly decrease antiviral antibodies, allowing the virus to effectively target cancer cells [133, 134]. Another way of delivering oncolytic viruses is by pre-infecting T cells or syngeneic carrier cells and thus have them act as delivery vehicles to tumour sites [135, 136]. In order to have an efficient delivery, the host's own T cells need to be iso-

lated and loaded with the virus; this method, therefore, allows the virus to pass undetected even in presence of neutralizing antibodies [127, 137].

1.4 Research objectives

In this work, we attempted to apply the aptamer technology in order to prevent the neutralization of the vesicular stomatitis virus by neutralizing antibodies and to improve the delivery of the virus to cancer cells. This project was done in collaboration with Dr. John Bell from the Ottawa Hospital Research Institute and resulted in two publications, which are partially presented in chapters 2 and 3 [138, 139].

Chapters of this thesis are divided into specific objectives of the project. The first one consisted of selecting aptamers for both the VSV as well as for nAbs and testing their binding efficiency *in vitro* that was done in collaboration with Dr. Anna Zamay. Next, we applied these specific oligonucleotide sequences for cell-based assays in order to quantify their blocking and shielding effect and their capacity for improving viral infectivity. These experiments were performed in collaboration with Dr. Anna Zamay and Shahrokh Ghobadloo. Finally, we selected aptamers for CT26, a cancer cell line, and combined these with virus-binding aptamers to achieve targeted delivery of VSV.

The last chapter consists of work that was done in collaboration with Dr. Matthias Lechmann and his graduate student, Simon Kreiser, from Erlangen University in Germany. Their laboratory focuses on the study of CD83, a maturation marker for dendritic cells, and its effects on the immune system. The project consisted of selecting aptamers for CD83 in order to facilitate these studies, and potentially achieve inhibiting or regulating effects with CD83-expressing molecules.

Chapter 2

Aptamers to VSV and anti-VSV neutralizing antibodies

2.1 Background

Viral-based therapeutics (e.g. gene therapy and viral vaccines) hold great promise for the treatment of many diseases, specifically cancer. As it has been previously mentioned, *in vivo* trials demonstrated that oncolytic viruses (OVs) can be inactivated by neutralizing antibodies and rapidly cleared from the circulation. Therefore, a prerequisite for successful virotherapy is that the virus must gain access to the tumour cell, which requires an extended circulation time without depletion by nAbs.

Even though a number of methods are currently under development in order to by-pass the neutralization problem, they suffer from some drawbacks. For example, polymer coating of the virus can lead to a loss of infectivity due to the formation of a permanent coat [131, 140]. A method that consists of pre-loading T cells with the virus requires isolation of patient's T cells, their activation, followed by back-infusion to the patient, which makes it impractical for clinical use.

In this section, we envisaged the development of two sets of aptamers, binding to nAbs and VSV, in order to shield VSV and block the antibodies, thus allowing the virus to escape the host immune mechanism and neutralization. The former approach would be feasible if an aptamer can be selected to an antigen-binding fragment (Fab) of nAbs [138]. Ideally, aptamers should bind to soluble antibodies or to those expressed on the surface of B cells.

Therefore, for the selection of these aptamers, we conjugated the antibodies with protein G coated magnetic beads. Protein G, isolated from bacteria, was first reported in 1973 due to its binding properties specific to the heavy chain or the Fc-domain of immunoglobulins [141, 142]. Using beads coated with this protein, the IgG antibodies found in biological samples can be isolated; furthermore, as the Fc domain of the antibody is bound to the bead, we increase the chances of selecting Fab-binding aptamers.

As for the aptamers to the virus itself, they should bind efficiently enough to prevent the binding of nAbs; however, these oligonucleotides should not prevent the virus from infecting tumour cells. This selection was done by Dr. Anna Zamay, and consisted of two main parts: ten rounds of cell-SELEX [143], followed by a selection on polypropylene plates using an antibody-displacement method [139].

The affinity of selected aptamers for antibodies and virus was tested using flow cytometry and resulted in over 30 aptamers that had favourable binding to their targets and promising blocking and shielding effects.

2.2 Materials and methods

2.2.1 DNA library and primers

The 80 nucleotide (nt) DNA library contained a central randomized sequence of 40 nt flanked by 20 nt primer-hybridization sites (5' - CTC CTC TGA CTG TAA CCA CG$(N)_{40}$GCA

TAG GTA GTC CAG AAG CC - 3'). The forward primer (FP) labeled with 6-carboxyfluorescein (6-FAM) fluorescent dye (5' - (6-FAM)-CTC CTC TGA CTG TAA CCA CG - 3') and the non-labeled reverse primer (RP, 5'-GGC TTC TGG ACT ACC TAT GC - 3') were used in PCR reactions for the synthesis of single-stranded DNA molecules. The non-labeled FP and RP were used for PCR reactions in order to generate double-stranded DNA molecules used for cloning. All oligonucleotides were synthesized by Integrated DNA Technologies (IDT, Iowa, USA).

PCR was carried out in a Mastercycler pro S thermal cycler (Eppendorf, Ontario, Canada). In addition to the DNA template, 50 μl of the PCR reaction mixture contained 1× Green GoTaq Flexi Buffer, 2.5 mM $MgCl_2$, 0.025 U/μl GoTaq Hot Start Polymerase, and 200 μM dNTPs (Promega Corporation, USA). For the symmetric amplification, 300 nM of 6-FAM-labeled FP and 300 nM of unlabeled RP were used. For the asymmetric amplification, the concentration of the forward primer was 20 times higher than the concentration of the reverse primer (1 μM and 50 nM, respectively). The following settings were used for the thermal cycler: melting at 94°C for 30 s, annealing at 56°C for 15 s and extending at 72°C for 15 s.

2.2.2 Aptamer selection

Anti-nAbs aptamers PureProteome Protein G magnetic beads and PureProteome magnetic stand were purchased from Millipore (Massachusetts, USA). The beads were suspended and washed in Dulbecco's Phosphate Buffered Saline (DPBS) from Sigma-Aldrich (Ontario, Canada), and incubated with rabbit serum containing 3.5 mg/mL of polyclonal anti-VSV neutralizing antibodies (nAbs) (Jennerex Inc, California, USA) at room temperature for 15 min with continuous mixing. The presence of nAbs on beads was confirmed by incubating the beads with 10 ng/μl of Alexa Fluor 488 chicken anti-rabbit IgG (H+L) (Invitrogen, California, USA); the fluorescence of the beads was monitored with a Gallios

flow cytometer (Beckman Coulter, California, USA) and analyzed with FlowJo software (Oregon, USA).

Aptamer selection was done using the previously developed SELEX method. DNA library was denatured at 95°C for 5 min and then snap cooled on ice for 10 min in order to obtain renatured DNA structures. The DNA (200 nM) was then incubated with 5×10^5 of beads coupled with anti-VSV nAbs for 1 hr with continuous mixing at room temperature. To separate bound from unbound DNA, the beads were washed three times with DPBS. Bound DNA was then eluted from beads by denaturing at 85°C for 10 min.

For the first 5 rounds, we performed a positive selection followed by a negative selection step to protein G magnetic beads where the eluted DNA was mixed with beads alone. The solution was incubated, with continuous mixing, for 1 hr at room temperature. Unbound DNA was collected and amplified by symmetric and asymmetric PCR reactions. The asymmetric product was then concentrated and purified with 30 kDa Nanosep Centrifugal Devices (Pall, New York, USA) and used for a following round of selection. In rounds 6 to 10, the beads for the negative selection step were coupled with non-VSV antibodies prior to their incubation with the eluted DNA. In rounds 11 to 15, two negative selections, beads alone and beads with non-specific antibodies, respectively, preceded the positive selection step. Unbound DNA was then collected and used for incubation with anti-VSV nAbs coupled with magnetic beads. Fifteen cycles of symmetric PCR, followed by 20 cycles of asymmetric PCR were used for the amplification of single-stranded DNA after the elution of DNA from the beads (Figure 2.1). The affinity of aptamers to nAbs-coated beads during the selection was monitored using flow cytometry. A total of 150 nM of 6-FAM-labeled DNA, obtained from asymmetric PCR amplification after each selection round, was continuously mixed with magnetic beads coupled with nAbs for 1 hr at room temperature. Following the incubation step, the beads were washed, re-suspended in DPBS buffer and subjected to flow cytometry analysis (Figure 2.3).

Anti-VSV aptamers The virus used for this selection was generously provided by

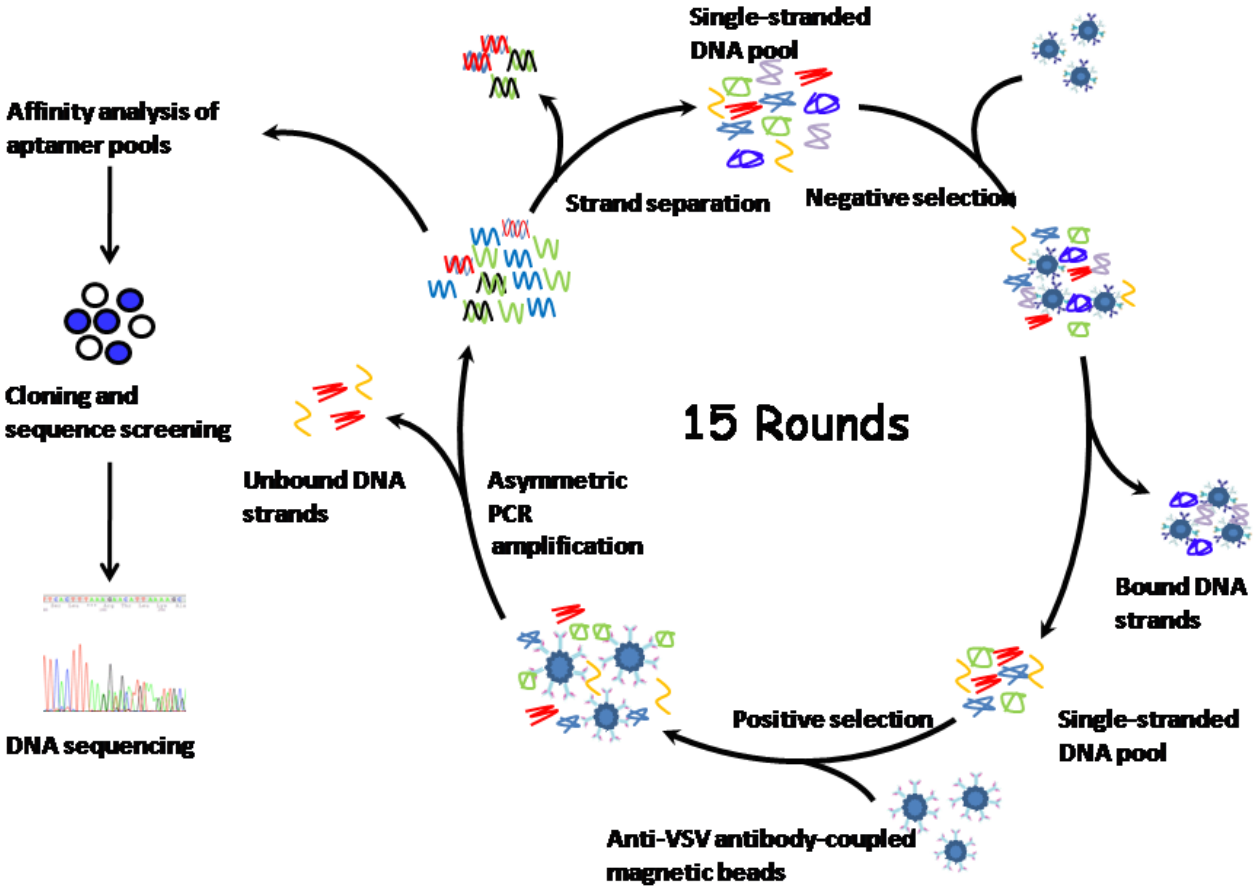

Figure 2.1: A schematic representation of aptamer selection to anti-VSV neutralizing antibodies. The SELEX (Systematic evolution of ligands by exponential enrichment) procedure consisted of 15 rounds iterating 3 major steps: (i) negative selection to beads and non-VSV Abs on the beads, (ii) positive selection to anti-VSV nAbs on the beads and (iii) symmetric and asymmetric PCR amplification. Selected aptamer pools were analyzed by flow cytometry. The best pool was cloned and sequenced. Reproduced with permission from Journal of American Chemical Society 134(41), 17168-17177. Copyright 2012 American Chemical Society.

Jennerex Inc. Prior to each aptamer round of selection, the virus was washed by centrifugation at $14,000 \times g$ and resuspended in DPBS.

For the aptamer selection, we used 2×10^{10} plaque forming units (PFUs) for each round and incubated with 100 nM of DNA for 30 min at 25°C. Non-bound DNA was removed by centrifugation of the virus and washing two times with DPBS. Bound DNA was eluted by denaturing at 95°C, centrifuging viral debris, and collecting the supernatant. Amplification and purification of aptamer pools was the same as the one used for selection of anti-nAbs aptamers. After first four rounds of positive selection, we did three rounds of negative selection against human blood cells, mouse blood cells and mouse blood plasma in order to make the aptamers applicable for *in vivo* use. In total, ten rounds of selection were performed using this cell-SELEX method (Figure 2.5) (Figure 2.2). The tenth aptamer pool, which showed the highest affinity to the virus, was chosen for cloning and sequencing (Table 2.2).

In order to obtain aptamers that can bind to the same site as the antibodies, we did a selection using a competitive approach. For this, we used 200 nM of unlabeled anti-VSV aptamer pool from round seven and incubated it overnight on a polypropylene 96-well plate (Corning, NY). The following day, wells were washed once with DPBS and then incubated with 1×10^7 PFUs of VSV for 30 min. The wells were washed again to remove unbound VSV, followed by the addition of another layer of the aptamer pool and incubation at 37°C for 1 hour. Subsequently, three different concentrations of rabbit serum containing polyclonal anti-VSV nAbs were added to each well – low (0.5 μg/ml), moderate (2.5 μg/ml) and high (3.8 μg/ml) – and incubated for 5, 30 and 60 min, respectively. The supernatant was then collected and each fraction was amplified and used for the subsequent round of selection on a plate. In total, we did five of these rounds, after which the pools were analyzed by flow with a competitive binding assay (Figure 2.6). Moderate pool 10 and strong pool 11 were cloned and sequenced.

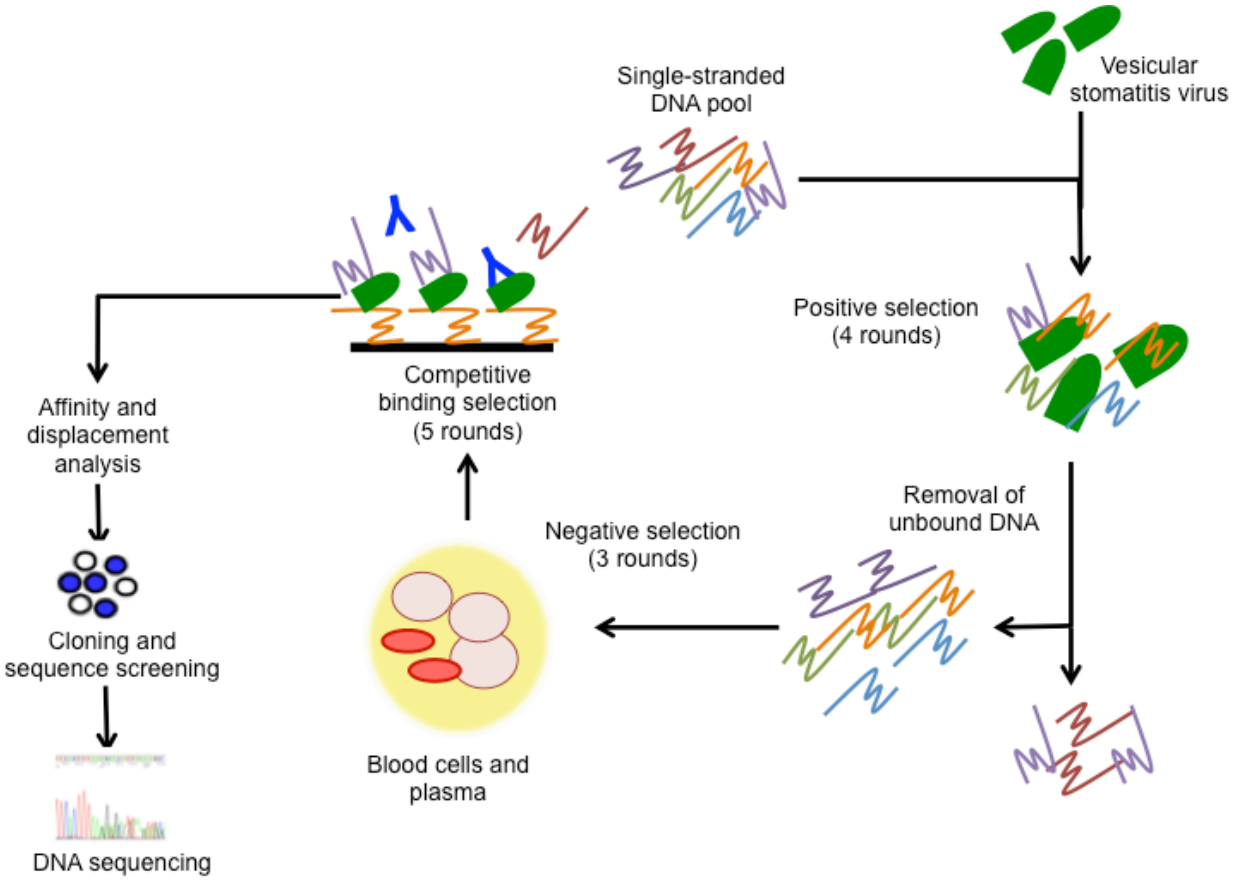

Figure 2.2: A schematic representation of aptamer selection to vesicular stomatitis virus. The SELEX (Systematic evolution of ligands by exponential enrichment) procedure consisted of 15 rounds consisting of 3 major steps: (i) positive selection to VSV, (ii) negative selection to mouse and human blood and plasma, and (iii) competitive binding selection. Selected aptamer pools were analyzed by flow cytometry. The best pools were cloned and sequenced.

2.2.3 Competitive binding assay

Anti-nAbs aptamers A total of 200 nM of each aptamer pool was mixed with 10 ng/μl of DyLight 488-conjugated anti-VSV polyclonal antibody (Rockland Inc, Pennsylvania, USA) and incubated for 1 hr at room temperature. To this solution, 6×10^8 PFUs of VSV were added, incubated at 37°C for 30 min and subjected to flow cytometry analysis. Virus particles were then gated and their total fluorescence was quantified. Virus alone, antibody alone, virus and antibody, and DPBS buffer were used as controls (Figure 2.4).

Anti-VSV aptamers VSV (1×10^7 PFUs) was preincubated with 0.1 mg/ml yeast RNA in DPBS for 30 minutes at 25°C. We then added 200 nM of 6-FAM-labeled amplified anti-VSV pools and incubated for an additional 30 min. Subsequently, samples were centrifuged to remove unbound aptamers, resuspended in DPBS, and subjected to flow cytometry analysis. After the analysis, anti-VSV antibody was added to the same vials at a final concentration of 2 mg/ml and the mixture was incubated again for 60 minutes at 37°C. Finally, the virus was centrifuged again to remove unbound antibodies and aptamers. VSV was resuspended in DPBS and subjected to a second flow cytometry analysis (Figure 2.6).

2.2.4 Aptamer cloning and sequencing

An aptamer pool was amplified by symmetric PCR using non-labeled primers and purified with AxyPrep DNA Gel Extraction Kit (Axygen Biosciences, California, USA). The aptamer pool was then cloned into *Escherichia coli* (*E. coli*) using the pETBlue-1 Perfectly Blunt Cloning Kit (Invitrogen, California, USA). Plasmids containing the insert were isolated from bacterial colonies with GeneJET Plasmid Miniprep Kit (Thermo Fisher Scientific Inc., Massachusetts, USA) and amplified by PCR. Individual aptamers were screened for their binding to their target and the clones that had fitting results were chosen for sequencing in Génome Québec (Québec, Canada).

Once the sequences were obtained, synthetic aptamers were ordered from IDT. To increase the number of potential aptamer candidates, we ordered the clones with and without primer-binding sites. The long aptamers (with primer-binding sites) were amplified with 6-FAM-labeled primers and purified. The dissociation constants for these aptamers were estimated by incubating the target with different concentrations of aptamers, running the samples on flow cytometry, and finally analyzing the data on excel (Table 2.1 and Table 2.2).

2.2.5 Statistical analysis

Statistical analysis was done using a one-way ANOVA and Tukey post test. A p-value below or equal to 0.05 was considered to be statistically significant and indicate significant difference.

2.3 Results and discussion

2.3.1 Anti-nAbs aptamers

In order to obtain aptamers that bind anti-VSV neutralizing antibodies, we used rabbit serum as the substrate containing a polyclonal pool of antibodies. Rabbits that have been immunized with vesicular stomatitis virus express high amounts of neutralizing antibodies; this has been confirmed with plaque forming assays, as incubation of VSV with this serum can completely inhibit viral infection *in vitro* [92]. Therefore, we used magnetic beads coated with protein G in order to isolate these polyclonal antibodies from rabbit serum. We assumed that a portion of these antibodies would be non-specific to the virus; to eliminate aptamers that would bind to them, we used rabbit serum that was not in contact with VSV for our negative selection. The presence of both of these types of antibodies was

confirmed by flow cytometry using fluorescently-labeled secondary antibodies (Figure 2.3 A).

Aptamer selection was performed using a modified SELEX method, with a different negative selection every five rounds: protein G beads only, beads coupled to non-VSV antibodies, and both. The selection was stopped after 15 rounds, when no further increase of pool affinity to nAbs was observed (Figure 2.3 C). The aptamer selection started with 3×10^{15} sequences of the DNA library. Many of the aptamer sequences in collected fractions may be present in very low concentrations. Therefore, an initial symmetric amplification is required to increase the concentration of available templates. Sequentially, in order to obtain the fluorescently labeled single-stranded aptamer pools for affinity analysis, an asymmetric amplification is performed.

In the first five rounds of selection, a constant increase of DNA affinity to nAbs was observed. However, when we introduced a negative selection to non-specific antibodies, it decreased. This loss of binding could be explained by elimination of aptamers to common structures among all antibodies. As we introduced the two negative selections, the binding of pools increased by more than threefold compared to the native DNA library (Figure 2.4 C). In addition, we hypothesized that small differences in pools binding to VSV nAbs and non-VSV Abs were because each pool contained many aptamer sequences that could bind to different parts of antibodies. Furthermore, as mentioned above, both VSV nAbs and non-VSV Abs were used from crude rabbit serum and thus consisted of a complex mixture of polyclonal antibodies. Taken together, these effects could explain the lack of average specificity of our pools.

Five pools with high affinity and specificity for anti-VSV antibodies were tested by flow cytometry using a competitive binding assay. Fluorescently-labeled anti-VSV nAbs and unlabeled aptamer pools were preincubated and then added to the virus. The complex of fluorescently-labeled antibody with the virus was monitored with the presence of different aptamer pools, using the DNA library as a control (Figure 2.4). A decrease of fluorescence

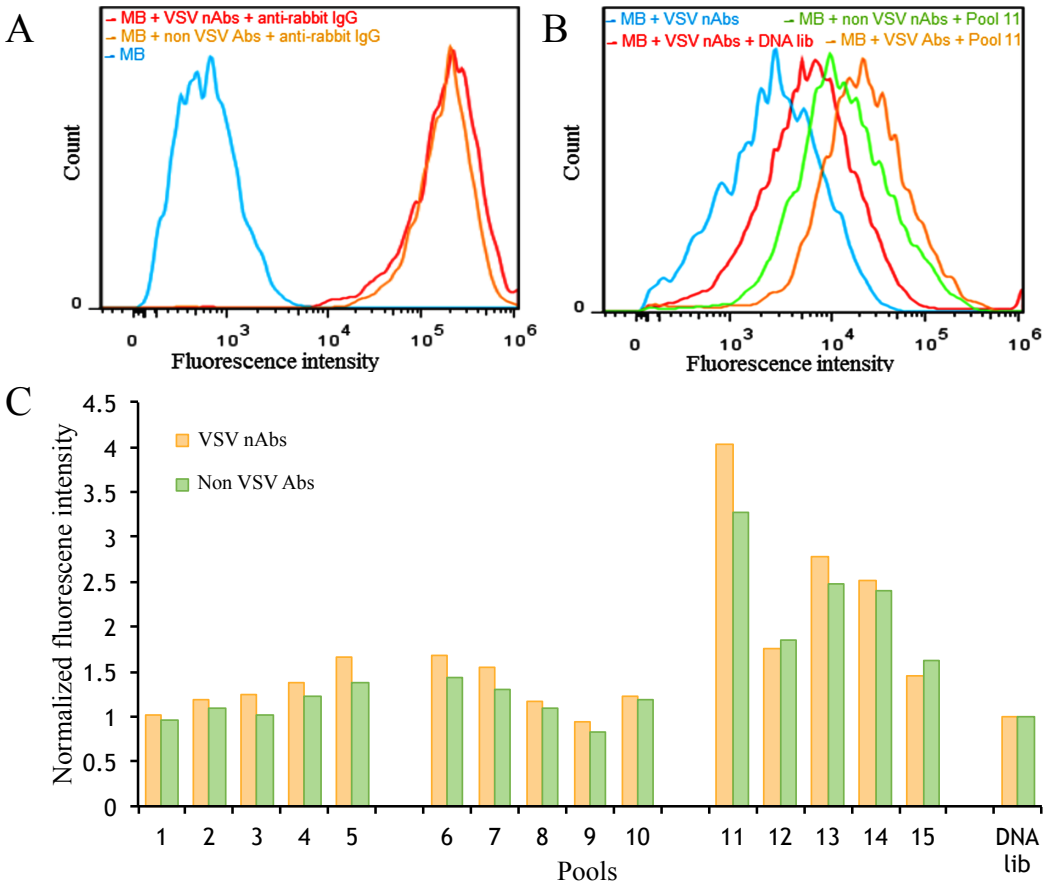

Figure 2.3: Affinity of different aptamer pools to anti-VSV neutralizing antibodies. Flow cytometry histograms showing (A) magnetic beads (MB) alone (blue), and MB with a secondary Alexa 488 labeled antibody coupled to non-VSV (orange) and anti-VSV (red) neutralizing antibodies (nAbs), (B) binding of aptamer pool 11 to anti-VSV nAbs on magnetic beads (orange), non-VSV antibody (green), and magnetic beads with anti-VSV nAbs (blue) compared with native DNA library binding to anti-VSV nAbs on magnetic beads (red). (C) Comparative binding of 6-FAM-labeled aptamer pools to anti-VSV nAbs (purple) and non-VSV antibodies (pink). Initial DNA library was used as a control (green) and to normalize the fluorescence of aptamer pools. Reproduced with permission from Journal of American Chemical Society 134(41), 17168-17177. Copyright 2012 American Chemical Society.

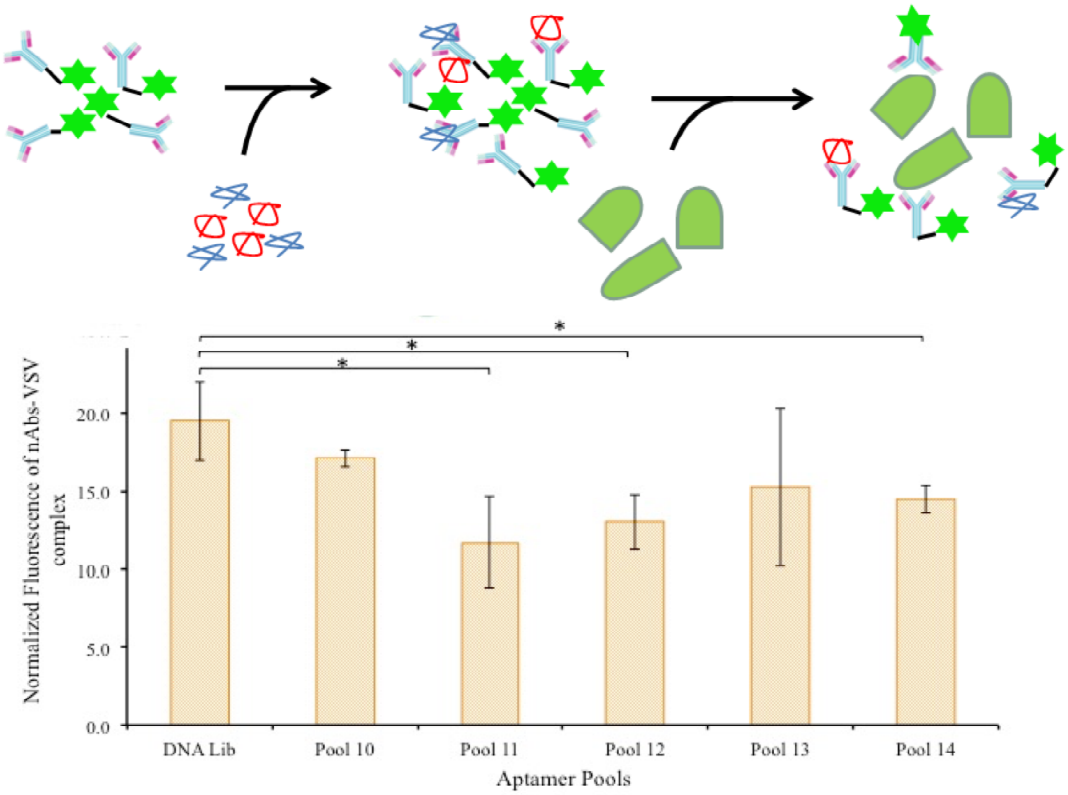

Figure 2.4: Competitive binding assay of selected aptamer pools. (A) A schematic depicting the assay, where labeled antibodies were preincubated with aptamer pools and then mixed with VSV. Virus fluorescence was then monitored by flow cytometry. (B) The results for each pool were compared to the initial DNA library and were normalized to the virus incubated without DNA. (* = $p < 0.5$)Adapted with permission from Journal of American Chemical Society 134(41), 17168-17177. Copyright 2012 American Chemical Society.

signal of nAbs-virus complex was an indication that the pool competed with nAbs for binding the virus. Pools 11, 12 and 13 showed the lowest fluorescence and were chosen for cloning. Individual aptamer clones were then screened by flow cytometry for their binding to VSV nAbs and non-VSV Abs. The ones with desirable affinity and specificity were synthesized by IDT; sequences and estimated dissociation constants for aptamers ranged from 10 nM to 780 nM (Table 2.1). These aptamers were then screened *in vitro* for their ability to prevent the binding of neutralizing antibodies to the virus, which is presented and discussed in Chapter 3.

2.3.2 Anti-VSV aptamers

The first round of selection for shielding aptamers to VSV was done using a cell-SELEX procedure. Briefly, each round consisted of several steps: incubation of DNA library with VSV, removal of unbound DNA from VSV, separation of bound DNA sequences from virus, DNA amplification by symmetric and asymmetric PCR, and purification of single-stranded aptamers after PCR (Figure 2.2). For *in vivo* applications of aptamers against VSV, it is necessary to prepare aptamer pools that do not bind to blood cells and plasma proteins and are stable and active in the blood stream. Therefore, after first four positive rounds of selection, three rounds of negative selection against human blood cells, mouse blood cells, and human plasma were performed. These negative rounds of selection resulted in a decrease of overall affinity of the aptamers, as is shown in Figure 2.5 A, which was also observed in the selection of aptamers to neutralizing antibodies. In this case, the decrease could be due to a depletion of aptamers by DNA-binding cells, such as leukocytes and DNA-binding proteins [144, 145]. Pool 10 was cloned, sequences and analyzed for its binding to the virus; seven of the aptamer clones were binding stronger than the aptamer pool (Figure 2.5 B).

Table 2.1: List of aptamer sequences selected for anti-VSV neutralizing antibodies and their apparent dissociation constants for VSV nAbs and non-VSV Abs.

Name	Sequence (5'–3')[a]	K_d anti-VSV nAbs (nM)	K_d non-VSV Abs (nM)
C1	fCCCAGAAACAGCACCCTTACATCGACTGGACCTTCCGCGcr	780	610
C3	fACTAGGACGCTTGGGAGGGGGGGTGGGGTGTCCGGTCGCGcr	780	370
C4	fCCGGGGAATCTAGGGGAGGGCGGGTGGGTCAATTGAGCCGcr	80	225
C5	fTGTGCCAAAGAGAGTGGTGGGGGGGTGGGCGGAACTCGCGcr	570	>1000
C6	fACTAGGACGCTTGGGAGGGGGGGTGGGGTGTCCGGTCGCGcr	10	70
C7	fCCAACCACACATCCTTCCATCGACATGGACCCACCGTTCCcr	230	>1000
C8	fTGAAGCGAACCGATGGTGGGGGGGTGGGTGGAAACGGAGAcr	170	280
C9	fACCGCCTTCCACCGTTCTCCACCACCCCTCAAACAACCCTcr	105	>1000
C10	fCCACCGAGCCTACCACATGTGACATCCCAGGACATAGCTGcr	575	>1000

[a] f, ctcctctgactgtaaccacg (sequence of the forward primer); cr, gcataggtagtccagaagcc (reverse-complement of the reverse primer); sequences were ordered both with and without the primer-binding sites; Dissociation constant K_d values were determined for long sequences only.

The next selection step was performed using a competitive approach (Figure 2.2). An unlabeled aptamer pool with affinity for VSV was incubated in a 96-well plate in order to allow DNA to nonspecifically adhere to the plastic. For this purpose, we screened different polypropylene and polystyrene plates in order to identify the one that facilitated maximal adsorption of DNA. As expected, polypropylene proved to be the ideal candidate, as it showed the highest adsorption [146]. Subsequently, the virus, preincubated with an anti-VSV aptamer pool, was added to the well. Ability of the virus to adhere onto the plate was previously verified with an intercalating viral RNA dye, YOYO-1, and analyzed with a fluorescence plate reader. Finally, the sandwich-like complex of aptamers and virus was disrupted by addition of antibodies at three relative concentrations: low, moderate, and high (0.5, 2, and 3 μg/ml, respectively). Aptamers that were displaced from the surface of the virus with these different antibody concentrations were separately collected, amplified, and used for further selection. In addition, we changed incubation times of nAbs according to their used concentration; we hypothesized that aptamers with longer dissociation rates might take longer to be displaced by nAbs, and therefore incubated higher antibody concentration doses for a longer period of time.

Binding analysis of these rounds revealed an increase in binding affinity of the strong pool throughout the selection process. Binding of the moderate pool did not significantly increase until the tenth round, and we observed a decrease of affinity for the weak pool during the competitive selection. However, in round 11, the weak pool had a higher affinity for the target than the moderate pool.

Moreover, all weak, moderate, and strong aptamer pools were analyzed for their ability to bind the virus and be displaced by anti-VSV nAbs. 6-FAM-labeled aptamers were preincubated with virus and analyzed by flow cytometry. Neutralizing anti-VSV antibodies were then added to the mixture and incubated an additional hour. The displacement of aptamers from the surface was estimated by monitoring the reduction of virus fluorescence. The best pools corresponding to weak, moderate, and strong aptamers can be

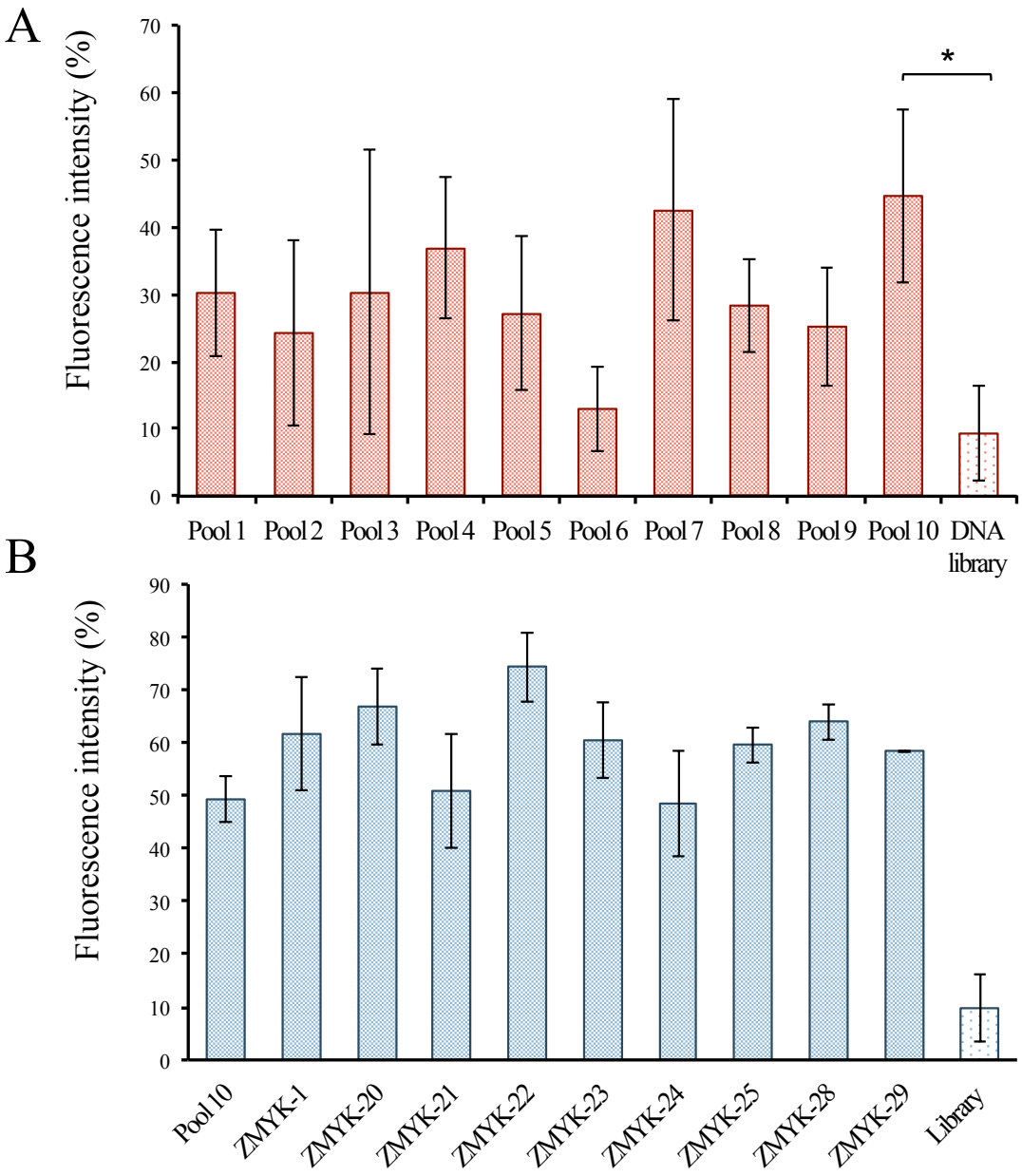

Figure 2.5: Affinity analysis of aptamer pools and clones selected for the vesicular stomatitis virus measured by flow cytometry. (A) Aptamer pools were selected using a traditional cell-SELEX method consisiting of positive and negative selections. (* = $p < 0.5$) (B) Clones were isolated from the tenth aptamer pool and their binding to VSV was analyzed by flow cytometry. Difference between the library and the clones is statistically significant (** = $p < 0.1$) Adapted with permission from Journal of American Chemical Society 84(3), 1677-1686. Copyright 2012 American Chemical Society.

seen in Figure 2.6. For weak pool 11, there was not a significant difference of fluorescence between the two concentrations of antibodies (3.8 μg/ml and 2.5 mg/ml), suggesting that the aptamers that bound to epitope-binding sites can be displaced with low concentrations of nAbs. Moderate pool 10 was partially displaced with the antibody at a lower concentration, and the additional dose of antibody of 2.5 mg/ml led to further reduction of fluorescence. Strong pool 11 had a high binding affinity and was not displaced significantly with antibodies at a concentration of 3.8 μg/ml. However, the high concentration of antibodies shifted the fluorescence curve back to the same intensity as the virus alone, indicating that nearly all aptamers bound to VSV had been replaced. Finally, moderate pool 10 and strong pool 11 were cloned and sequenced (Table 2.2).

2.4 Conclusion

Vesicular stomatitis virus is an efficient oncolytic virus that is mostly used as a model virus due to its broad tropism. However, the main setback for this oncotherapy is the fact that multiple injections in a host result in high doses of neutralizing antibodies, which prevent the virus from reaching tumour sites. In the first part of this project, we attempted to select aptamers for the purpose of developing shielding and blocking oligonucleotides to facilitate the bypassing of the immune system by the virus. Blocking aptamers were selected to bind to the anti-VSV neutralizing antibodies, whereas shielding aptamers were selected for their affinity to the virus itself.

Anti-nAbs aptamers were selected using magnetic beads in order to facilitate the separation of bound and non-bound oligonucleotides. Furthermore, the fact that the antibodies were binding to the beads through their Fc domains increased the chances of selecting aptamers that would interact with the Fab domain on these antibodies.

As for the anti-VSV aptamers, they were selected using two different methods: a traditional cell-SELEX, as well as a competitive displacement approach. The latter was done

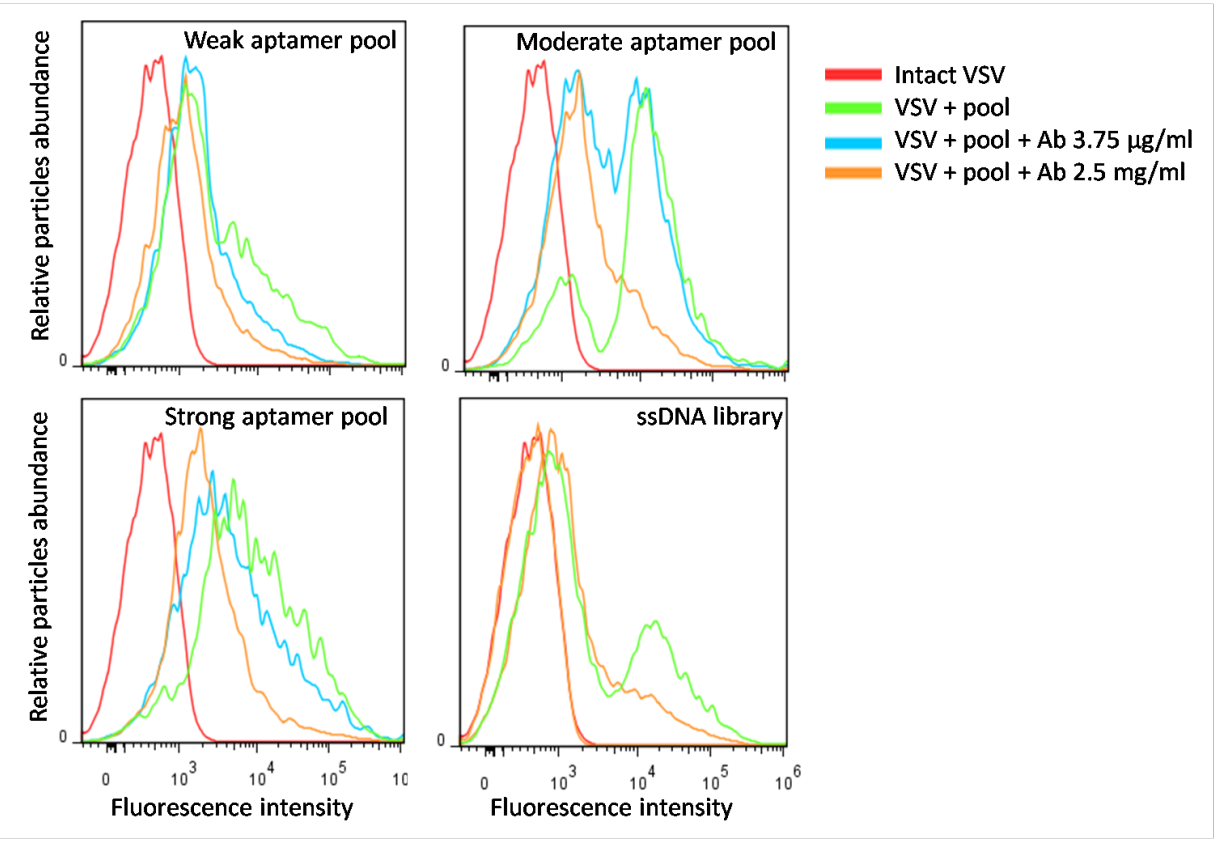

Figure 2.6: Competitive analysis of weak, moderate and strong pools selected for vesicular stomatitis virus analyzed by flow cytometry. VSV was incubated with anti-VSV aptamers or DNA library (green), followed by addition of neutralizing antibodies (3.8 μg/ml (blue) or 2.5 mg/ml (orange)); virus alone (red) was used as a control. Adapted from Macmillan Publishers Ltd: Molecular Therapy – Nucleic Acids 3:e167, 2014 freely available under the terms of the Creative Commons Attributions License.

Table 2.2: List of aptamer sequences selected for vesicular stomatitis virus selected using SELEX method and competitive selection including their apparent dissociation constants.

Name[a]	Sequence (5'–3')[b]	K_d (nM)
Z-1	fGTGGGGGTCCTGTGGTTGGTGTGGTGGTGAGATGTGGTGGcr	N/A
Z-20	fCCATCACCCTATTATCTCATTATCTCGTTTTCCCTATGCcr	780
Z-21	fCGGGAACCAAATCACGTCCTAGATTGTGATGAACCTCGGCcr	80
Z-22	fGCGACAACACGGACGGTTGAGACTTTAATTCTGCTCACGGcr	570
Z-23	fGGGACCTATCAGGCGATGTGAAAACTCTTATACCACTGGcr	10
Z-24	fGGCGGTCCCTTCTTTTTGTGTTTATGTTGTTCTCTTTTCGcr	230
Z-25	fCCGCAACCGAGCTTCGACCTACACTTACGATGTGTCCCACcr	170
Z-28	fCCACCATGCACGACCCACGCAATGACAGTAACACACCTCGcr	100
Z-29	fCACATCCTACGTTTGCCACGCGCTACTCCGCCATCTACCCcr	570
M50	fCCATCACCCTATTATCTCATTATCTCGTTTTCCCTATGcr	N/A
S37	fGCATAGCGGGGGAGATGGGGGATGACTTGGGTGTGATGGGcr	N/A
S39	fGCACTTCACTTCTCCTCTGACTGTAACCACGCcr	N/A

[a] f, ctcctctgactgtaaccacg (sequence of the forward primer); cr, gcataggtagtccagaagcc (reverse-complement of the reverse primer); clones selected with traditional SELEX approach.

[b] Z = selected using SELEX approach; M = selected using competitive approach, moderate pool; S = selected using competitive approach, strong pool.

in order to obtain aptamers that would share the same binding sites as the neutralizing antibodies.

In this work, aptamer binding was analyzed with flow cytometry, both for their affinity and their efficacy in displacing antibodies bound to the vesicular stomatitis virus. Selected DNA aptamers were then used for *in vitro* and *in vivo* assays (discussed in the following chapter) to further examine their blocking and shielding effect.

Chapter 3

In vitro aptamer-facilitated protection of virus from neutralizing antibodies

3.1 Background

In our previous chapter, we presented our results for the development of anti-nAbs and anti-VSV aptamers and explored their potential in preventing the inhibition of viral infection by displacement assays and flow cytometry. In this chapter, we propose an improved aptamer-based technology, named Aptamer-Facilitated Virus Protection (AptaVIP), which is based on enhancing the survival of VSV in the presence of nAbs. For this, we use our two types of DNA aptamers: blocking and shielding aptamers. Blocking aptamers will ideally bind to antigen-binding fragments of neutralizing antibodies (nAbs) and prevent neutralization of a virus; shielding aptamers will bind to the virus and mask it from recognition by nAbs, thus allowing the virus to attach to and infect cancer cells (Figure 3.1).

It is important to be able to measure the virus titer in order to determine the amount

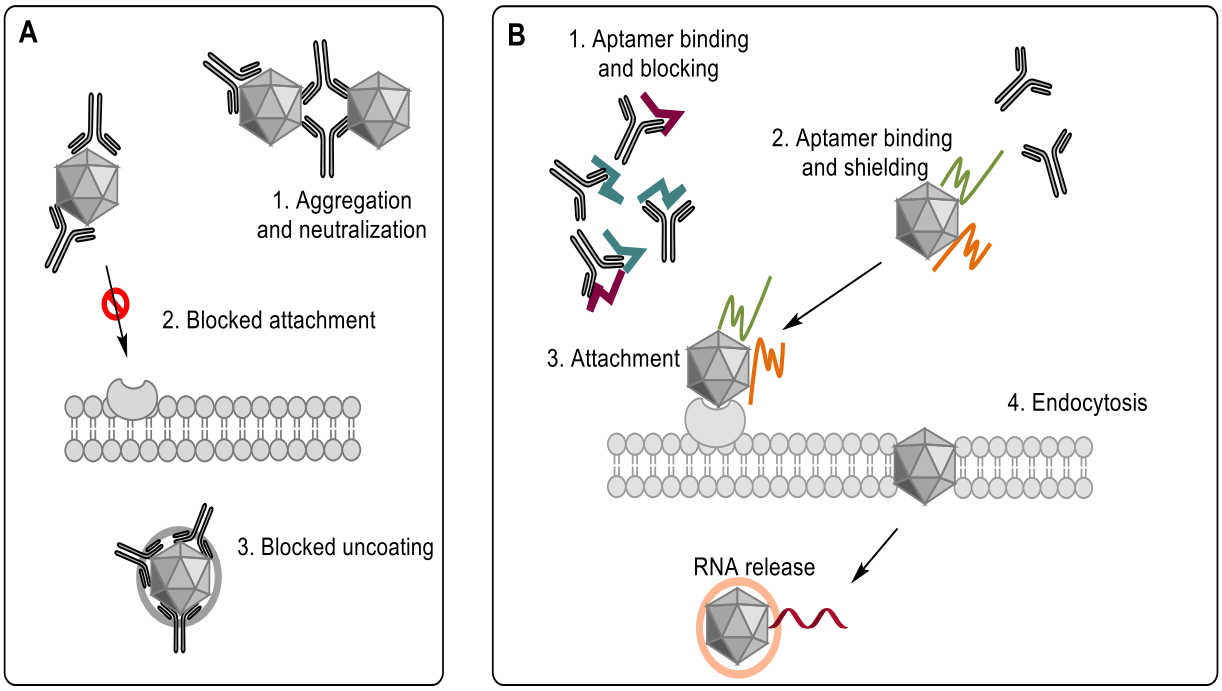

Figure 3.1: (A) Neutralizing antibodies (nAbs) bind to vesicular stomatitis virus and prevent it from infecting the cell by (i) aggregating the virus, (ii) blocking attachment of virus to the cell membrane, and/or (iii) preventing uncoating of virus inside the cell. (B) Aptamers binding to nAbs or to VSV can block the antibodies or shield the virus, thus allowing it to infect the cell. Reproduced from Macmillan Publishers Ltd: Molecular Therapy – Nucleic Acids 3:e167, 2014 freely available under the terms of the Creative Commons Attributions License.

of infectious particles. This can be done using a variety of different methods, including nanoparticle tracking analysis (NTA), quantitative polymerase chain reaction (qPCR), transmission electron microscopy (TEM), as well as capillary electrophoresis, which was recently developed in our laboratory [147–149]. However, the majority of these techniques tend to overestimate the number of infectious particles, as viruses tend to aggregate or contain non-infectious units [150]. Therefore, the most widely used approach is the plaque forming assay as it facilitates the measurement of infectious viral particles. This method is executed by preparing serial dilutions of the viral stock, which are then spread on a cellular monolayer. These monolayers are then covered with a gel, such as agarose or carboxymethyl cellulose, which prevents the virus from spreading further than the neighbouring cells. Finally, after incubation, infected cells are marked with circular-shaped plaques; it is estimated that each plaque is caused by a single viral particle [151].

A similar plaque forming assay is used for antibody titration in order to determine their level of viral neutralization. When the virus is incubated with nAbs, the plaque formation will be completely inhibited; we used this approach to inspect the effect of our aptamers on viral infectivity. Plaque forming assays were done in collaboration with Dr. Anna Zamay and Shahrokh Ghobadloo.

Aptamers have been tested *in vivo* in different groups for a number of applications [52, 152, 153]. For example, the previously mentioned aptamer targeting Axl, a tyrosine kinase receptor, was successfully used for inhibition of Axl-dependent phosphorylations and thus lead to inhibition of tumour growth in a mouse xenograft model [56]. We attempted to achieve delivery of the vesicular stomatitis virus in VSV-immunized mice by injecting both blocking and shielding aptamers with the virus and monitoring its replication in the tumour. However, we were not able to obtain the desired effect, either with monomeric aptamers or with tetrameric modifications.

3.2 Materials and methods

3.2.1 Vesicular stomatitis virus

Original vesicular stomatitis virus sample was provided by Jennerex (California, USA). It was then propagated and purified as described by Diallo et al [92]. Briefly, Vero African green monkey kidney cells were seeded in high glucose Dulbecco's modified Eagle medium (DMEM) supplemented with 10% fetal bovine serum (FBS). When cultures reached about 95% confluency, they were infected with the virus at a concentration of 2×10^5 plaque forming units (PFUs) per 150-mm petri dish. After approximately 24 hours, the supernatant containing the virus was collected and purified by centrifugation and sucrose gradient. Aliquoted viral samples were titered and stored at -80°C.

Viral infectivity assay Aptamer-shielded nAbs were prepared by incubating whole rabbit serum containing nAbs with 1 μM aptamers in DPBS for one hour at 37°C. Aptamer-binding nAbs were then incubated with VSV (2×10^6 PFUs) for 1 hr at 37°C. Consequently, the aptamer-nAb-virus mixture was serially diluted in serum-free medium and added to a Vero cell monolayer (0.4×10^6 cells per well) in a twelve-well culture plate. The final concentration of aptamers was 132 nM per well. After one hour at 37°C in a 5% CO_2 humidified incubator (Thermo Fisher Scientific Inc, Massachusetts, USA), all media were removed and the cells were overlaid with 1% agarose dissolved in DMEM supplemented with 10% fetal bovine serum (Sigma-Aldrich, Ontario, Canada). Following a 24-hour incubation, cells infected with VSV expressing yellow fluorescent protein (YFP) were visualized using Alfa Innotech Imaging System. In addition, a standard plaque assay was performed, where the same plates were fixed with methanol-acetic acid fixative (3:1 ratio) and stained with Coomassie Brilliant Blue R solution (Sigma-Aldrich, Ontario, Canada) in order to visualize and count the plaques.

Rabbit serum containing polyclonal anti-VSV antibodies was provided by Jennerex and

stored at -20°C.

3.2.2 96-well plate assays

For the neutralizing antibody assay, a procedure published by Diallo et al. was followed [92]. Briefly, Vero cells were plated at a density of 1.25×10^4 cells/well in 100 μl of Dulbecco's modified Eagle medium (DMEM) containing 10% fetal bovine serum and incubated overnight at 37°C. The following day, rabbit serum containing anti-VSV antibodies was prepared in seven different dilutions: $100\times$, $500\times$, $1,000\times$, $1,500\times$, $2,000\times$, $2,500\times$, and $5,000\times$. Subsequently, each concentration (performed in triplicates) was plated in a 96-well plate, to which 1×10^4 PFUs of virus was added and incubated at 37°C for 1 hour. The mixture was then transferred onto Vero cells and incubated overnight at 37°C. The infection of cells was monitored by fluorescence using FluorChem Q (Alpha Innotech, California, USA) imaging system (Figure 3.2 B).

For VSV aptamer assays on 96-well plates, 1×10^4 PFUs of YFP-VSV were coated with aptamers at five different concentrations (0.10, 0.25, 0.50, 1.0, and 10 μM) at 37°C for 1 hour. Coated virus was then added to a $2,000\times$ dilution of rabbit serum with anti-VSV antibodies and incubated at 37°C for 1 hour. The remaining procedure was the same as mentioned above, where the mixture was added onto Vero cells, incubated overnight, and finally imaged in order to observe the fluorescence.

3.2.3 Screening and analysis of aptamer clones by plaque forming assays

For the plaque forming assay, Vero cells were plated at a density of 2.5×10^5 cells/well in 1 ml of DMEM containing 10% fetal bovine serum and incubated overnight at 37°C. The following day, 1×10^4 PFUs of YFP-VSV were incubated with or without VSV aptamers

(final concentration 1 μM) in serum-free medium for 1 hour at 37°C. For the screening of aptamer clones, a 500× dilution of serum was used and incubated with or without anti-nAbs aptamers in serum-free medium for 1 hour. Serum and virus were then mixed together and placed at 37°C for 1 hour. The mixture was diluted in order to obtain three different concentrations of virus: 100, 500, and 1,000 PFUs in 250 μl, and added to Vero cells. After 1 hour of incubation, a layer of 0.5% low-melting point agarose (IBI Scientific, Iowa, USA) with Dulbecco's modified Eagle medium supplemented with 10% fetal bovine serum was added and the plates were left to incubate for 24 hours. The following day, the plates were imaged and the plaques were counted.

3.2.4 Effect of dimeric and tetrameric aptamers on VSV infectivity

For dimeric and tetrameric forms of aptamers, an oligonucleotide bridge linking two or four aptamers together was constructed, which consisted of one or two oligonucleotide strands connected by a central complementary sequence. The sequence of these bridging nucleic acids is 5' - GGT TAC AGT CAG AGG AGT TAA CAC AAC CCC AAT TGG CTT CTG GAC TAC C - 3' and 5' - GGT TAC AGT CAG AGG AGT TTT GGG GTT GTG TTT TGG CTT CTG GAC TAC C - 3'. Each end of the bridge consisted of a complementary flank to facilitate the annealing of an aptamer (Figure 3.5 A). To prepare the dimeric and tetrameric aptamers, after heating at 95°C, the sides of the bridge were mixed equally, followed by their mixing with the aptamer pool in equal amounts. Subsequently, the complex resulted in two or four aptamers annealing to each bridge construct. For plaque forming assays, oligonucleotides were incubated with undiluted serum or 1×10^4 PFUs of VSV, or both for 5 minutes. The serum and the virus were then mixed together and incubated for one hour at 37°C. The virus was then diluted to 100 PFUs and added to the monolayer of Vero cells in a 12-well plate. Dissociation constants for these aptamers were

found according to the procedure described in the previous chapter.

To test the stability of these different aptamer constructs, 20 μl of 100 μM of each aptamer construct was incubated in 1 ml of human serum (BioReclamation, Hicksville, NY) at 37°C and aliquoted during a 24-hour period. Samples were stored in -80°C until they could be analyzed by real-time PCR (Bio-Rad CFX; Bio-Rad Laboratories, California, USA) using Platinum SYBR Green qPCR supermix-UDG reagent (Invitrogen, California, USA) and aptamer-specific primers. Each sample was diluted in ddH_2O and 10^4 molecules were added to the qPCR supermix. The amplification reaction was monitored with the following thermocycler conditions: 50°C for 2 minutes, 95°C for 2 minutes, and 40 cycles at 95°C for 15 seconds, followed by 60°C for 30 seconds. The amount of aptamers in serum was extrapolated from a standard curve obtained from a serial dilution of aptamers in serum at 0 hour incubation (Figure 3.7).

For the aggregation assay, Vero cells were plated in a 96-well plate at a density of 1.25×10^4 cells/well. Aptamers in monomeric, dimeric or tetrameric form (4 μM) were incubated with premixed equimolar solution of VSV-YFP and VSV-RFP for 1 hour at 37°C. Following this incubation, the mixture was diluted and 25 PFUs were added to the cells and incubated at 37°C. After 10 hours, the cells were visualized by microscopy (Eclipse Ti, Nikon Corporation, Tokyo, Japan) and the number of infected cells expressing YFP, RFP, or both, were counted (Figure 3.6).

3.2.5 Statistical analysis

All experiments were performed in triplicate. Statistical analysis was done using a one-way ANOVA and Tukey post test. A p-value below or equal to 0.05 was considered to be statistically significant and indicate significant difference.

3.2.6 Mouse *in vivo* experiments

For the initial experiment, we used a total of 30 Balb/c mice that were divided in four groups. Half of each group, fifteen in total, were vaccinated against VSV by receiving two injections of 5×10^8 PFUs/100μl of VSVΔ51, per mouse, in a span of two weeks. All of the mice were then injected subcutaneously with 1×10^6 of CT26.LacZ in the right hind flank; the tumours were grown and the treatment started after 12 days. Virus and aptamer injections were done intravenously (i.v.).

The four groups had different injections on the first day, consisting of VSV alone, VSV with anti-VSV aptamers, VSV with anti-nAbs aptamers, and VSV with anti-VSV and anti-nAbs aptamers. For these treatments, we used VSV with a firefly (*Photinus pyralis*) luciferase (Fluc) gene inserted between G an L genes, which allows *in vivo* imaging of animals. The virus was grown in Vero cell line and purified by sucrose gradient banding and centrifugation. Injected aptamer concentration was 10 μg/g for a total amount of DNA of 800 μg per mouse. The following day, the mice received aptamer injections, without the virus, and were then imaged with an *in vivo* imaging system with an exposure time of 30 sec after receiving 200 μl of 10 mg/ml of D-luciferin and isoflurane. On day 3, the mice received the aptamers, were imaged, and sacrificed after we did not observe any signal in the immunized group. The tumours were extracted, homogenized and subjected to a plaque forming assay in order to detect if any virus reached the tumour site.

For the second trial, involving multimeric aptamers, 16 Balb/c mice were used – 8 of them immunized against VSV – and divided into two groups. The preparation of mice was the same as in the previous experiment. However, in this case, we injected 20 μg/g of DNA per mouse. On the first day, one group received VSV alone and the second received VSV with tetrameric aptamers for both VSV and nAbs. The second and third day, the first group received DPBS only, whereas the second one received a dose of tetrameric aptamers for both targets, followed by imaging. The mice were sacrificed on the third day

(Figure 3.8).

3.3 Results and discussion

Analysis of shielding and blocking aptamers by plaque forming assay For our *in vitro* experiments, we used neutralizing antibodies obtained from rabbit serum. We performed a titration experiment in order to determine the optimal concentration necessary for neutralization of the virus. By varying the amount of virus and rabbit serum dilutions, we found that using antibody dilution of up to $2,000\times$ did not show any YFP expression in the cells, which indicated complete neutralization of the virus (Figure 3.2).

The initial screening was done in 96-well plates as it allowed us to analyze all of the clones. Anti-VSV or anti-nAbs aptamer clones were incubated with their respective targets and then mixed and incubated an additional hour. Subsequently, the mixture was added to the monolayer of cells. The following day, the fluorescence expression of these cells was analyzed. Even in presence of neutralizing antibodies, some cells were infected with the virus, which indicated that aptamer clones in those plates had shielding or blocking effects. These clones were then selected for further assays.

The plaque forming assay enables us to determine the viral potential to infect cells, which we will refer to as infectivity henceforth. As previously mentioned, when incubated with neutralizing antibodies, the virus is completely inhibited, and is unable to form any plaques on the cell monolayer (0% infectivity). On the other hand, when the nAbs are not added to the cells, the virus is free to infect them, and is considered to be 100% infectivity. For the anti-VSV aptamer sequences obtained from SELEX and moderate and strong pools, we found that clones Z-23, Z-22, S-31 (from strong pool) and M-50 (from moderate pool) had the ability to prevent the neutralization of virus by anti-VSV antibodies. As for anti-nAbs aptamers, four clones (C4s, C5s, C7s, and C9) proved to have the highest blocking efficacy. Rabbit antibodies can have around 200 genes encoding

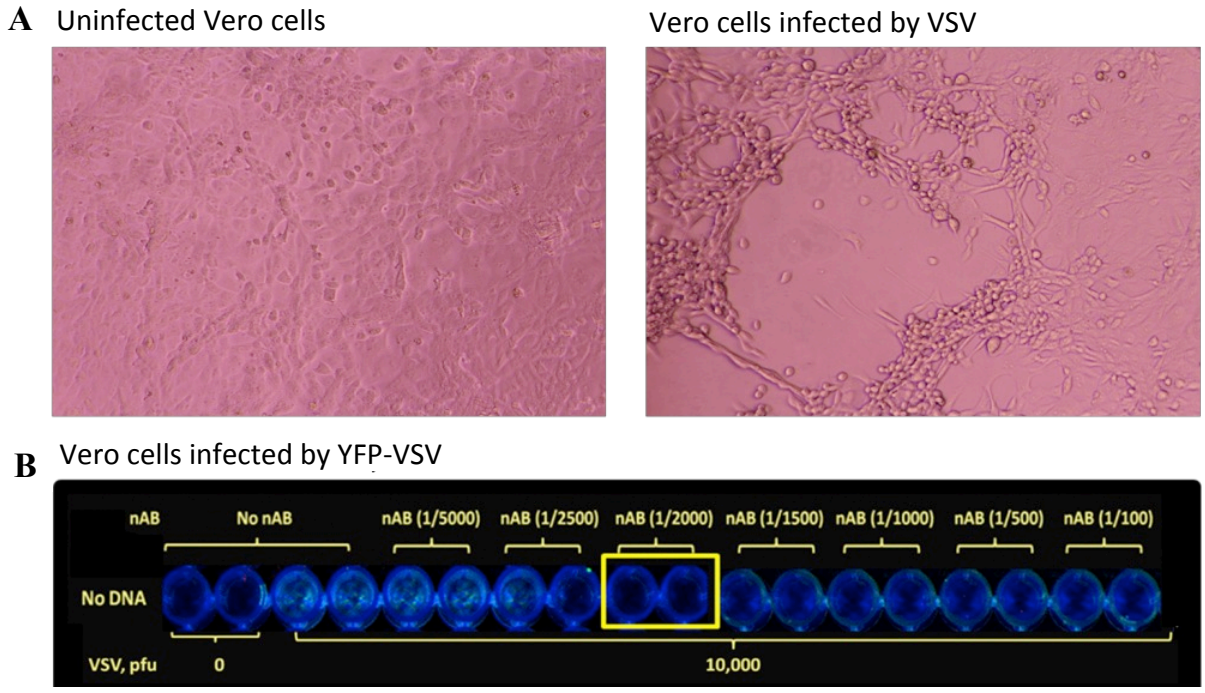

Figure 3.2: Rabbit serum titration for neutralization of vesicular stomatitis virus following a 24-hour incubation. (A) Brightfield images of a healthy Vero cell culture (left panel) and one infected by vesicular stomatitis virus (right panel). (B) Imaging of a 96-well plate with Vero cells and their YFP expression with different rabbit serum dilutions. When the virus is incubated with dilutions of $2,000\times$ or lower, it is completely neutralized and thus unable to infect the cells. Reproduced from Macmillan Publishers Ltd: Molecular Therapy – Nucleic Acids 3:e167, 2014 freely available under the terms of the Creative Commons Attributions License.

for the variable domain of the heavy chain. However, up to 80% of these are similar in sequence. This homology could explain why using only four aptamer sequences is sufficient for obtaining a blocking effect, as one aptamer could bind to a number of different antibody clones [154]. To determine the optimal concentration of aptamers for the plaque forming assay, we performed another titration experiment. Both VSV and anti-VSV antibodies were incubated with their respective aptamer pools varying from 1 to 10 fM concentrations. Two of the highest concentrations (1 and 10 μM) showed the best potency, whereas the shielding effect of aptamer concentrations below 10 nM dropped significantly (Figure 3.3).

The best aptamers were finally combined into a synthetic pool, incubated with their respective targets and then added to the monolayer of Vero cells. The results are presented in Figure 3.4. Incubation of the virus with the native DNA library led to 32% infectivity of Vero cells. This effect led us to believe that due to the polyclonal nature of the antibodies, it is better to have a variety of aptamers that could bind nAb variants. Pools for nAbs or VSV tested individually showed an increase of infection of 20%. The combination of pools for both targets, however, resulted in the highest increase, with 61% of additional plaques, suggesting a synergistic mechanism. Therefore, the best results are obtained when combining pools to achieve higher specificity and a larger number of different aptamers.

Since degradation of aptamers by nucleases results in their instability in serum, we modified our oligonucleotides by constructing their dimeric and tetrameric counterparts to increase their potency *in vivo* [155]. For this purpose, we generated dimeric and tetrameric aptamers, linked by an oligonucleotide bridge. These were constructed by bridging monomers using a single- or double-stranded DNA bridge, respectively (Figure 3.5). Each strand consisted of extremities that were complementary to forward and reverse primer-binding domains of aptamers. Some primer regions can participate in the folding of our aptamers, therefore having two different binding sites decreased the risk of disrupting the secondary structure that may be important in binding the target. The apparent dissociation constant for monomeric and dimeric pools remained similar (71$\pm$15 nM and

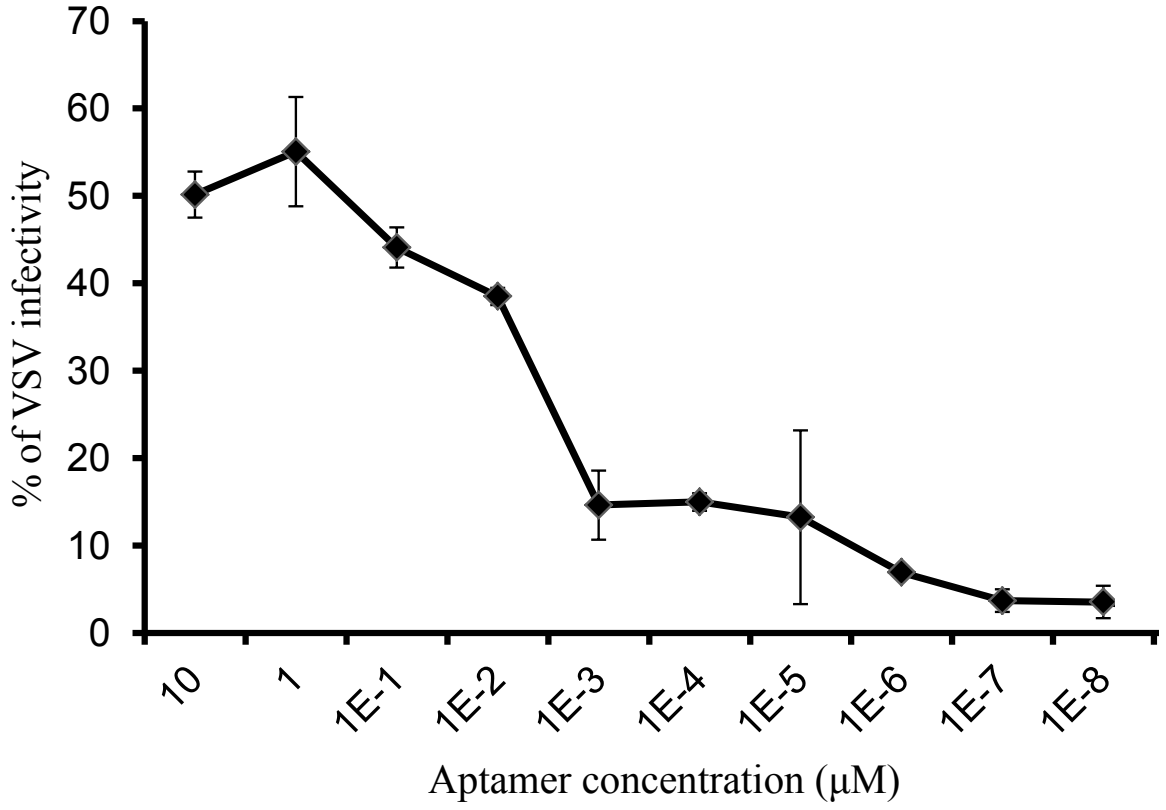

Figure 3.3: Titration of aptamer pools for optimal enhancement of virus infectivity. Anti-VSV and anti-nAbs aptamer pools were incubated with their respective targets and added to a monolayer of Vero cells. Viral infectivity was determined by a plaque forming assay and compared to a positive control, which consisted of virus without nAbs and was considered to be 100%. Adapted from Macmillan Publishers Ltd: Molecular Therapy – Nucleic Acids 3:e167, 2014 freely available under the terms of the Creative Commons Attributions License.

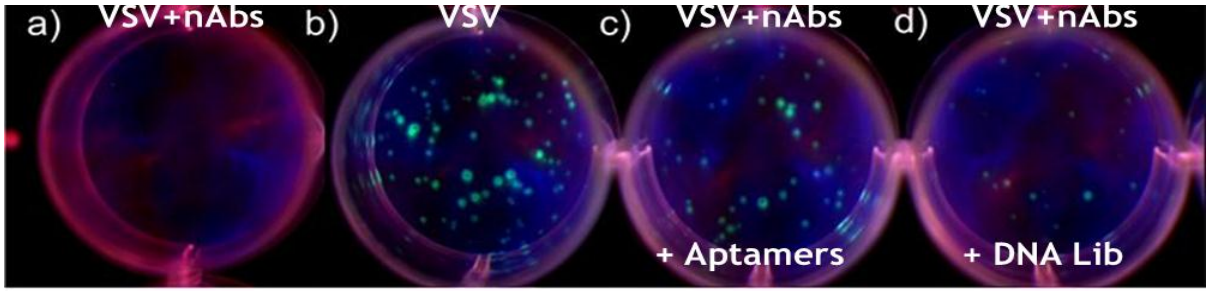

nAbs	nAbs Aptamers	VSV Aptamers	VSV	Infection (%)
+	-	-	+	0
-	-	-	+	100 ± 7
+	-	Pool	+	16 ± 2
+	Pool	-	+	20 ± 5
+	Pool	Pool	+	61 ± 3
+	DNA library	-	+	15 ± 1
+	-	DNA library	+	17 ± 2
+	DNA Library	DNA Library	+	32 ± 6

Figure 3.4: Plaque forming assay evaluating viral infectivity in presence of aptamers. Neutralizing antibodies were preincubated with or without anti-nAbs aptamers and were added to vesicular stomatitis virus preincubated with anti-VSV aptamers. Cells infected with (a) VSV and nAbs (0% infectivity), (b) VSV without nAbs (100% infectivity), (c) VSV with anti-VSV aptamers and nAbs with anti-nAbs aptamers, and (d) VSV and nAbs with DNA library. Adapted from Macmillan Publishers Ltd: Molecular Therapy – Nucleic Acids 3:e167, 2014 freely available under the terms of the Creative Commons Attributions License.

87±6 nM, respectively), whereas a fourfold decrease for the tetrameric pool (22±9 nM) was observed. The binding increase of the tetrameric construct could be explained by the increase of aptamer's avidity. In combination with the results obtained from plaque forming assays where we did not see a significant change of viral infectivity with the dimeric pool, we can assume that this construct did not bind well to its targets (Figure 3.5 B).

In order to mimic more closely an *in vivo* environment, we incubated aptamers binding to nAbs with whole, undiluted rabbit serum for 5 minutes. The short incubation time imitated the effect of introducing aptamers to blood-circulating antibodies. The mixture was then added to the solution of VSV and anti-VSV aptamers and was incubated for an additional hour, after which it was diluted for the plaque forming assay. With the use of anti-VSV dimers and tetramers, virus infectivity with VSV aptamers remained approximately the same, with a difference of ±2%. However, the use of dimeric and tetrameric forms for anti-nAbs aptamers resulted in an increase by 12 and 28% of viral infectivity, respectively. The combination of aptamer pools in a dimeric form did not have an increasing effect on VSV infectivity. Conversely, this pool combination with a tetrameric bridge increased the infectivity to 77% (Figure 3.5 B).

To elucidate possible reasons for obtaining this increase of infectivity, we hypothesized that the aptamers might have an effect on the aggregation of the virus, which could increase the number of infectious particles. Therefore, we performed an aggregation assay, which consisted of incubating both yellow and red fluorescent protein-expressing viruses with or without aptamers, followed by the addition of the mixture to the monolayer of Vero cells in a 96-well plate. Co-localization of the two kinds of viruses would indicate their aggregation, as they could both be infecting the cell simultaneously. Expression of yellow or red protein in cells was counted and averaged. Aggregation in the control sample, consisting of viruses without the aptamers, was 8±2%, which correlated with previously reported literature [156]. Incubating VSV with the pool of aptamers, either in their monomeric, dimeric or tetrameric state, resulted in a significant decrease of aggregation, with only 3,

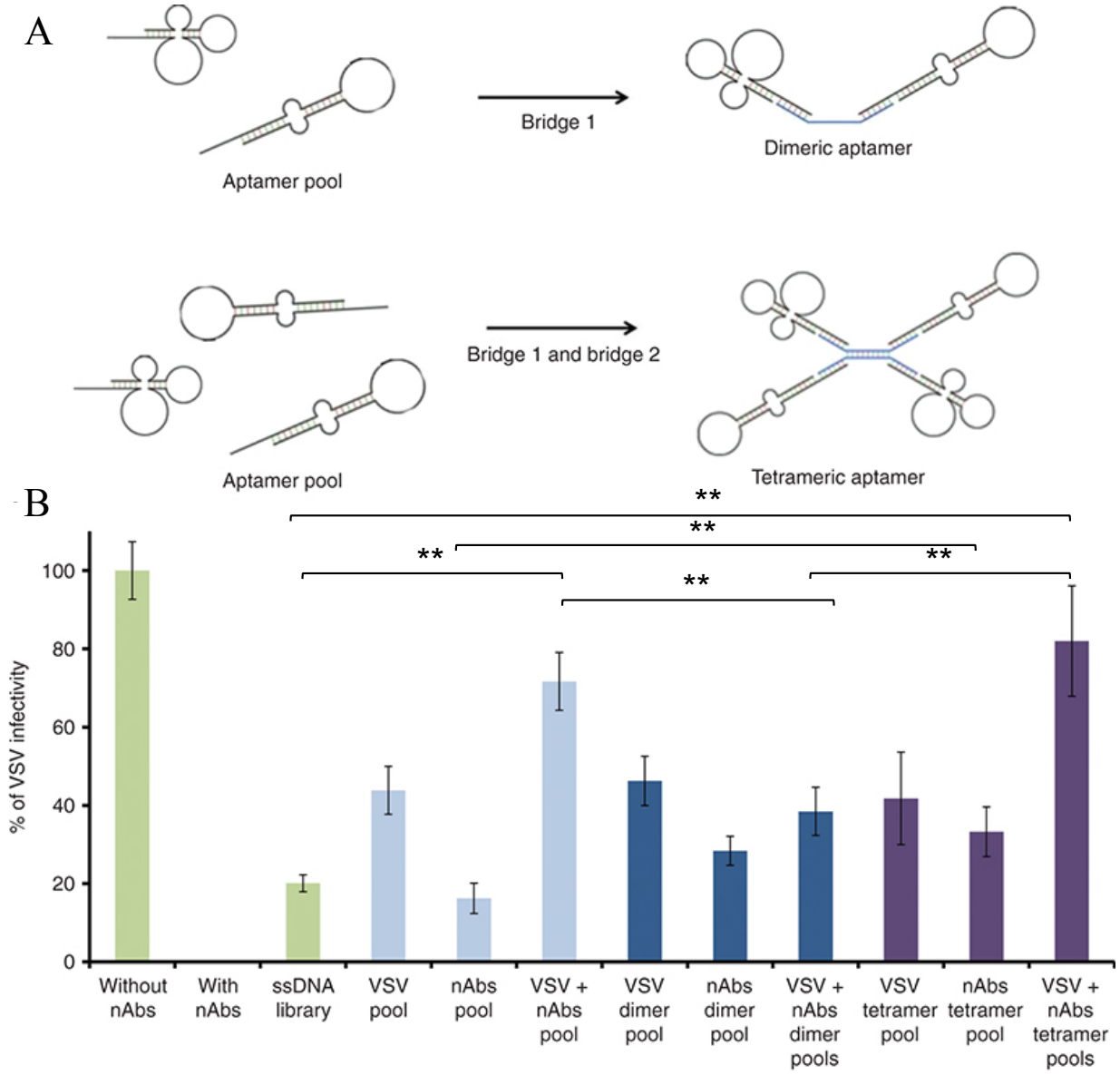

Figure 3.5: (A) A schematic showing the construction of dimeric and tetrameric aptamers. (B) Plaque forming assay results showing the infectivity of VSV with monomeric (light blue), dimeric (dark blue) and tetrameric (purple) aptamer pools in presence of neutralizing antibodies. (** = $p < 0.1$) Reproduced from Macmillan Publishers Ltd: Molecular Therapy – Nucleic Acids 3:e167, 2014 freely available under the terms of the Creative Commons Attributions License.

5 and 4%, of cells expressing both YFP and RFP (Figure 3.6 B). This decrease suggests that there may be a repulsion of viral particles from one another caused by the negatively charged nucleotides, which could also interfere with viral neutralization caused by anti-VSV antibodies.

Another factor that could explain the increase of viral infectivity may be the fact that these multivalent modifications increase the stability of aptamers in serum. The amount of aptamers after their incubation in human serum was analyzed using real-time PCR. Based on the standard curve, there was about five times less of the monomeric form after a 24-hour incubation period in serum (Figure 3.7 A). However, investigating the melting curve of various samples indicates that this loss is at least two times greater. It is clear that a significant portion of amplified products consists of smaller, degraded aptamers (Figure 3.7 B). We speculate that the absence of degraded dimeric and tetrameric aptamers is due to the fact that they became less accessible to exonucleases.

A different modification that was explored in our laboratory consisted of using biotinylated aptamers and incubating them with streptavidin in order to form tetrameric counterparts. However, this method did not prove to be successful as we did not observe a significant increase of infectivity in plaque forming assays.

We obtained neutralizing antibodies from mice immunized with VSV and tested our anti-VSV antibodies on mouse neutralizing antibodies. Although the viral infectivity was not augmented as much as it was with rabbit nAbs, we did observe on average 10% increase in plaque numbers. This led us to believe that *in vivo* experiments on mice might be successful. Furthermore, if the nAbs aptamers do not succeed in blocking the neutralizing effect due to the difference and great abundance of nAbs, we envisaged that the anti-VSV aptamers would be more universal. Thus, we carried out our *in vivo* experiments with groups of mice which were injected with anti-VSV aptamers alone, anti-nAbs aptamers alone, or both. As we used virus expressing the firefly luciferase, we expected to see luminescence once the virus infected the tumour site. This result was observed in mice

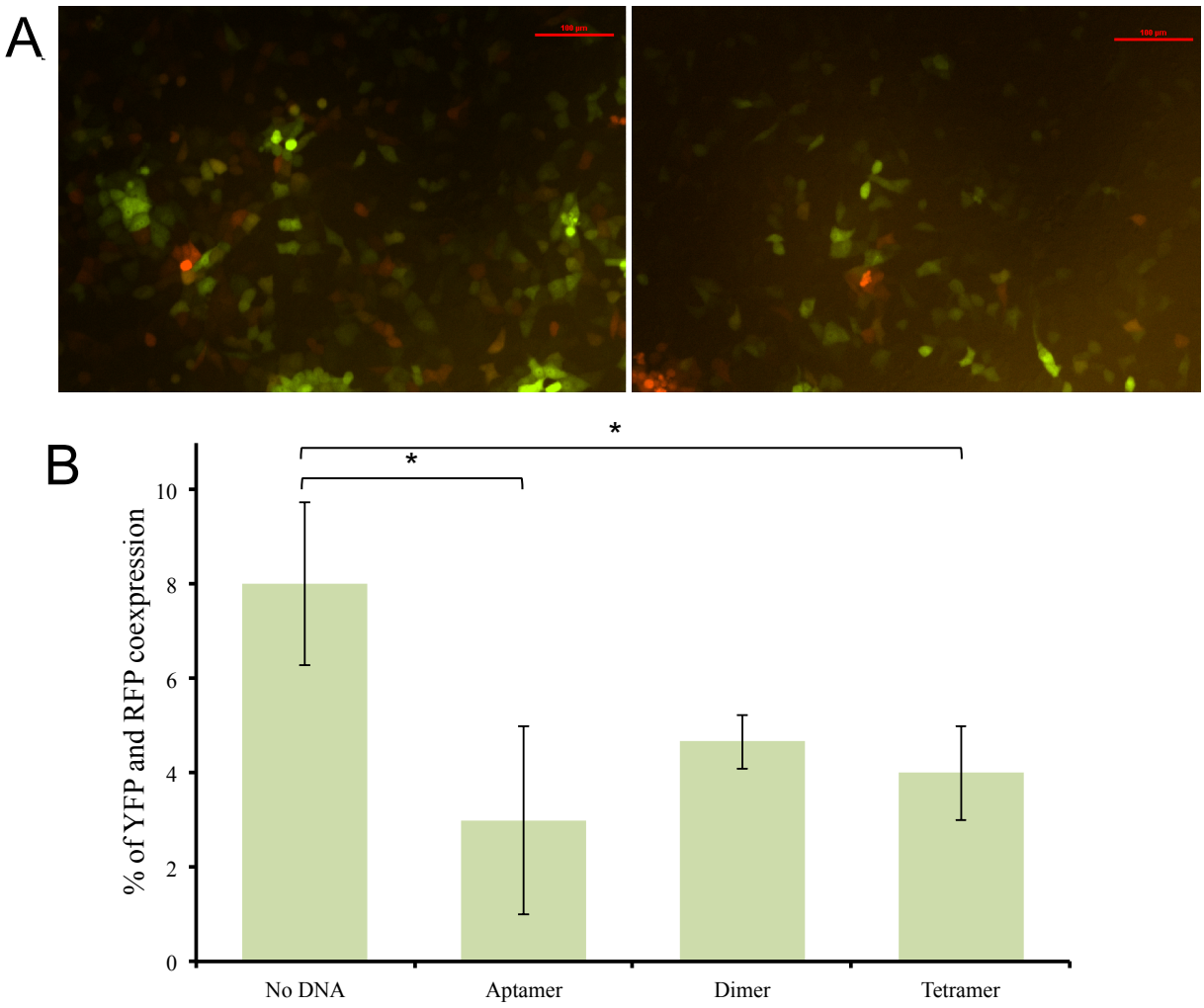

Figure 3.6: (A) Overlay of YFP and RFP expression in Vero cells infected without and with aptamers. (B) Aggregation percentage in cells infected with virus alone or virus incubated with monomeric, dimeric, or tetrameric aptamers. Reproduced from Macmillan Publishers Ltd: Molecular Therapy – Nucleic Acids 3:e167, 2014 freely available under the terms of the Creative Commons Attributions License.

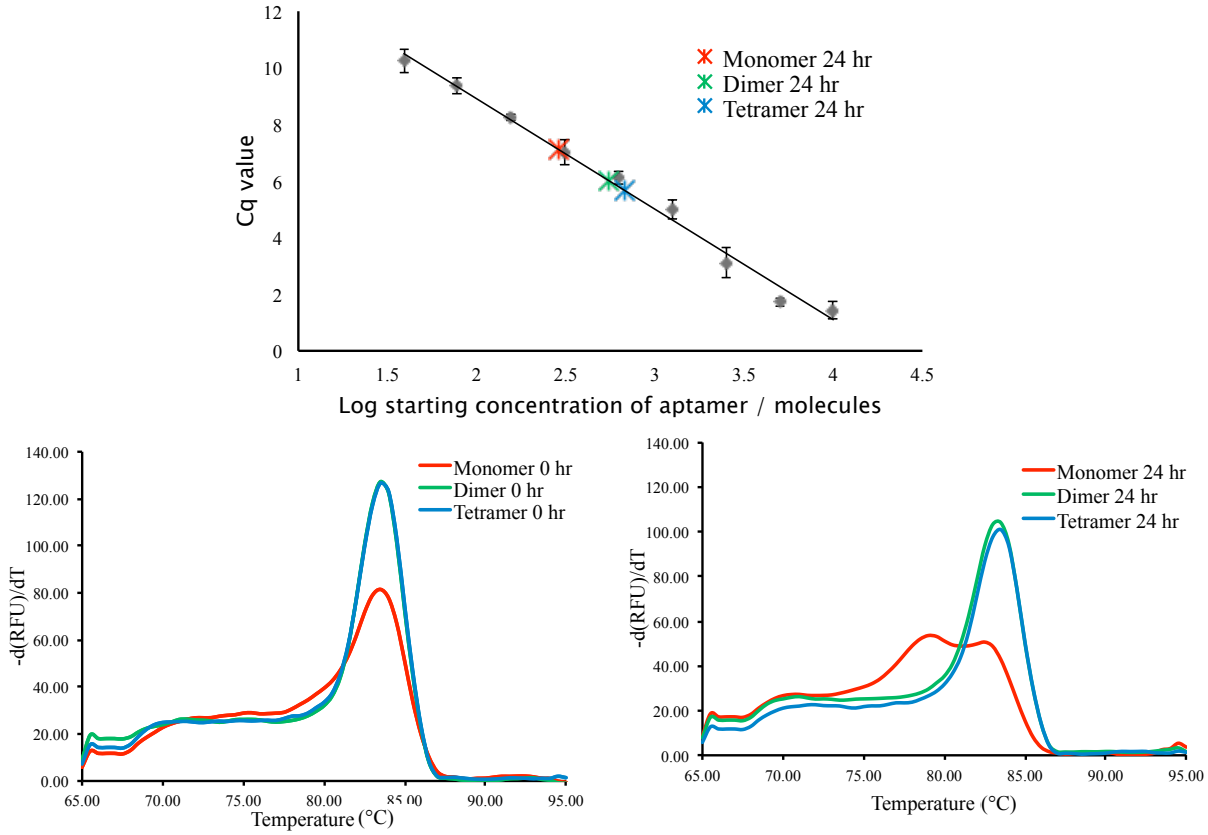

Figure 3.7: Real-time PCR (qPCR) showing degradation of monomeric, dimeric and tetrameric aptamers. (A) Standard curve showing the remaining concentration of different aptamer pools, and (B) melting curve of monomeric, dimeric and tetrameric aptamers before and after a 24-hour incubation in serum. Reproduced from Macmillan Publishers Ltd: Molecular Therapy – Nucleic Acids 3:e167, 2014 freely available under the terms of the Creative Commons Attributions License.

that were not immunized against VSV—the treatment worked well and by the end of day 3 the tumours were significantly reduced. However, immunized mice, which were expressing high doses of antibodies, did not have any luciferase expression at their tumour site, indicating that the virus did not reach the cancerous cells. The minimum number of cells expressing luciferase that can be detected with a live imaging software is approximately 1×10^3 cells [157, 158]. Moreover, when the tumour is infected, it takes several hours for the virus to replicate and produce a high enough copy number to be detectable. For these reasons, we extracted the tumours after sacrificing the mice and carried out plaque forming assays—no plaque formation was detected.

Since our tetrameric aptamers proved to have a better shielding and protecting effect, we attempted a second *in vivo* trial with these modified oligonucleotides. Moreover, we hypothesized that one of the reasons why the assays did not work was due to DNA stability. Therefore, the tetrameric DNA would be more efficient in mice. IgG concentrations in rabbit serum can be as high as 5-20 mg/ml, and up to 12% of these can be immunogen-specific [154]. We hypothesized that by doubling the amount of aptamers we might increase blocking and shielding effects. Even though the oligonucleotides were again well tolerated, there was no difference in tumour luminescence of the immunized groups (Figure 3.8), nor were any plaques formed after a post-mortem plaque forming assay.

Even though the aptamers worked well *in vitro*, viral protection and shielding was not achieved *in vivo*. This might be due to a number of reasons. Aptamers might be binding non-specifically to different components in blood. Furthermore, the aptamers for nAbs were selected to rabbit serum. Even though here was a blocking effect in mouse serum, it was not optimal. Therefore, in order to obtain a successful delivery of the virus to tumour sites *in vivo*, "personalized" aptamers might be the key as they should bind with high efficiency and specificity to the host's own nAbs.

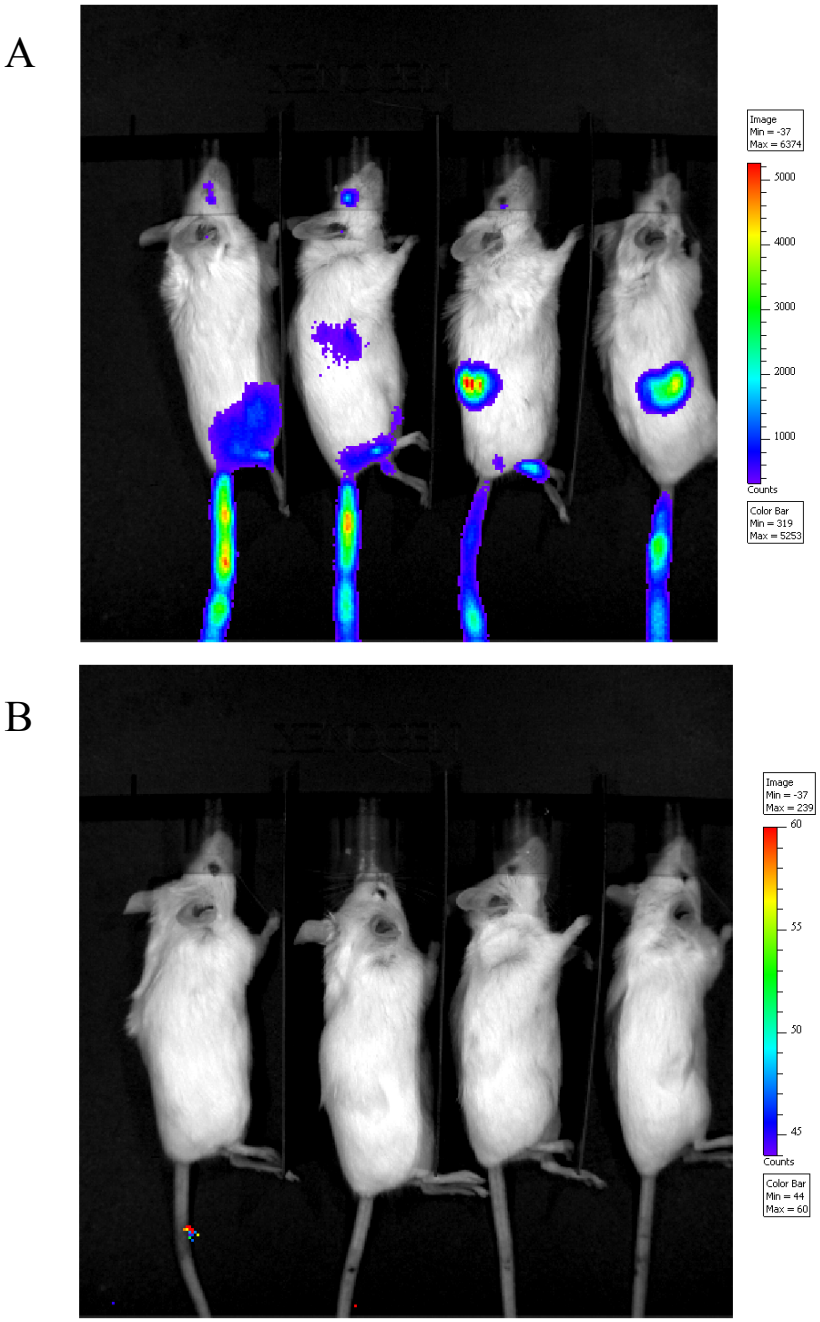

Figure 3.8: Mice with CT26.LacZ subcutaneous tumours injected with anti-VSV and anti-nAbs tetrameric aptamers and firefly luciferase expressing VSV; (A) not immunized prior to the treatment and (B) immunized against VSV by receiving two doses of VSV prior to the treatment.

3.4 Conclusion

In this chapter, we used aptamers which were selected for vesicular stomatitis virus and its neutralizing antibodies in order to obtain a blocking and shielding effect *in vitro*. We applied a plaque forming method to determine the viral infectivity increase in presence of nAbs. Furthermore, by modifying our aptamers in order to make their multivalent counterparts, we were able to achieve a higher increase of viral infectivity in presence of nAbs. This proof-of-principle method demonstrated the possibility of using aptamers in combination with oncolytic viruses in order to achieve more efficient therapeutics.

In vivo assays with aptamers did not prove to be successful, potentially due to DNA degradation or ineffective binding of blocking aptamers. In order to potentially improve this form of therapy, anti-nAbs aptamers should be selected for neutralizing antibodies isolated from the same mouse that will be injected with the VSV. This personalized approach ensures that the aptamers bind with high affinity and specificity to the same nAbs that are responsible for the neutralization of the injected virus.

Chapter 4

Aptamers for enhancing delivery of vesicular stomatitis virus to cancer cells

4.1 Background

Vesicular stomatitis virus is a potent oncolytic virus taking advantage of defective interferon pathways in tumour cells. However, $VSV\Delta51$, as well as the wild type and the majority of other VSV mutants, lack a great selectivity for cancer cells. Therefore, the virus can infect normal cells, but will not be able to replicate and lyse them as effectively [99].

In order to improve viral selectivity, we envisioned the development of an aptamer that would target specifically cancer cells. Aptamer-nanoparticle conjugates have been used in other laboratories to target cells for an efficient delivery of such agents as liposomes, micelles and polymeric nanoparticles [159–161].

Here, we demonstrate the application of such bifunctional aptamers for targeting of a cancer cell line, by selecting aptamers and conjugating them to our previously developed

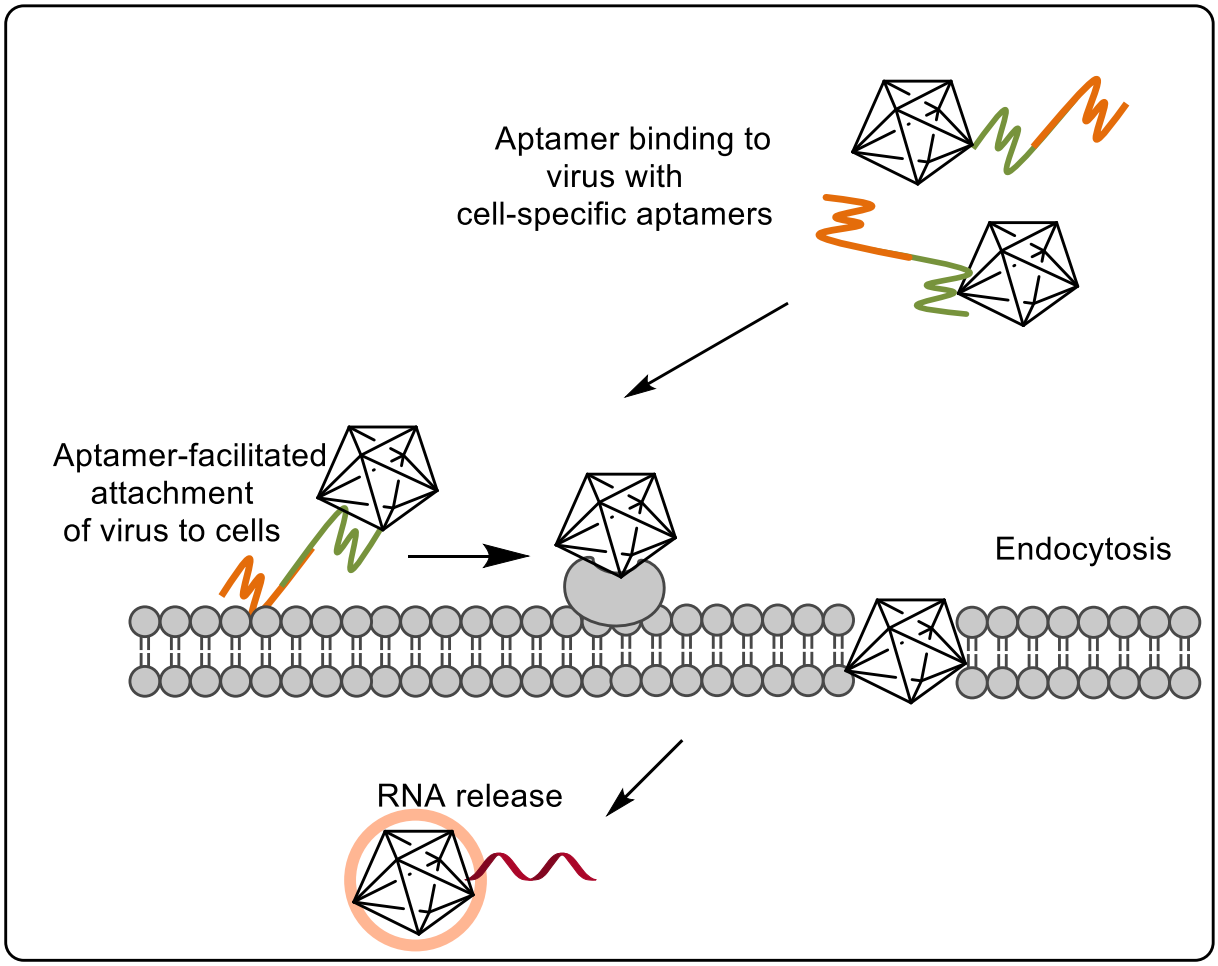

Figure 4.1: A schematic of aptamer-facilitated viral delivery to targeted cancer cells. A multifunctional aptamer binding to both the virus and the targeted cell would facilitate cancer cell-specific viral infection.

anti-VSV aptamers. We decided to use the CT26.CL25 cell line (CT26 hereafter), an undifferentiated colon carcinoma cell line. When these cells are administered subcutaneously to mice, they develop lethal tumours; this model is used for testing immunotherapy protocols, including the efficiency of oncolytic viruses *in vivo* [92, 97].

The design of bifunctional aptamers was applied to a modified plaque forming assay, which consisted of removing the virus after a reduced incubation time in order to examine aptamer's ability to target and deliver the virus to cancer cells. Our results showed that the use of anti-VSV and CT-26 aptamers conjugated with a tetrameric bridge increased the ratio of washed to unwashed plaques by twofold, making viral delivery to cancer cells more efficient.

4.2 Materials and methods

4.2.1 DNA library and primers

The DNA library used for this aptamer selection was 100 nucleotides long and consisted of 60 nucleotide long partially-defined internal region, $(XY)_4N_4(XY)_5N_3(XY)_5N_4(XY)_5N_3(XY)_4$ where X = 45:5:45:5, Y = 5:45:5:45 and N = 25:25:25:25 for ratios of A/C/G/T. The randomized region was flanked by 20-nucleotide long primer binding sites. The forward primer (5' - CTC CTC TGA CTG TAA CCA CG - 3') was labeled with Cy5 or 6-FAM fluorophores, and the reverse primer (5' - GGC TTC TGG ACT ACC TAT GC - 3') was labeled with a phosphate group at the 3 position for exonuclease digestion. All oligonucleotides were ordered from Integrated DNA Technologies (Iowa, USA).

4.2.2 Anti-CT26 aptamer selection

CT26 cells were plated in a 12-well plate at 0.4×10^6 cells per well and incubated until 90% confluency has been attained. The first round of selection was done with 1 μM of native

ssDNA library. The cells were incubated with the DNA at 37°C for 10 min, followed by a washing step with Dulbecco's phosphate buffered saline (DPBS) solution. The number of washes was increased after round 2 to two washes per selection, and after round 7 to three washes in order to make the selection process more stringent. We then added calcium and magnesium-free DPBS to the cellular monolayer and incubated at 37°C for 10 min. Detached cells and DNA were then collected from wells and stored at -20°C until ready for amplification. Symmetrically amplified DNA was separated on a 3% agarose gel, purified with a DNA gel extraction kit (Thermo Scientific, Massachusetts, USA), and digested with a lambda exonuclease (New England Biolabs, Massachusetts, USA) to generate single-stranded DNA. For rounds 2 to 10, 150 nM of ssDNA purified from the previous round of selection was used. After round 8, a negative selection was introduced, where cells were first incubated in a well with Vero cells at 37°C for 10 min. The supernatant was then recovered and subjected to a positive selection on CT26 cells, as described above.

Once 10 rounds of selection were completed, the binding of aptamer pools was analyzed. Purified ssDNA (100 nM) labeled with Cy5 at the 5' position was incubated with 5×10^5 cells for 10 min at 37°C. These were then spun down for 5 min and the supernatant was removed. Cells were resuspended in DPBS and subjected to flow cytometry analysis. Pools 8 and 9 showed the highest affinity for the targeted cells and were thus selected for high throughput sequencing (HTS).

For HTS, the pools were prepared by attaching an 8-base barcode to the 5' end of the aptamers, amplified by symmetric PCR, purified using a gel purification kit and finally combined with 13 other barcoded pools from other lab members. The DNA was sequenced using Illumina's MiSeq paired-end 2×150 bp platform, which resulted in 2,267,916 sequences that contained our specific barcode. These were analyzed using Galaxy, a web-based data analysis tool for grouping and ranking of sequences, as well as a tool for identification of sequence similarities, Multiple Em for Motif Elicitation (MEME) [162]. Selected sequences were ordered from IDT and analyzed by flow cytometry to determine their binding poten-

tial to both CT26 and Vero cell lines. The sequences that seemed to have high binding and selectivity to CT26 cells during the initial screening by flow cytometry were ordered with a Cy5 or 6-FAM labels and were then titrated with concentrations ranging from 32 to 750 nM in order to measure their dissociation constants to both cell lines.

4.2.3 Microscopy analysis

CT26 and Vero cells were plated in a 4-well chamber slide (ibidi, LLC, Germany) with 5×10^4 cells per well. Once the cells reached 90% confluency, the media was removed and replaced with 200 nM of 6-FAM- or Cy5-labeled aptamer. Following a 10-min incubation at 37°C, the supernatant was removed and the cells were washed with serum-free DMEM (20 min) and with DPBS (5 min). Buffer and chamber wells were then removed from the slide, the cells were mounted with Vectashield mounting media with DAPI (Vector Laboratories Inc, California, USA), and covered with a glass slip (Fisherbrand, Fisher Scientific, New Hampshire, USA). For membrane-staining, DiO membrane dye (3,3'-dioctadecyloxacarbocyanine Perchlorate, Thermo Fisher Scientific, Massachusetts, USA) was used at a concentration of 1 mM and incubated with CT26 cells for 20 min, followed by the aforementioned slide preparation. Microscopy images were obtained with a Nikon A1 MP confocal microscope (Tokyo, Japan).

4.2.4 Design and analysis of multivalent aptamers by plaque forming assays

We designed three bridges partially complementary to the primer-binding sites of anti-VSV and anti-CT26 aptamers and complementary to each other in the central region; the latter consisted of three different lengths: 20, 30 and 40 bp (Table 4.1). Pool of anti-VSV aptamers (M50, Z28, S31, S37 and S39), anti-CT26 aptamers (CT1, CT2, CT3, CT4, CT5, CT6, CT8, CT51, and CT78) and both strands of each bridge were mixed in equimolar

amounts and annealed by heating at 95°C for 2 minutes, followed by a gradual cooling from 75°C to 40°C. Each construct was then tested with a plaque forming assay to evaluate the ability of the bridge to bring the two targets together.

For the plaque forming assay, Vero cells were plated at a density of 2.5×10^5 cells/well in 1 ml of DMEM containing 10% fetal bovine serum and incubated overnight at 37°C. The following day, 100 PFUs of YFP-VSV were incubated with or without 1 μM of aptamers (bridged or non-bridged) in serum-free medium for 1 hour at 37°C. The solution was then added to the monolayer of cells and incubated for 10, 30 or 45 min, after which the media was removed and washed two times with fresh serum-free medium. After another 50, 30 or 15 minutes of incubation (overall incubation time of 1 hour), a layer of 0.5% agarose (Invitrogen, California, USA) with Dulbeccos modified Eagle medium, supplemented with 10% fetal bovine serum was added, and the plates were left to incubate for 24 hours. The following day, the plates were imaged and the plaques were counted.

Table 4.1: List of bridge sequences used for the design of tetrameric aptamers.

Name[a]	Sequence (5'–3')[b]	Length[c]
S Bridge	GGTTACAGTCAGAGGAGTTAACACAACCCCAATTGGCTTCTGGACTACC	13
cS Bridge	GGTTACAGTCAGAGGAGTTTTGGGGTTGTGTTTTGGCTTCTGGACTACC	13
M Bridge	GGTTACAGTCAGAGGAGTTAACACAACCCCAAAACACAACCCCAATTGGCTTCTGGACTACC	26
cM Bridge	GGTTACAGTCAGAGGAGTTTTGGGGTTGTGTTTTGGGGTTGTGTTTTGGCTTCTGGACTACC	26
L Bridge	GGTTACAGTCAGAGGAGTTAACACAACCCCAAAACACAACCCCAAAACACAACCCCAATTGGCTTCTGGACTACC	39
cL Bridge	GGTTACAGTCAGAGGAGTTTTGGGGTTGTGTTTTGGGGTTGTGTTTTGGGGTTGTGTTTTGGCTTCTGGACTACC	39

[a] S = Small, M = Medium, L = Long, c = complementary
[b] Magenta: region complementary to the 5' domain of aptamers; Green: region complementary to the 3' domain of aptamers.
[c] Length (bp) is defined for the central region of the bridge only.

4.2.5 Statistical analysis

All experiments were performed in triplicate. Statistical analysis was done using a one-way ANOVA and Tukey post test. A p-value below or equal to 0.05 was considered to be statistically significant and indicate significant difference.

4.3 Results and discussion

The aptamer selection against CT26 cells was carried out in order to ameliorate the delivery of the vesicular stomatitis virus by bridging the anti-VSV aptamers to the tumour-binding aptamers. To achieve a higher specificity, Vero cells were used for negative selection for rounds 8 to 10. Moreover, for this selection, we used a more structured library (R*Y*) that was designed by the Liu group. In their work, they showed that, by using this library, they were able to select for aptamers with a higher affinity and selectivity due to the "predetermined" nucleotides that were more statistically favourable [13].

Even though asymmetric amplification is beneficial in reducing the number of purification steps, we have encountered some issues in previous selections. Since our library is randomized, the chances of obtaining sequences that are partially complementary to the primers are fairly high. Upon asymmetric amplification of aptamers, we observed the incorporation of multiple forward-primer sequences, marked with a tail-like trace on the gel. Therefore, we needed to include a gel purification step of our 100 nucleotide base pair product. In order to increase the yield of this purification step, we opted for symmetric amplification, followed by an exonuclease digestion of the phosphate-labeled anti-sense strand [163]. The increased length of our library (100 nucleotides) was also more beneficial during the gel purification step, resulting in a higher recovery yield.

Another modification that we introduced to our aptamer selection protocol was the way we identified the aptamer sequences. Instead of going through the cloning process and

picking colonies containing aptamer clones, we opted for high throughput sequencing. As it has been demonstrated by the Shutze group, high affinity sequences can be identified as early as in round three [18]. Therefore, we only performed ten rounds of selection and did not attempt to achieve a maximal binding affinity of the pool, but chose the highest affinity pools among the ten. These were then combined and labeled with a specific barcode. The HiSeq system has the potential to decode up to 176 Gb (gigabases), enabling us to combine several different pools, simply by differentiating them with barcodes. In our case, sequencing of 14 individually-barcoded aptamer pools generated a total of 15,944,766 sequences, which is another advantage of using this platform, as we obtain a much more detailed view of aptamer pools. However, analysis of generated data can also be quite challenging and overwhelming due to the complexity of the raw data and requirement for some level of expertise in the computational field [164].

For the analysis of one aptamer pool's 2,485,790 sequences, we used the publicly available Galaxy software [165–167]. Although our selection started with a 100-nucleotide library, we found that some retrieved sequences were only 80 nucleotides long. Since we work simultaneously with both of these libraries, we attributed the presence of these oligonucleotides to a cross-contamination that occurred either in our laboratory or in IDT during their synthesis. Table 4.2 is representative of the top ten sequences (from CT1 to CT10) that had the highest abundance in the aptamer pool selected for CT26. These abundances are lower than reported by the Shutze group; we attributed this decrease in abundance to the complexity of our target, which will generate a higher number of binding aptamers than if it were a single purified protein (e.g. streptavidin) [18].

Aptamers that have the highest affinity may share a similar motif, but may not necessarily have the exact same sequence. Therefore, not one of these motif-containing aptamers would be the most abundant in the pool. For this reason, we used a motif search programme, MEME, to identify 20 of the most common patterns in 1000 of the most abundant sequences of the pool [18, 162, 168]. The search identified mostly the top se-

Table 4.2: List of aptamer sequences obtained by high throughput sequencing and their overall abundance in the pool

Name	Number of reads[a]	Abundance (%)
CT1	159026	6.4
CT2	5963	0.24
CT3	3840	0.15
CT4	3321	0.13
CT5	2610	0.10
CT6	2397	0.096
CT7	1493	0.060
CT8	1207	0.049
CT9	712	0029
CT10	572	0.023
CT51	234	0.0094
CT78	163	0.0066

[a] Total number of sequences in pool = 2,485,790

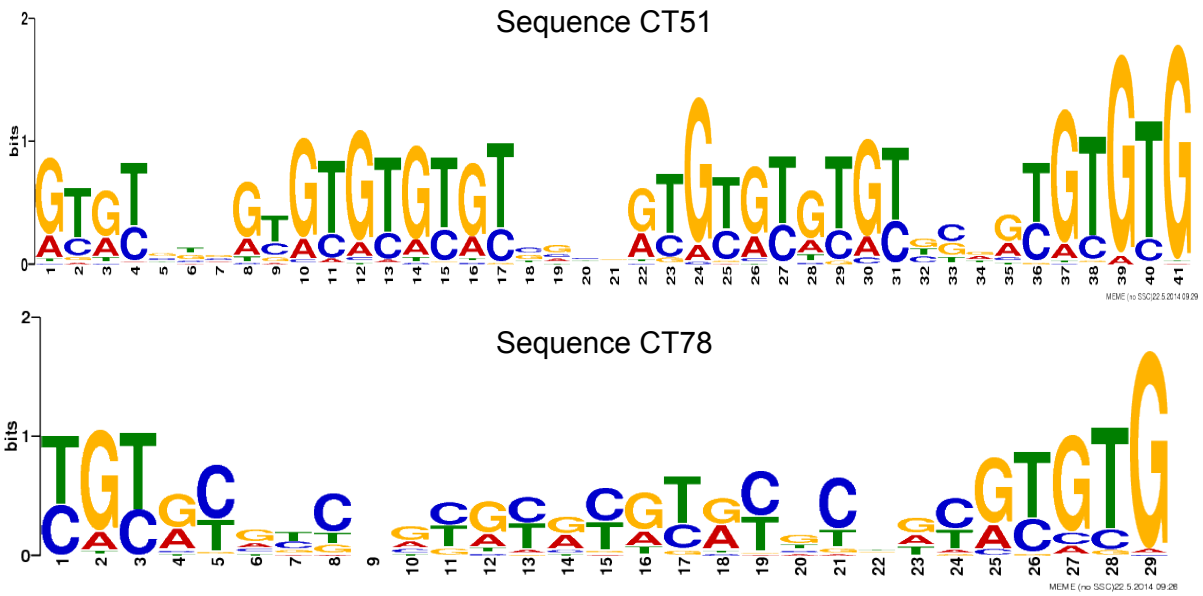

Figure 4.2: Graphical representation of two motifs that were identified in the sequenced anti-CT26 aptamer pool, for aptamer sequences CT51 and CT78.

quences (based on their abundance) that had only minor differences and were probably generated due to PCR mutations; however, there were also two patterns that were highly present among different sequences but only ranked as numbers 51 and 78 in abundance (Figure 4.2). A pool could contain a group of aptamer sequences that share a similar pattern and compete with each other for binding to the target. These two were also, among the total of nine sequences, chosen for synthesis and further analysis. Among those, seven were part of the ten most abundant ones; sequences CT7, CT8 and CT9 were excluded as they shared motifs with higher-ranked aptamers. Finally, CT2 and CT78 had the highest affinity for CT26, as well as specificity; binding of CT2 to Vero cells was minimal and thus we were unable to calculate the K_d for this interaction (Table 4.3).

Synthetic aptamers were amplified in order to produce their labeled counterparts and analyze their binding affinity to CT26 cells. Even though they all had higher mean fluorescence when compared to the library, some did prove to be better binders (Figure 4.3). Out of the nine candidates, we selected five aptamer sequences and ordered them with a Cy5

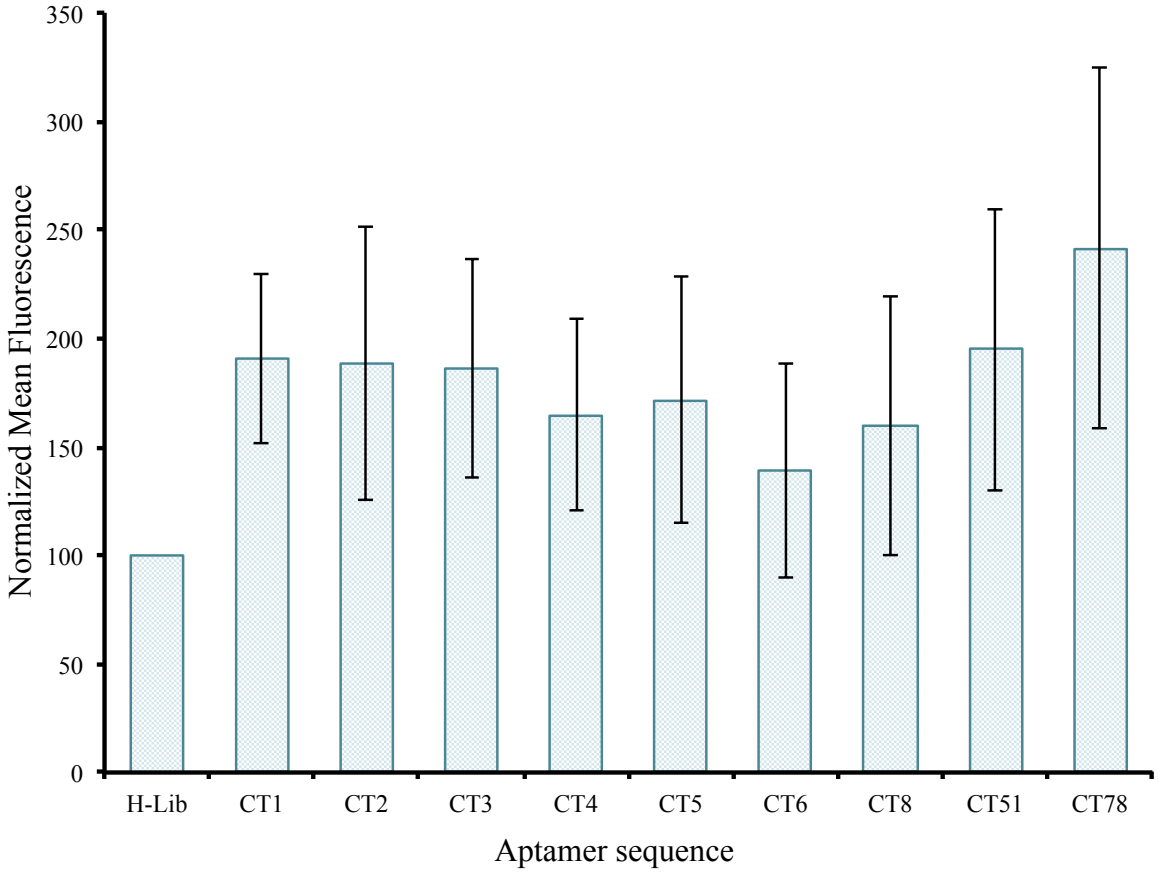

Figure 4.3: Flow cytometry analysis of selected aptamers after analysis of high throughput sequencing data. The analysis was done by incubating 300 nM of Cy5-labeled DNA with 1×10^5 CT26 cells and washing one time with DPBS.

label on their 5' end for further analysis. Although aptamer sequence CT1 was the most abundant in our pool, making up more than 6% of total sequences, we found that it was also highly abundant in other aptamer pools that contained different barcodes and were sequenced at the same time. We suspected that this sequence was very promiscuous and able to bind to many targets and/or was a contamination present in one of our reagents, in low abundance. To date, the source of the sequence has not been identified, but we did confirm its promiscuity, as it proved to have relatively low dissociation constants for both cell lines. Along with this aptamer, sequences CT3 and CT5 also had poor selectivity for the target of interest (Table 4.3).

Table 4.3: List of aptamer sequences selected for CT26 and their dissociation constants to CT26 and Vero cell lines.

Name	Sequence (5'–3')[a]	K_d CT26 (nM)	K_d Vero (nM)
CT1	fTGACCCGAGATTCTAGTGATTGCTTGTTCGGTATGTTCGcr	123	68
CT2	fTGTGCCAAAGAGAGTGGTGGGGGGGTGGGCGGAACTCGCGcr	178	>1000
CT3	fACGTATGTAGACGCCTACGTATCTCGGATGTGTGTTCTGATGTGCACGTTTTATGTGTAGcr	527	425
CT4	fGCGTATGTAGACATGCTTGTATCTCGCGTGGGTATTGAGACGTATGCGCCGCGCGTGTGTcr	N/A	N/A
CT5	fGCATACGTACCAATGCACATGTGGAATGTAGACGCAGAAATGCGTAGATGGTATGTGCGCcr	107	98
CT6	fCCATCACCCTATTATCTCATTATCTCGTTTTCCCTATGCGcr	N/A	N/A
CT8	fGGGACCTATCAGGCGATGTGAAAACTCTTATACCACTGGcr	N/A	N/A
CT51	fGCCTGTACGGCGAAGAGTCCCCCCGATGTGTGTGCAGGGATGCGTGTGTTGTGCGCTCGGcr	N/A	N/A
CT78	fCAGGGTACGTGTACGCGTGTACTGCACGTGTGTGTTGCCAGGCCGACGTGTGATGTGCGGcr	195	1600

[a] f, ctcctctgactgtaaccacg (sequence of the forward primer); cr, gcataggtagtccagaagcc (reverse-complement of the reverse primer).

Binding of the two aptamers with high affinity and specificity was visualized with confocal microscopy. Figure 4.4 is representative of the binding of FAM-labeled CT78 aptamer to CT26 cells, as well as two controls: a non-specific aptamer with CT26, and the CT78 aptamer with Vero cells. A distinct fluorescent pattern around the cells is indicative of aptamer binding to the surface of the cells (Figure 4.4 D). However, for the CT2 aptamer, we did not observe this pattern, but the dye was spread inside the cell, indicating possible internalization of the oligonucleotide (data not shown).

We designed three different bridge constructs with the central, double stranded region composed of different sizes - 13, 26 and 39 base pairs, using a template of a construct that was previously developed in our laboratory [139, 169]. This middle region was flanked by parts that were partially complementary to the primer-binding sites of both anti-VSV and anti-CT26 aptamers. Both of these types of aptamers were mixed in equimolar amounts to the bridge in order to obtain the desired construct, which had a theoretical linear length of 4.4, 8.8 and 13 nm, respectively. Although we were unable to control the annealing location of aptamers, since they all shared the same primer-binding sites, we assumed that the majority of constructs contained both types of aptamers as they were added in equal parts. This will be tested by capillary electrophoresis, as this instrument will allow us to control the separation temperature inside the capillary and should not lead to the separation of complementary DNA strands.

Each construct was tested using a plaque forming assay. Briefly, multimeric aptamers were incubated with the virus prior to adding the solution to the monolayer of CT26 cells in a 12-well plate. The virus was allowed to infect the cells for 10 or 45 minutes and was then washed away with serum free media. Non-washed wells were used as a positive control. The cells were incubated overnight and the plaque formations were counted the following day. Data was analyzed by calculating the ratio of plaques formed for washed samples to unwashed ones for each assay; therefore, a higher ratio indicated higher infectivity after washing the virus away (Figure 4.5). The ratio for the medium and long bridges was higher

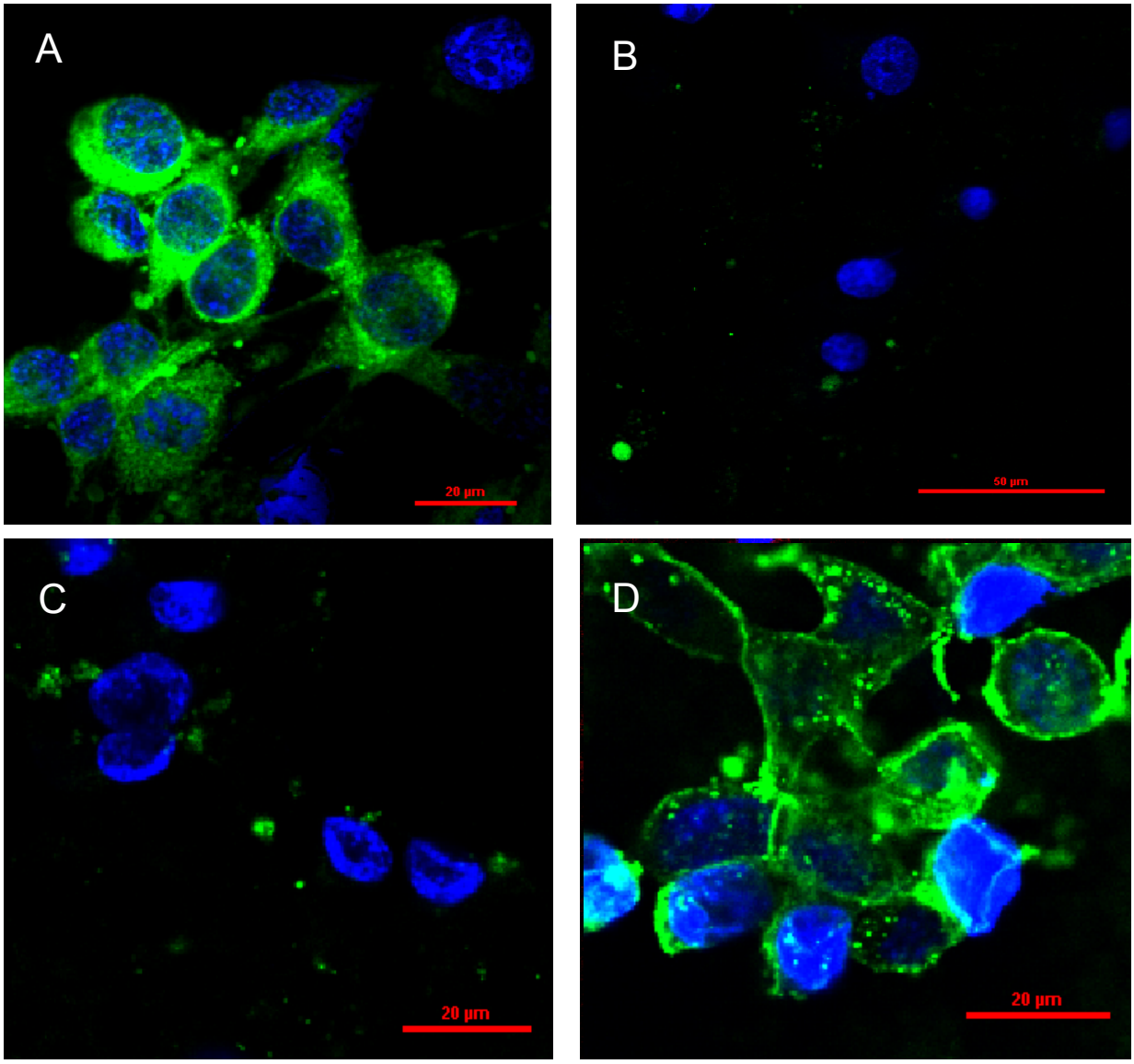

Figure 4.4: Confocal fluorescence microscopy images of live cells showing DAPI to stain the nuclei and A) CT26 cells stained with DiO membrane dye; (B) Vero cells incubated with FAM-labeled CT78 aptamer; (C) CT26 cells incubated with a non-specific FAM-labeled oligonucleotide; and (D) CT26 cells incubated with FAM-labeled CT78 aptamer.

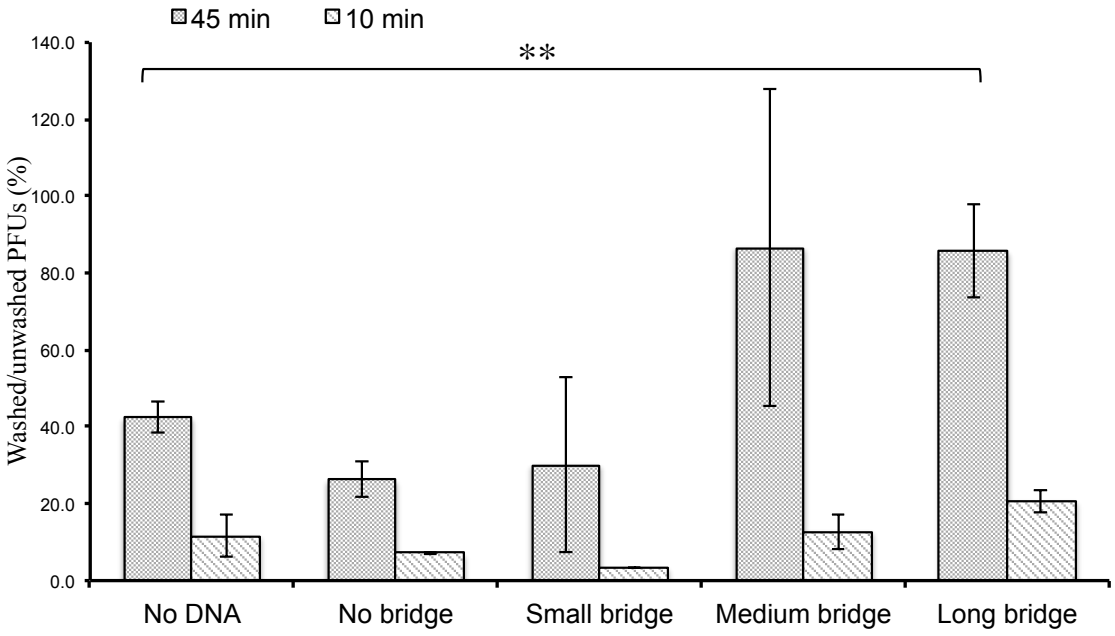

Figure 4.5: Plaque forming assay of tetrameric aptamers using small, medium and long bridges incubated with VSV. The mixture was added to a monolayer of CT26 cells, incubated for 10 or 45 minutes, and then washed away. The bars represent the ratio of number of plaques of washed to unwashed cells. (** = $p < 0.1$)

when the virus was allowed to infect the cells for 45 minutes, whereas there was no difference when the virus was washed after 10 minutes. The small bridge did not have an effect on the increase of viral infectivity. This could be attributed to the fact that this bridge was too short, and thus the two, relatively large targets, were not able to bind simultaneously. The shortness of the bridge is also responsible for this construct's low melting temperature (47°C), which could also contribute to the lack of this aptamer's effectiveness — at 37°C, the construct may not be fully annealed. Therefore, for further experiments, we decided to use medium and long bridges in order to form the tetrameric aptamers.

In order to ensure that the observed effect was not caused by the bridge alone, we generated a tetrameric construct using a non-specific pool of aptamers that was previously selected for vaccinia virus (NV2, NV6, NV14, NV51) by Dr. Anna Zamay [80]. The use of

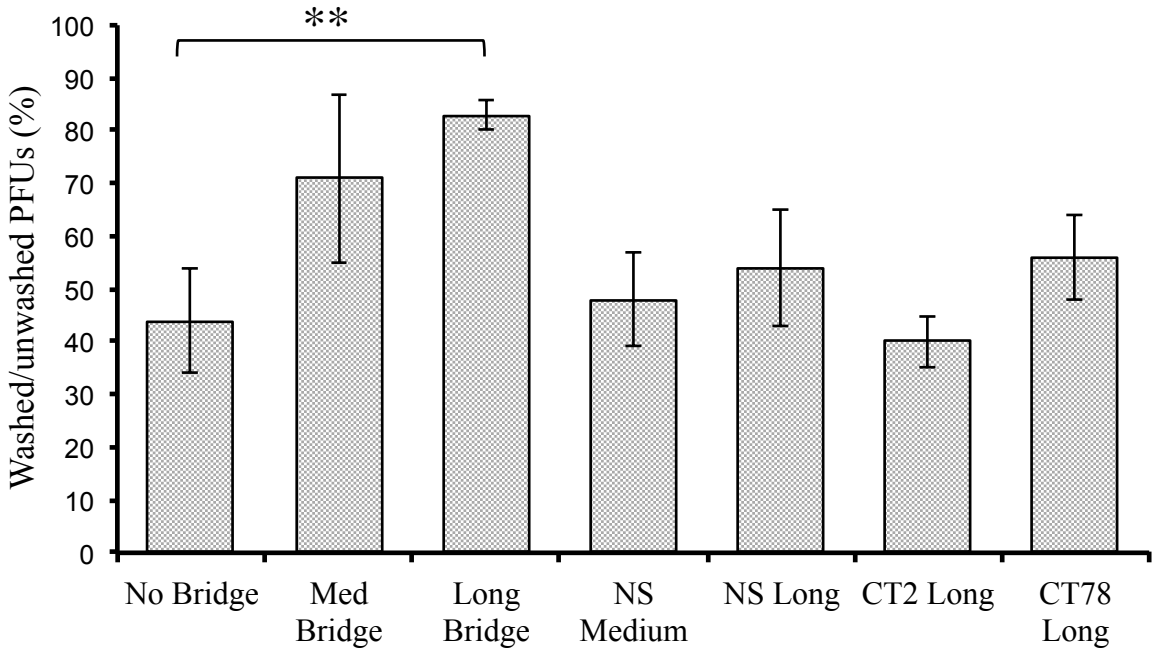

Figure 4.6: Plaque forming assay of tetrameric aptamers using medium and long bridges annealed with VSV- and CT26-specific aptamers and non-specific (NS) ones. The complex, together with VSV, was added to a monolayer of CT26 cells, incubated for 45 minutes, and then washed away. The bars represent a ratio of number of plaques of washed to unwashed wells. (** = $p < 0.1$)

these non-specific aptamers, as well as the aptamers without the bridge, resulted in a lower ratio of washed to unwashed number of plaques. Furthermore, we tested our best-binding aptamers (CT2 and CT78) individually to see if we could obtain an even higher increase of infectivity; this was not the case. Therefore, the optimal results were obtained using a combination of all of the CT26-binding aptamers. This was expected, as a cell is a complex system, and the use of multiple aptamers that would bind to a number of different sites would achieve maximal binding.

4.4 Conclusion

In this work, we selected aptamers to the CT26 cancer cell line in order to achieve a more efficient delivery of the vesicular stomatitis virus. The selection was done using a regular cell-SELEX, followed by high-throughput sequencing of selected pools. This analysis resulted in identification of nine aptamer sequences, two of which proved to have high affinity and selectivity for the targeted cell line. Furthermore, we designed a tetrameric construct by combining these aptamers together with an anti-VSV aptamer pool. A modified plaque forming assay, which involved the washing of the cellular monolayer, demonstrated this multimeric construct's ability to improve the delivery of the virus.

The mechanism of this effect still needs to be elucidated. One way of doing so is by observing the outcome of adding the virus and tetramer mixture to the cells in a microfluidic device in order to see if they are indeed "attaching" the virus to the target in a dynamically changing environment. Furthermore, we would like to identify the binding targets of our two best aptamers by isolating their specific biomarkers using a pull-down method and identifying them by mass spectrometry.

Chapter 5

Aptamers to CD83: A biomarker for dendritic cells

5.1 Background

In 2005, Berezovski et al. published a non-equilibrium capillary electrophoresis of equilibrium mixtures (NECEEM) method and applied it for aptamer selection [170]. NECEEM is based on the fact that molecules separated by capillary electrophoresis will migrate according to their size-to-charge ratio; therefore, oligonucleotides (ligand), which are negatively charged, will elute slower than most proteins (target) [170, 171]. Moreover, when an equilibrium mixture of a target and its ligand is injected into a capillary, and an electric field is applied, the components – target, ligand and complex – are separated. As the separation occurs in run buffers, the solution will no longer be in equilibrium, which will lead to dissociation of the complex, marked by "smears" that can appear around the ligand or the target peaks (Figure 5.1) [171].

In the first proof-of-principle NECEEM application, the Krylov group selected aptamers for protein farnesyltransferase (PFTase) in a single round, showing that more efficient

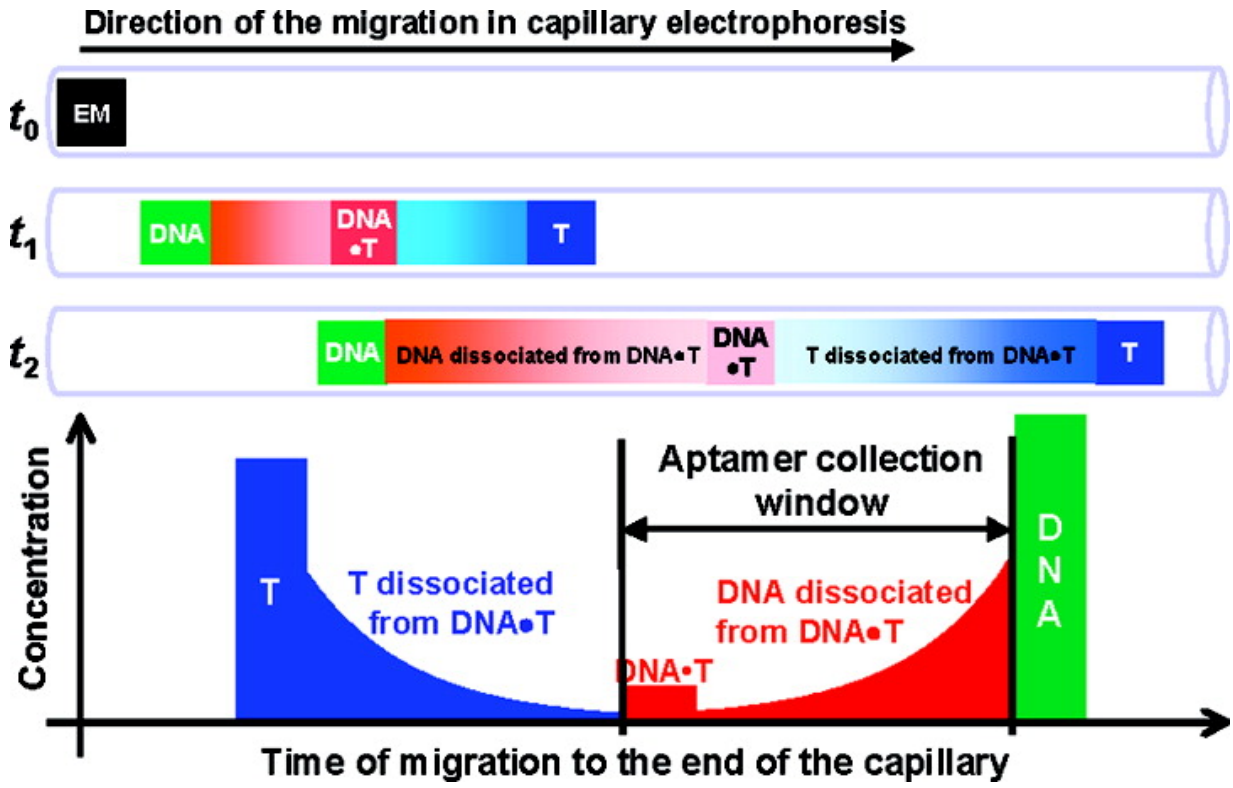

Figure 5.1: A schematic of NECEEM-based separation of DNA and its target. An equilibrium mixture (target, DNA and complex) is injected and separated by capillary electrophoresis. The target is usually eluted first, followed by the complex and, finally, the DNA. The ligand continuously separates from the target, leaving a smear around their peaks. Reproduced with permission from Journal of American Chemical Society 127(9), 3165-3171. Copyright 2005 American Chemical Society.

partitioning can be achieved using this method [170]. This was further supported when the technique was applied to select aptamers using a non-SELEX procedure (i.e. without having to amplify the DNA between rounds of selection) in order to isolate binding oligonucleotides after only three rounds [172].

One of the known biomarkers of dendritic cell (DC) maturation is CD83, which is expressed on their cellular surface [115,173]. CD83 is a 45 kDa glycoprotein which appears to have selective expression and upregulation on mature dendritic cells (mDCs) [174]. These findings hint at its involvement and importance in immune regulation [112]. Furthermore, it has been reported that some viruses such as measles and vaccinia virus have found a way of evading the immune system by suppressing the maturation of DCs or by inhibiting mDCs' capacity to stimulate T cells [175,176]. In line with these findings, the Steinkasserer group made the connection between human simplex virus type 1 (HSV-1), which also blocks DC-stimulation of T cells, with CD83: infection by HSV-1 leads to a complete and specific degradation of CD83 [177,178].

In this section, we applied the NECEEM method, in combination with cell-SELEX, in order to select aptamers for a purified extracellular domain of the human CD83 protein. Using the purified domain resulted in the use of a more facile method of aptamer selection, whereas the cell-SELEX protocol enabled the selection of aptamers that are more specific for the mature dendritic cells. This project was completed in collaboration with Dr. Matthias Lechmann and Dr. Simon Kreiser, from Erlangen University, Germany. Selecting aptamers for this specific target will facilitate future studies about CD83 and its involvement with the immune system regulation.

5.2 Materials and methods

5.2.1 Chemicals and materials

The extracellular human CD83 domain (hCD83ext) was donated by the Department of Dermatology, University of Erlangen-Nuremberg (Erlangen, Germany). Fused-silica capillaries were purchased from Polymicro (Arizona, USA). All solutions were prepared with deionized water and filtered through a 0.22 μm PVDF filter (Millipore, Massachusetts, USA). GoTaq Hot Start Polymerase, dNTPs Mix and other PCR components were purchased from Promega (Wisconsin, USA).

5.2.2 DNA library and primers

The native DNA library contained a central randomized sequence of 40 nucleotides flanked by 20-nt primer hybridization sites (5 ' -CTC CTC TGA CTG TAA CCA CG-$(N)_{40}$-GCATAG GTA GTC CAG AAG CC - 3'). The forward primer (FP) labeled with Alexa Fluor 488 (5' - /5Alex488N/CTC CTC TGA CTG TAA CCA CG - 3') and the reverse primer (RP) labeled with biotin (5' - /5Biosg/GGC TTCTGG ACT ACCTAT GC - 3') were used for generation of single-stranded DNA. Unlabeled FP and RP were used for PCR reactions to generate double-stranded DNA, which was used for cloning of aptamer pools. All oligonucleotides were custom synthesized by Integrated DNA Technologies (Iowa, USA). For flow cytometric analysis, FP used for amplification of DNA pools and clones was labeled with Alexa Fluor 647.

Prior to each round of selection, the DNA library was denatured by heating at 95°C for 5 min and immediately transferred on ice. For the first round, the solution was prepared in incubation buffer (50 mM tris-acetate, 50 mM NaCl and 5 mM $MgCl_2$, pH 8.2) containing 1 μM (200 nM for following rounds) of native DNA library and 10 μM of hCD83ext protein; the mixture was incubated at 23°C for 25 min.

5.2.3 Aptamer selection

Before each separation, the capillary was rinsed with 100 mM HCl, 100 mM NaOH, ddH_2O and running buffer at 20 psi. All separations were carried out on PA800 capillary electrophoresis instrument (Beckman Coulter, California, USA) equipped with a laser-induced fluorescence (LIF) detector. DNA labeled with Alexa Fluor 488 was excited with a laser at 488 nm and the emission was monitored at 520 nm. Separation was carried out in a capillary with an inner diameter of 75 μm, outer diameter of 365 μm, and total length of 73.5 cm (63.5 cm to the detection window). Inlet and outlet reservoirs contained the electrophoresis run buffer (25 mM tris-acetate, pH 8.2). The absorbance of hCD83 protein was detected by UV at 280 nm. The capillary was prefilled with the run buffer and the samples were injected for 5 s at 0.5 psi (3.4 kPa); the capillary temperature was maintained at 20°C. The equilibrium mixture containing DNA-protein mixture was injected into the capillary (injection plug length 9.23 mm, volume 18 nl) pre-filled with buffer. Separations were performed by applying a voltage of 25 kV, resulting in an electric field of 340 V/cm. A fraction was collected from 5 to 12 min by replacing the regular outlet reservoir with a fraction collection vial containing running buffer in order to collect aptamers bound to protein (Figure 5.2).

After collecting the aptamer-containing fraction by CE, single-stranded DNA was generated with 15 cycles of symmetric, followed by 20 cycles of asymmetric amplification. PCR was carried out in a Mastercycler pro S thermal cycler (Eppendorf, Germany). In addition to the DNA sequence template, the PCR reaction mixture contained 1× Green GoTaq Flexi Buffer, 2.5 mM $MgCl_2$, 10 mM dNTPs Mix, and 0.025 U/μl of Taq DNA Polymerase. For symmetric amplification, we used 300 nM of Alexa Fluor 488 labeled FP and biotin-labeled RP. Following settings were used for the thermal cycler: melting at 94°C for 30 s, annealing at 56°C for 15 sec and extending at 72°C for 15 s. Double-stranded DNA was then removed using streptavidin coated magnetic beads (Promega). For asym-

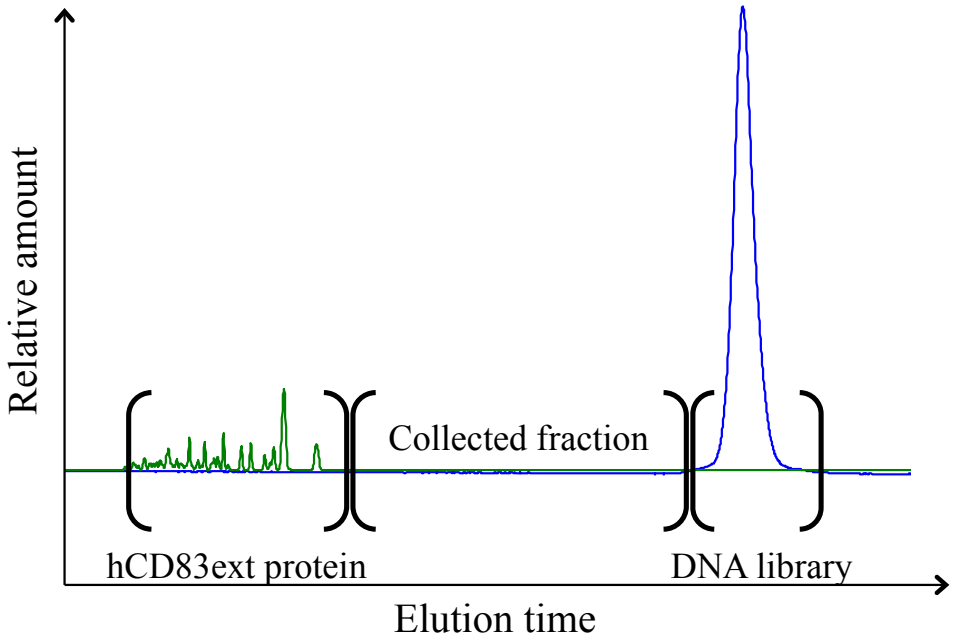

Figure 5.2: A combination of two electropherograms representing the collected fraction for aptamer selection facilitated by capillary electrophoresis using a non-equilibrium capillary electrophoresis of equilibrium mixtures (NECEEM) method. The fraction was collected between the hCD83ext protein (green) and fluorescently-labeled DNA library (blue).

metric amplification, the concentration of FP was 20 times higher than the concentration of the RP (1 μM and 50 nM, respectively); the product was purified with 30 kDa Nanosep Centrifugal Devices (Pall Corporation, New York, USA). Enriched and purified aptamer pools were then used for following rounds of selection, which was repeated up 10 times.

5.2.4 Flow cytometry analysis of enriched DNA libraries

The specificity of enriched DNA libraries for hCD83ext was determined by analyzing their binding to immature (iDCs) and mature dendritic cells (mDCs). This was done in collaboration with Simon Kreiser and Dr. Matthias Lechmann in Erlangen University, Germany. Human iDCs and mDCs were obtained from healthy donors by leukapheresis using leukoreduction system chambers (LRSC). The peripheral blood mononuclear cells (PBMCs) were isolated by density centrifugation and plastic adherence. These cells were then cultured in Dendritic Cell Medium (CellGenix GmbH, Freiburg, Germany) supplemented with human recombinant GM-CSF (800 U/ml on day one, 400 U/ml on day four, CellGenix GmbH) and IL-4 (250 U/ml on day one and day four, CellGenix GmbH). After four days, the differentiated iDCs were matured by adding human recombinant $IL-1\beta$ (200 U/ml, CellGenix GmbH), IL-6 (1000 U/ml, CellGenix GmbH), TNF-α (10 ng/ml, Boehringer Ingelheim, Ingelheim, Germany) and PGE-2 (1 μ/ml, Pfizer, New York, USA) to the culture medium and incubating the cells for 24 hours.

Prior to the affinity analysis, Alexa Fluor 647 labeled aptamer pools were denatured by heating at 95°C for 5 min in DPBS and directly transferred on ice for 10 min. Immature and mature dendritic cells (2×10^5 cells/sample) were incubated with 1 nmol of salmon sperm DNA (Rockland Inc., Pennsylvania, USA) and 50 pmol of the aptamer pool in 500 μl of DPBS for 30 min on ice. The cells were then centrifuged at $300 \times g$ for 5 min at 4°C in order to separate bound and unbound ssDNA, washed two times and re-suspended in DPBS. A solution of 50 pmol of native DNA library was used as a control. Binding

of DNA sequences was analyzed by determining the level of fluorescence of cells with a FACSCanto II cytometer (Becton Dickinson, New Jersey, USA).

As per results of flow cytometry analyses, pool 9 was selected to be improved for its binding to mDCs. For this, we used 1×10^6 cells and incubated with 20 nmol of salmon sperm DNA and 100 pmol of aptamer pool. The cells were centrifuged to separate bound and unbound ssDNA, washed two times and re-suspended in DPBS. The solution was then subjected to a fluorescence-activated cell sorting system, FACSAria III (Becton Dickinson) in order to separate the mDCs that contained on their surface ssDNA. The separation resulted with 17,000 cells which were spun down, re-suspended in DPBS and used as a template for symmetric/asymmetric PCR amplification. Single-stranded DNA was then separated and purified.

Finally, this purified enriched pool 9, and pools 7 and 8, were subjected to a cell-SELEX selection. First, we removed dead cells using MACS Cell Isolation Kit (Miltenyl Biotec, Germany) and obtained 1×10^5 cells. They were then incubated with 4 nmol of salmon sperm DNA and 25 pmol of enriched aptamer pools for 20 min on ice. The cells were centrifuged, washed two times, and re-suspended in DPBS. The solution was then heated at 95°C for 5 min to release DNA bound to cells. Following the denaturing step, cellular debris was removed by maximal centrifugation for 20 min. The supernatant was collected and used as a template for symmetric/asymmetric PCR amplification. Binding of these enriched aptamer pools (pools 7B, 8B and 9B) was analyzed by flow cytometry where native DNA library was used as a control.

5.2.5 Aptamer pool sequencing

Aptamer pool 9B was amplified by symmetric PCR using unlabeled primers and purified with AxyPrep DNA Gel Extraction Kit (Axygen Biosciences, California, USA). The DNA was then cloned into *Escherichia coli* (*E. coli*) using the pETBlue-1 Perfectly Blunt

Cloning Kit (Invitrogen, California, USA). Plasmids containing the insert were isolated from bacterial colonies with GeneJET Plasmid Miniprep Kit (Thermo Fisher Scientific Inc., Massachusetts, USA) and amplified by PCR. Individual aptamers were screened for their binding to their target and the clones that had fitting results were chosen for sequencing in Génome Québec facilities (Québec, Canada).

Selected aptamer pool 9B was also sent to ACGT Inc (Illinois, USA) for high throughput sequencing (HTS). The ends of DNA were treated in order to be phosphorylated and then ligated into concatemers. The resulting library was run and sequenced on Illumina MiSeq Personal Sequencer (Illumina, California, USA). The samples were analyzed in ACGT facilities by screening for nucleotide sequences containing primer-binding sites of our DNA library. Once the sequence information was received, the most abundant aptamer sequences were ordered from IDT.

Both synthetic aptamers and aptamers obtained by cloning were analyzed for their binding to mature and immature dendritic cells (Figures 5.5 and 5.6).

5.3 Results and discussion

This aptamer selection was done using a purified sample of the extracellular domain of human CD83, in its folded state, which simplifies the selection process, as there is no need to use CD83-expressing dendritic cells [174]. We took advantage of capillary electrophoresis (CE) and the previously published NECEEM method to select aptamers against hCD83ext [172]. CE-laser induced fluorescence (CE-LIF) is a sensitive technique, allowing the detection of as little as 10 fmol of fluorescein. However, during the initial rounds of aptamer selection, the complex is not easily visualized due to the enormous heterogeneity of the library and the low amount of binding aptamers. Therefore, it is important to identify the fraction collection window before starting the selection. This window was established by determining the elution time of the protein with a UV detector at 280 nm and that

of the DNA library, which was fluorescently labeled. The fraction was collected up to the point where the free DNA is eluted (Figure 5.2).

After each round of selection, purified and amplified DNA was incubated with an excess of the target protein and separated by capillary electrophoresis. Asymmetrically amplified ssDNA was labeled with Alexa Fluor 488, which enabled us to visualize it by CE-LIF. We observed a peak that had a faster migration time than that of the free DNA, which we attributed to DNA interacting with the target protein. This protein-DNA complex was visualized after the third round and gradually increased in the following rounds. We did a total of ten selections by capillary electrophoresis, after which the collected pools were analyzed under the same conditions in order to determine their binding affinity to hCD83ext (Figure 5.3).

The main role of dendritic cells is to process and present antigens to T cells [179]. Therefore, when they come into contact with compounds, it is expected of them to have a certain adhesion to these bodies. We found that the native DNA library had a significant amount of binding to both types of DCs. To eliminate this non-specific binding, we incubated the cells with salmon sperm DNA, which served as masking DNA, prior to the incubation of the cells with selected aptamer pools.

Binding of collected fractions to CD83-expressing mature dendritic cells was analyzed in Erlangen University, Germany. Ideally, selected pools would have a high affinity for matured DCs and have minimal binding to their immature counterparts. After the initial screening of all pools obtained by CE selection, we determined that pools 7, 8 and 9 had a promising affinity and selectivity for the targeted cells; these were used for additional rounds of cell-SELEX.

In order to increase the affinity of pool 9, we performed one round of selection using fluorescence-activated cell sorting on mature dendritic cells. This method allowed us to isolate the cells which were fluorescent, and therefore had bound aptamers on their surface.

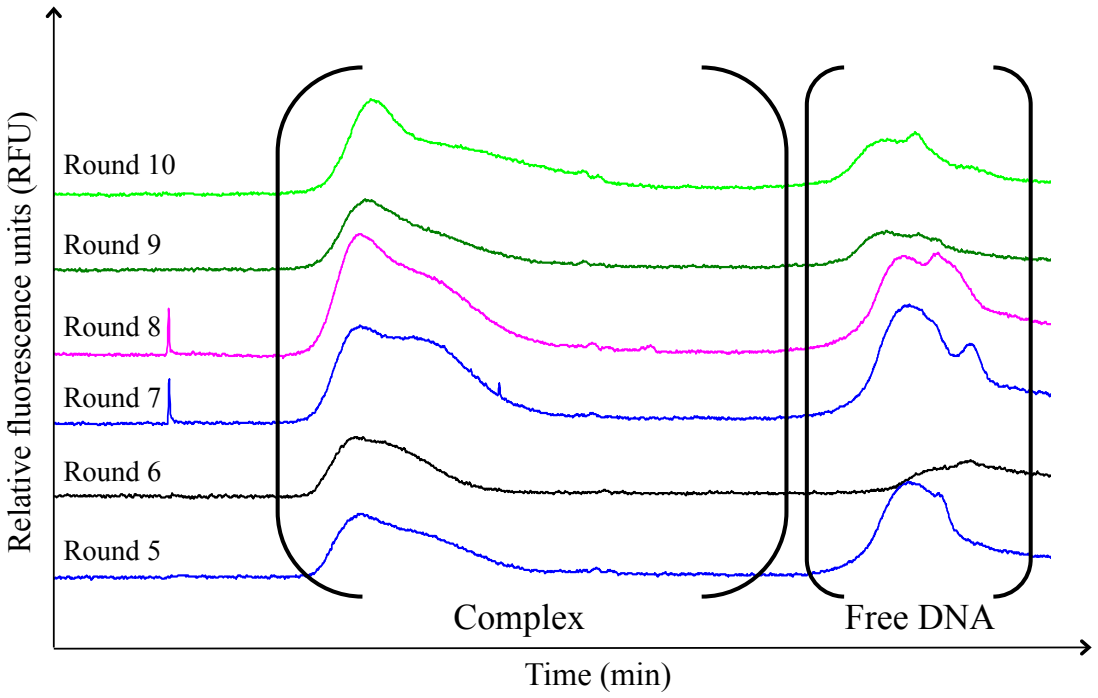

Figure 5.3: Electropherograms of different rounds of selection and their binding to the extracellular human CD83 domain (hCD83ext). Each round was amplified and purified before being incubated with the protein target and subjected to capillary electrophoresis separation.

Finally, the three top pools (7, 8 and 9) were subjected to one final selection. Since DNA can bind non-specifically to dead or dying cells and thus eliminate some potentially high-binding aptamers, we used a dead-cell removal kit before undergoing this selection. Final resulting pools, which we named 7B, 8B and 9B, were tested for their affinity to mDCs with flow cytometry (Figure 5.4). For rounds 7 and 8, we observed only partial binding, as the majority of cells were not fluorescing. However, for round 9, there was about a 5-fold increase in fluorescence compared to the DNA library, and a 10-fold increase compared to mDCs alone.

To identify individual sequences from pool 9B, we initially cloned the pool and isolated 20 colonies (Table 5.1). Sanger sequencing allowed us to identify the repetitive oligonucleotides (clone 1 and clone 4), which were repeated two and three times, respectively. All aptamer sequences were tested for their binding to mature and immature dendritic cells. Clones 1, 2 and 10 were identified as the sequences with the highest affinity and specificity. These were chemically synthesized and titrated in a range of concentrations from 1 to 1000 nM. All three aptamers had a higher specificity for mDCs than iDCs.

Pool 9B also underwent high throughput sequencing. This was done using a concatemer approach, where the aptamers were treated and ligated in order to form long and continuous DNA strands. This method has the advantage of eliminating the need for pool barcoding, as each pool is treated and sequenced separately. The analysis resulted in a total of 764,841 aptamer sequences. As expected, the two cloned sequences that were found in duplicate and triplicate were the top two sequences obtained by HTS (Tables 5.1 and 5.2).

The most abundant aptamer sequences were analyzed by flow cytometry for their binding to mature and immature dendritic cells. Apparent dissociation constants can be estimated by titrating different aptamer concentrations and analyzing their binding intensity to the target. By plotting these values, the K_d value is estimated when 50% of binding saturation is reached. Interestingly, even though the dissociation constants for the majority of the clones were similar for iDCs and mDCs, higher fluorescence was observed when the

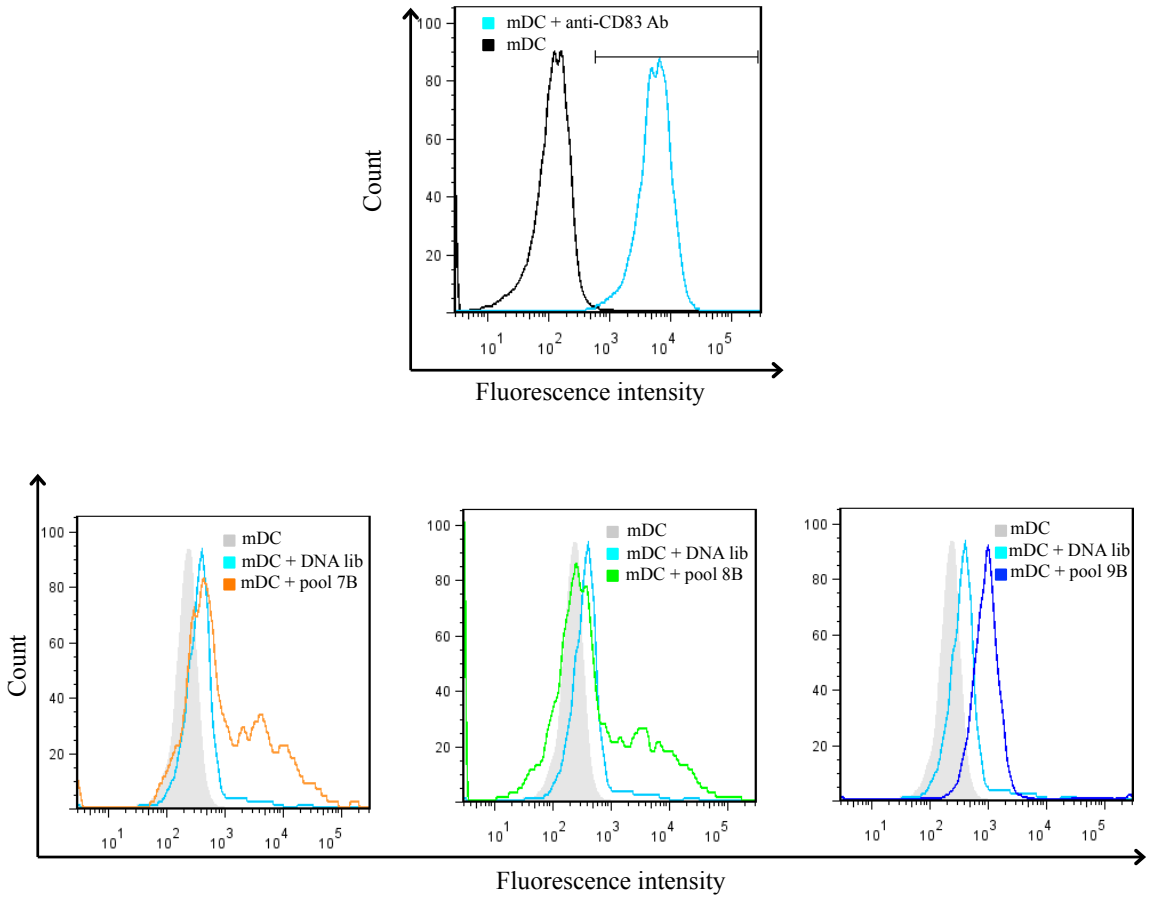

Figure 5.4: Flow cyometry analysis of aptamer pools binding to hCD83ext. All three pools were subjected to capillary electrophoresis-facilitated selection and one round of cell-SELEX. Additionally, round 9B underwent an aptamer selection using fluorescence-activated cell sorting.

Table 5.1: List of aptamer sequences selected for CD83 identified by cloning and Sanger sequencing and their abundance obtained by HTS.

Name	Sequence (5'–3')[a]	Abundance (%)
Clone 1[b]	fGTCGAGGCCGCGTGCCCTCTCTTCCCCTTACGTGCTCGGCcr	4.1
Clone 2	fCCCTCCCAGGTCCTTCTTTCCCTCCTTTCTGTCACTGCCGcr	1.2
Clone 3	fTACCACCCGTGACCCTCACATCCCTCCTCTGTTCTCCGTGcr	0.010
Clone 4[c]	fTTGTCCCGCTGTTGTTCGTTGTCTCTTCTTTTCCCGTGGTcr	4.2
Clone 5	fCCATACTTGCCCCCGACATTTGTCCCCTTTCCCGTTCCTcr	0.00013
Clone 7	fTCGCGTATATCACACCTCGAATCTGTCCCCTGTTGTTCTGcr	0.039
Clone 8	fTGCCACCCCCCTGTGTCCCCTATCCATCTATGCCCCCTTCcr	0.0034
Clone 10	fGTCATGTCCGTCGAGCCGTCCCCCGCCATCTCCTCCTGCTcr	0.050
Clone 13	fGCCCCGCTCACTATAATCTCGTCGCACCTTCCATATGCCAcr	0.00039
Clone 14	fCGCCCTTCGTCATCTGTATGGTCTGCCTGTCCTGGTAACAcr	0.026
Clone 15	fTACTATGCGCACATATATCCCTACCTGCACCACCTCCCGGcr	0.0071
Clone 17	fACCTCCTGATATCCTCCCTGTCCGCCGTCTTGTTCTTATGcr	0.00013
Clone 19	fTCCTCGCCATCTTCCCATCGCCAAGCCCCCCTCCGCCTGCcr	0.0055

[a] f, ctcctctgactgtaaccacg (sequence of the forward primer); cr, gcataggtagtccagaagcc (reverse-complement of the reverse primer).
[b] Sequence repeated two times.
[c] Sequence repeated three times.

Table 5.2: List of aptamer sequences selected for CD83 and identified by high throughput sequencing.

Name	Sequence (5'–3')[a]	Abundance (%)
CD83 Apt1[b]	fTTGTCCCGCTGTTGTTCGTTGTCTCTTCTTTTCCCGTGGTcr	4.2
CD83 Apt2[c]	fGTCGAGGCCGCGTGCCCTCTCTTCCCCTTACGTGCTCGGCcr	4.1
CD83 Apt3	fTACCACCTTTTCTCTTTTCCGTTTCCCACTGCCTCGTACGcr	2.1
CD83 Apt4	fTACATGCCCTCCTCCCTACTCTCGTCCGATATTGACCTCTcr	1.7
CD83 Apt5	fGGCGGTCCCTTCTTTTTGTGTTTATGTTGTTCTCTTTTCGcr	1.4

[a] f, ctcctctgactgtaaccacg (sequence of the forward primer); cr, gcataggtagtccagaagcc (reverse-complement of the reverse primer).
[b] Sequence identical to Clone 4 in Table 5.1.
[c] Sequence identical to Clone 1 in Table 5.1.

aptamers were incubated with mature dendritic cells (Figures 5.5 and 5.6). The clone that was the most abundant in the pool, CD83 Apt1, appeared to have the highest selectivity (Figure 5.6).

5.4 Conclusion

For this project, we selected aptamers by applying a combination of NECEEM and cell-SELEX methods. The initial selection was performed on a recombinant extracellular domain of the CD83, which proved to be an efficient target for generation of pools using these methods. Selected pools were further improved by undergoing cell-SELEX on mature dendritic cells, which highly express the CD83 protein on their surface. After cloning and high-throughput sequencing, we isolated six aptamer sequences which appear to bind selectively to the mature dendritic cells.

Even though CD83 is the most abundant marker for maturation of DCs, it is not the only one; for example, CD80 and CD86 are also highly expressed on mDCs [178]. Therefore, further experiments, such as CD83 displacement assays or microscopy with

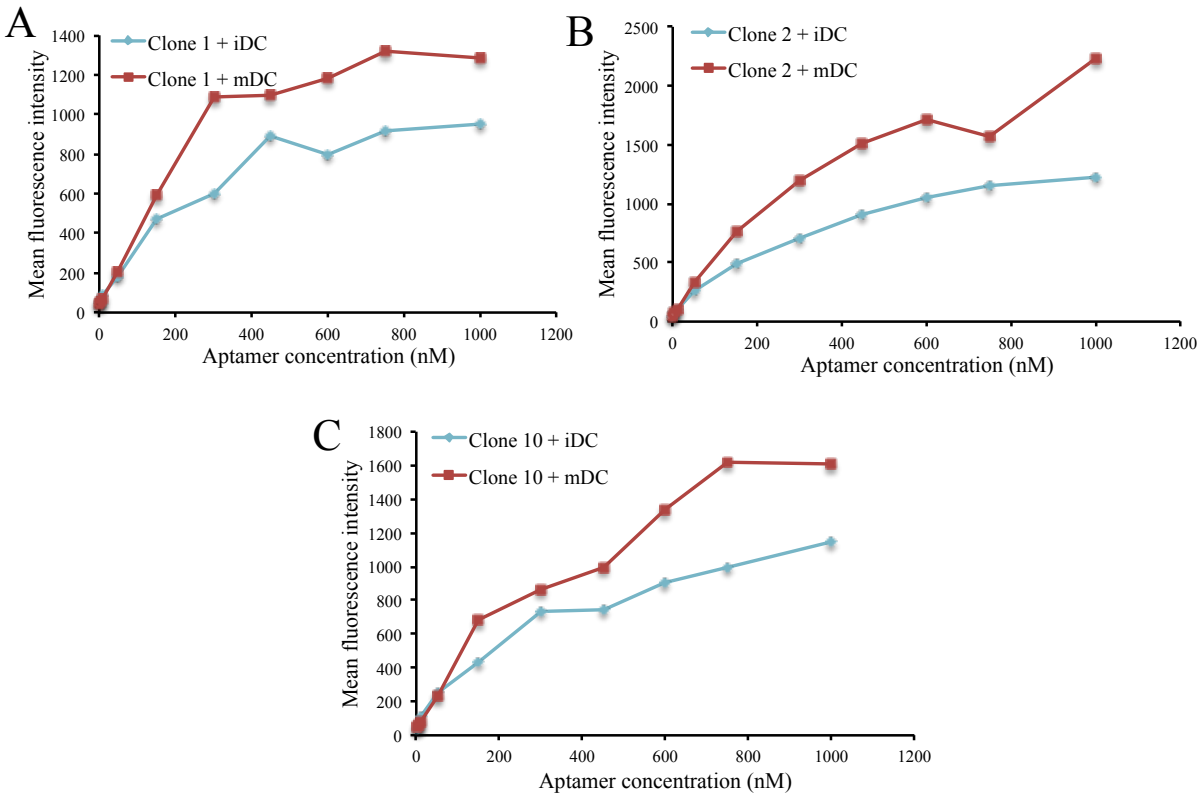

Figure 5.5: Flow cytometry analysis of selected aptamers and their binding to mature (red) and immature (blue) dendritic cells. Aptamers were obtained after cloning and sequencing of the pool of highest affinity and selectivity (pool 9B).

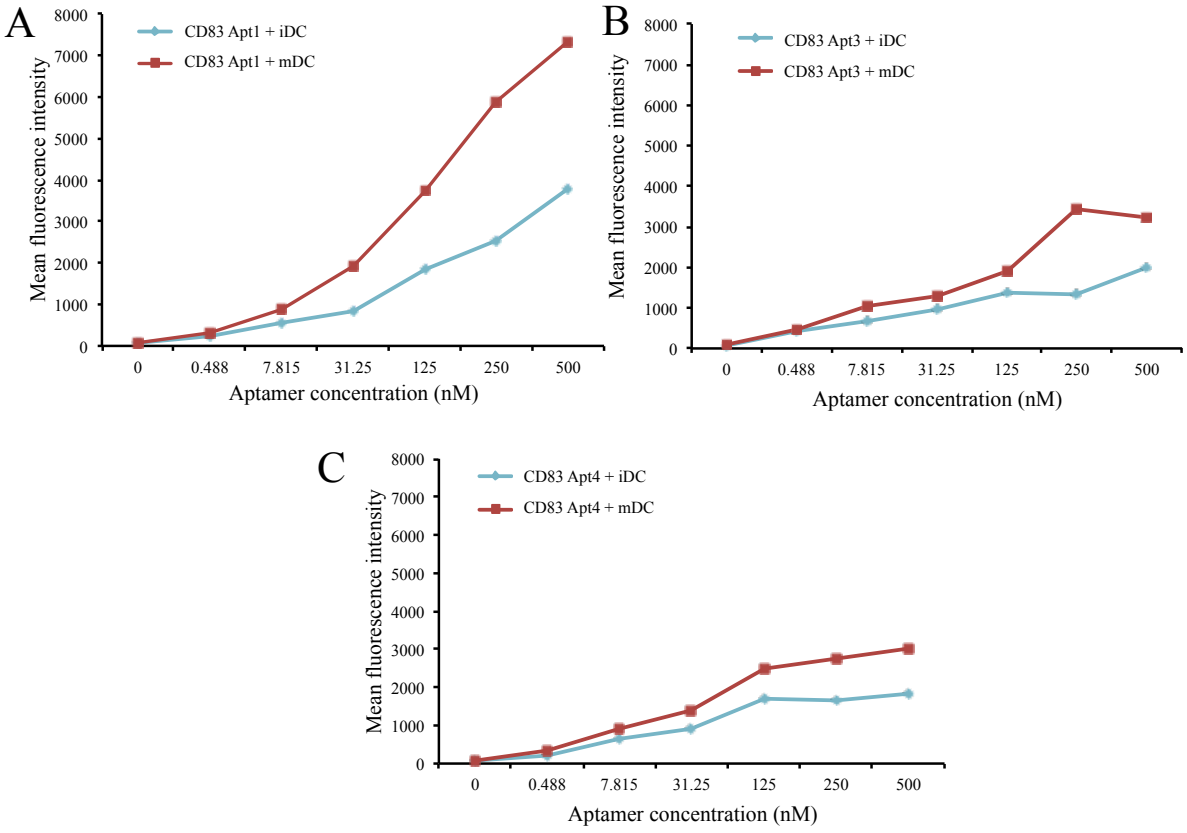

Figure 5.6: Flow cytometry analysis of selected aptamers and their binding to mature (red) and immature (blue) dendritic cells. Aptamers were obtained after the pool with highest affinity and selectivity (pool 9B) was sequenced by high throughput sequencing.

anti-CD83 antibodies, will need to be performed in order to confirm that these aptamers are, indeed, binding to their target.

Chapter 6

Conclusion and future directions

Oncolytic viruses promise to significantly improve current cancer treatments through their tumour-selective replication and multimodal attack against cancer cells. A variety of oncolytic viruses have already been adopted or specifically engineered to target or replicate in tumour cells, some of which are currently under clinical or preclinical studies [88]. Human trials have demonstrated that the use of oncolytic viruses is safe with much less toxicity compared to standard forms of cancer therapy, such as chemo- and radiation therapies. However, one of the biggest setbacks for oncolytic virus therapies is intravenous delivery of the virus, as it can be cleared from the bloodstream before it reaches the tumour cells. While viruses circulating in the bloodstream could be inactivated by complement proteins or the reticuloendothelial system, the most restrictive barrier to effective treatment is the acquired immunity to repeated infections due to neutralizing antibodies (nAbs).

The main focus of this thesis is the selection of different types of aptamers. The first three chapters address the development of aptamers with the final goal of obtaining protecting and shielding aptamers or a more efficient delivery of the virus to targeted cells. Following the selection and binding assessments, selected oligonucleotides proved to be successful in curtailing nAbs inhibition of virus infection of cell monoloyers *in vitro*. However, further attempts to apply protecting and shielding aptamers in mouse models

did not generate the desired result. A possible explanation is that, due to a large diversity of antibodies within different hosts, aptamers that were selected to bind to or be displaced by nAbs extracted from rabbit serum can not be applied to mice, or even possibly to a different rabbit host.

This project therefore served as a proof-of-principle to demonstrate the potential of selecting and applying aptamers to cancer therapy. Ideally, these would be used in combination with oncolytic viruses, selected on a "personalized" basis. We propose that the best approach would be to use neutralizing antibodies from a specific patient following one or multiple administrations of an oncolytic virus. Even though current selections are quite laborious and time-consuming, there have been many advances in aptamer technology that could lead us toward a future where aptamer selection would be automated by robotic systems and completed within several days [180–182].

Targeted delivery using aptamers is a method that has been applied to a number of "target-ligand" systems [39,183]. In Chapter 4, we design bifunctional aptamers that would bind to the targeted cancer cells, CT26, as well as the virus. *In vitro* analysis has shown a two-fold increase of viral delivery. In order to improve this effect, future work should focus on characterization of aptamers, such as identifying the binding receptor on the cellular surface. This can be done using a pull-down method with biotinylated aptamers, a method that has been explored for different projects [113, 184]. This way, we could use a more rational approach in selecting which aptamers to use. For example, targeting biomarkers that are only expressed on cancer cells will make the bifunctional aptamers more specific. Anti-VSV aptamers can be conjugated with other oligonucleotides that have been selected in our or other laboratories in order to deliver the virus to different types of cells. Moreover, the system can be used to target other agents to the cancer cells, such as miRNA or toxins, in order to obtain cytotoxicity.

The ability of the aptamer to efficiently deliver the virus to the targeted cells *in vivo* systems can further be explored using a microfluidics system, which would contain a cham-

ber with the monolayer of cells and an inlet/outlet to allow the media containing the virus to pass though. This experiment would help to identify whether the aptamers are able to bind to the target in a kinetic environment. If this is the case, the bifunctional construct could also be used for the targeting and oncotherapy of circulating tumour cells, which are usually responsible for the metastasis of tumours.

Finally, the targeting aptamers have the potential to be efficient delivery agents in an *in vivo* environment. Combined with the fact that the anti-VSV aptamers protect the virus from neutralizing antibodies, a more targeted, and thus more rapid delivery of VSV to the cancer cells could help overcome its neutralization. Furthermore, this approach could be more applicable in a broader sense, as the cancer biomarkers and the virus do not vary greatly from patient to patient.

The final chapter of the thesis focuses on the selection of aptamers to CD83, a biomarker of dendritic cells. The selection was done initially using capillary electrophoresis in order to identify oligonucleotides binding to purified recombinant CD83, followed by rounds of cell-SELEX to mature dendritic cells expressing the protein of interest. The selection was successful and resulted in several individual sequences that had a higher affinity to the mDCs when compared to the iDCs.

However, in order to be able to confirm that the aptamers are indeed binding to the desired target on the cell surface, further characterization assays need to be done. For example, one way to explore this would be perform a displacement analysis with anti-CD83 antibodies. If the aptamers are displaced, this would indicate their co-localization. Another method that could be explored is the aforementioned pull-down using biotinylated aptamers and streptavidin-coated beads. The pulled out protein would be analyzed by mass spectrometry or identified with Western blotting.

As we have previously mentioned, CD83 was also discovered to have a functional role—the soluble extracellular domain inhibits DC-mediated T-cell proliferation [115]. Therefore,

aptamers specific to CD83 could be further assessed in order to see if they have inhibiting properties when bound to the target. If this is the case, these could be used to further study and elucidate the mechanism of action of the CD83 protein.

Development of aptamer-based technology has the potential to improve viral oncotherapies as well as other types of therapies, as it is the case with a number of aptamers that are currently undergoing clinical studies.

List of publications

(1) Ghobadloo, S. M., Balcerzak, A. K., Gargaun, A., **Muharemagic, D.**, Mironov, G. G., Capicciotti, C. J., Briard, J.G., Ben R.N., & Berezovski, M.V. (2014). Carbohydrate-based ice recrystallization inhibitors increase infectivity and thermostability of viral vectors. Scientific Reports, 4.

(2) Wehbe, M., Labib, M., **Muharemagic, D.**, Zamay, A. S., & Berezovski, M. V. (2014). Switchable aptamers for biosensing and bioseparation of viruses (SwAps-V). Biosensors and Bioelectronics.

(3) **Muharemagic, D.**, Zamay, A., Ghobadloo, S. M., Evgin, L., Savitskaya, A., Bell, J. C., & Berezovski, M. V. (2014). Aptamer-facilitated Protection of Oncolytic Virus from Neutralizing Antibodies. Molecular Therapy. Nucleic Acids, 3, e167.

(4) Azizi, A., Mironov, G. G., **Muharemagic, D.**, Wehbe, M., Bell, J. C., & Berezovski, M. V. (2012). Viral quantitative capillary electrophoresis for counting and quality control of RNA viruses. Analytical Chemistry, 84(21), 9585-9591.

(5) **Muharemagic, D.**, Labib, M., Ghobadloo, S. M., Zamay, A. S., Bell, J. C., & Berezovski, M. V. (2012). Anti-Fab aptamers for shielding virus from neutralizing antibodies. Journal of the American Chemical Society, 134(41), 17168-17177.

(6) Labib, M., Zamay, A. S., **Muharemagic, D.**, Chechik, A. V., Bell, J. C., & Berezovski, M. V. (2012). Electrochemical differentiation of epitope-specific aptamers. Analytical Chemistry, 84(5), 2548-2556.

(7) Labib, M., Zamay, A. S., **Muharemagic, D.**, Chechik, A., Bell, J. C., & Berezovski, M. V. (2012). Electrochemical sensing of aptamer-facilitated virus immunoshielding. Analytical Chemistry, 84(3), 1677-1686.

(8) Labib, M., Zamay, A. S., **Muharemagic, D.**, Chechik, A. V., Bell, J. C., & Berezovski, M. V. (2012). Aptamer-based viability impedimetric sensor for viruses. Analytical Chemistry, 84(4), 1813-1816.

References

[1] O'Malley, R. P, Mariano, T. M, Siekierka, J, & Mathews, M. B. (1986) A mechanism for the control of protein synthesis by adenovirus VA RNAI. *Cell* **44**, 391–400.

[2] Dollins, C. M, Nair, S, & Sullenger, B. A. (2008) Aptamers in immunotherapy. *Human Gene Therapy* **19**, 443–450.

[3] Sullenger, B. A, Gallardo, H. F, Ungers, G. E, & Gilboa, E. (1990) Overexpression of TAR sequences renders cells resistant to human immunodeficiency virus replication. *Cell* **63**, 601–608.

[4] Eaton, B. E, Gold, L, & Zichi, D. A. (1995) Let's get specific: the relationship between specificity and affinity. *Chemistry & Biology* **2**, 633–638.

[5] Tuerk, C & Gold, L. (1990) Systematic evolution of ligands by exponential enrichment: RNA ligands to bacteriophage T4 DNA polymerase. *Science* **249**, 505–510.

[6] Ellington, A. D & Szostak, J. W. (1990) In vitro selection of RNA molecules that bind specific ligands. *Nature* **346**, 818–822.

[7] VEGF Inhibition Study in Ocular Neovascularization (V.I.S.I.O.N.) Clinical Trial Group, D'Amico, D. J, Masonson, H. N, Patel, M, Adamis, A. P, Cunningham, E. T, Guyer, D. R, & Katz, B. (2006) Pegaptanib sodium for neovascular age-related macular degeneration: two-year safety results of the two prospective, multicenter, controlled clinical trials. *Ophthalmology* **113**, 992–1001.e6.

[8] Siller-Matula, J. M, Merhi, Y, Tanguay, J. F, Duerschmied, D, Wagner, D. D, McGinness, K. E, Pendergrast, P. S, Chung, J. K, Tian, X, Schaub, R. G, & Jilma, B. (2012) ARC15105 is a potent antagonist of Von Willebrand factor mediated platelet activation and adhesion. *Arteriosclerosis, Thrombosis, and Vascular Biology* **32**, 902–909.

[9] Bates, P. J, Laber, D. A, Miller, D. M, & Thomas, S. D. (2009) Discovery and development of the G-rich oligonucleotide AS1411 as a novel treatment for cancer. *Experimental and Molecular Pathology.*

[10] Ninichuk, V, Clauss, S, Kulkarni, O, Schmid, H, Segerer, S, Radomska, E, Eulberg, D, Buchner, K, Selve, N, Klussmann, S, & Anders, H.-J. (2008) Late onset of Ccl2 blockade with the Spiegelmer mNOX-E36–3PEG prevents glomerulosclerosis and improves glomerular filtration rate in db/db mice. *The American Journal of Pathology* **172**, 628–637.

[11] Waters, E. K, Genga, R. M, Schwartz, M. C, Nelson, J. A, Schaub, R. G, Olson, K. A, Kurz, J. C, & McGinness, K. E. (2011) Aptamer ARC19499 mediates a procoagulant hemostatic effect by inhibiting tissue factor pathway inhibitor. *Blood* **117**, 5514–5522.

[12] Legiewicz, M, Lozupone, C, Knight, R, & Yarus, M. (2005) Size, constant sequences, and optimal selection. *RNA* **11**, 1701–1709.

[13] Ruff, K. M, Snyder, T. M, & Liu, D. R. (2010) Enhanced functional potential of nucleic acid aptamer libraries patterned to increase secondary structure. *Journal of the American Chemical Society* **132**, 9453–9464.

[14] Yegnasubramanian, S. (2013) Explanatory chapter: next generation sequencing. *Methods in Enzymology* **529**, 201–208.

[15] Bock, L. C, Griffin, L. C, Latham, J. A, Vermaas, E. H, & Toole, J. J. (1992) Selection of single-stranded DNA molecules that bind and inhibit human thrombin. *Nature* **355**, 564–566.

[16] Hoon, S, Zhou, B, Janda, K. D, & Brenner, S. (2011) Aptamer selection by high-throughput sequencing and informatic analysis. *Biotechniques*.

[17] Cho, M, Xiao, Y, Nie, J, Stewart, R, Csordas, A. T, Oh, S. S, Thomson, J. A, & Soh, H. T. (2010) Quantitative selection of DNA aptamers through microfluidic selection and high-throughput sequencing. *Proceedings of the National Academy of Sciences of the United States of America* **107**, 15373–15378.

[18] Schütze, T, Wilhelm, B, Greiner, N, Braun, H, Peter, F, Mörl, M, Erdmann, V. A, Lehrach, H, Konthur, Z, Menger, M, Arndt, P. F, & Glökler, J. (2011) Probing the SELEX process with next-generation sequencing. *PLoS ONE* **6**.

[19] White, R. R, Sullenger, B. A, & Rusconi, C. P. (2000) Developing aptamers into therapeutics. *Journal of Clinical Investigation* **106**, 929–934.

[20] Koshkin, A. A, Singh, S. K, Nielsen, P, Rajwanshi, V. K, Kumar, R, Meldgaard, M, Olsen, C. E, & Wengel, J. (1998) LNA (Locked Nucleic Acids): Synthesis of the adenine, cytosine, guanine, 5-methylcytosine, thymine and uracil bicyclonucleoside monomers, oligomerisation, and unprecedented nucleic acid recognition. *Tetrahedron* **54**, 3607–3630.

[21] Obika, S, Nanbu, D, Hari, Y, Andoh, J. I, Morio, K. I, Doi, T, & Imanishi, T. (1998) Stability and structural features of the duplexes containing nucleoside analogues with a fixed N-type conformation, 2'-O,4'-C- methyleneribonucleosides. *Tetrahedron Letters* **39**, 5401–5404.

[22] Braasch, D. A & Corey, D. R. (2001) Locked nucleic acid (LNA): Fine-tuning the recognition of DNA and RNA. *Chemistry & Biology* **8**, 1–7.

[23] Barciszewski, J, Medgaard, M, Koch, T, Kurreck, J, & Erdmann, V. A. (2009) Locked nucleic acid aptamers.

[24] Doessing, H & Vester, B. (2011) Locked and unlocked nucleosides in functional nucleic acids. *Molecules (Basel, Switzerland)* **16**, 4511–4526.

[25] Schmidt, K. S, Borkowski, S, Kurreck, J, Stephens, A. W, Bald, R, Hecht, M, Friebe, M, Dinkelborg, L, & Erdmann, V. A. (2004) Application of locked nucleic acids to improve aptamer in vivo stability and targeting function. *Nucleic Acids Research* **32**, 5757–5765.

[26] Hicke, B. J, Marion, C, Chang, Y. F, Gould, T, Lynott, C. K, Parma, D, Schmidt, P. G, & Warren, S. (2001) Tenascin-C aptamers are generated using tumor cells and purified protein. *Journal of Biological Chemistry* **276**, 48644–48654.

[27] Purschke, W. G, Radtke, F, Kleinjung, F, & Klussmann, S. (2003) A DNA Spiegelmer to staphylococcal enterotoxin B. *Nucleic Acids Research* **31**, 3027–3032.

[28] Kurreck, J. (2008) *Therapeutic Oligonucleotides*. (Royal Society of Chemistry).

[29] Klussmann, S, Nolte, A, Bald, R, Erdmann, V. A, & Fürste, J. P. (1996) Mirror-image RNA that binds D-adenosine. *Nature Biotechnology* **14**, 1112–1115.

[30] Nolte, A, Klussmann, S, Bald, R, Erdmann, V. A, & Fürste, J. P. (1996) Mirror-design of L-oligonucleotide ligands binding to L-arginine. *Nature Biotechnology* **14**, 1116–1119.

[31] Vater, A, Jarosch, F, Buchner, K, & Klussmann, S. (2003) Short bioactive Spiegelmers to migraine-associated calcitonin gene-related peptide rapidly identified by a novel approach: tailored-SELEX. *Nucleic Acids Research* **31**, e130.

[32] Di Giusto, D. A & King, G. C. (2004) Construction, stability, and activity of multivalent circular anticoagulant aptamers. *Journal of Biological Chemistry* **279**, 46483–46489.

[33] Santulli-Marotto, S, Nair, S. K, Rusconi, C, Sullenger, B, & Gilboa, E. (2003) Multivalent RNA aptamers that inhibit CTLA-4 and enhance tumor immunity. *Cancer Research* **63**, 7483–7489.

[34] Pastor, F, Kolonias, D, McNamara, J. O, & Gilboa, E. (2011) Targeting 4-1BB costimulation to disseminated tumor lesions with bi-specific oligonucleotide aptamers. *Molecular Therapy : The Journal of the American Society of Gene Therapy* **19**, 1878–1886.

[35] Aldaye, F. A & Sleiman, H. F. (2007) Modular access to structurally switchable 3D discrete DNA assemblies. *Journal of the American Chemical Society* **129**, 13376–13377.

[36] Rothemund, P. W. K. (2006) Folding DNA to create nanoscale shapes and patterns. *Nature* **440**, 297–302.

[37] Hamblin, G. D, Carneiro, K. M. M, Fakhoury, J. F, Bujold, K. E, & Sleiman, H. F. (2012) Rolling circle amplification-templated DNA nanotubes show increased stability and cell penetration ability. *Journal of the American Chemical Society* **134**, 2888–2891.

[38] Soundararajan, S, Wang, L, Sridharan, V, Chen, W, Courtenay-Luck, N, Jones, D, Spicer, E. K, & Fernandes, D. J. (2009) Plasma membrane nucleolin is a receptor for the anticancer aptamer AS1411 in MV4-11 leukemia cells. *Molecular Pharmacology* **76**, 984–991.

[39] Charoenphol, P & Bermudez, H. (2014) Aptamer-targeted DNA nanostructures for therapeutic delivery. *Molecular Pharmaceutics* **11**, 1721–1725.

[40] Edwardson, T. G. W, Carneiro, K. M. M, McLaughlin, C. K, Serpell, C. J, & Sleiman, H. F. (2013) Site-specific positioning of dendritic alkyl chains on DNA cages enables their geometry-dependent self-assembly. *Nature Chemistry* **5**, 868–875.

[41] Juul, S, Iacovelli, F, Falconi, M, Kragh, S. L, Christensen, B, Frøhlich, R, Franch, O, Kristoffersen, E. L, Stougaard, M, Leong, K. W, Ho, Y. P, Sørensen, E. S, Birkedal, V, Desideri, A, & Knudsen, B. R. (2013) Temperature-controlled encapsulation and release of an active enzyme in the cavity of a self-assembled DNA nanocage. *ACS Nano* **7**, 9724–9734.

[42] Lau, K. L, Hamblin, G. D, & Sleiman, H. F. (2014) Gold nanoparticle 3D-DNA building blocks: high purity preparation and use for modular access to nanoparticle assemblies. *Small (Weinheim an der Bergstrasse, Germany)* **10**, 660–666.

[43] Wu, C, Han, D, Chen, T, Peng, L, Zhu, G, You, M, Qiu, L, Sefah, K, Zhang, X, & Tan, W. (2013) Building a multifunctional aptamer-based DNA nanoassembly for targeted cancer therapy. *Journal of the American Chemical Society* **135**, 18644–18650.

[44] Fire, A & Xu, S. Q. (1995) Rolling replication of short DNA circles. *Proceedings of the National Academy of Sciences of the United States of America* **92**, 4641–4645.

[45] Zhu, G, Hu, R, Zhao, Z, Chen, Z, Zhang, X, & Tan, W. (2013) Noncanonical self-assembly of multifunctional DNA nanoflowers for biomedical applications. *Journal of the American Chemical Society* **135**, 16438–16445.

[46] Zhao, W, Cui, C. H, Bose, S, Guo, D, Shen, C, Wong, W. P, Halvorsen, K, Farokhzad, O. C, Teo, G. S. L, Phillips, J. A, Dorfman, D. M, Karnik, R, & Karp, J. M. (2012) Bioinspired multivalent DNA network for capture and release of cells. *Proceedings of the National Academy of Sciences of the United States of America* **109**, 19626–19631.

[47] Hu, R, Zhang, X, Zhao, Z, Zhu, G, Chen, T, Fu, T, & Tan, W. (2014) DNA nanoflowers for multiplexed cellular imaging and traceable targeted drug delivery. *Angewandte Chemie (International ed. in English)* **53**, 5821–5826.

[48] Katiyar-Agarwal, S, Morgan, R, Dahlbeck, D, Borsani, O, Villegas, A, Zhu, J.-K, Staskawicz, B. J, & Jin, H. (2006) A pathogen-inducible endogenous siRNA in plant immunity. *Proceedings of the National Academy of Sciences of the United States of America* **103**, 18002–18007.

[49] Perkel, J. M. (2009) RNAi therapeutics: A two-year update. *Science* **326**, 454–456.

[50] McNamara, J. O, Andrechek, E. R, Wang, Y, Viles, K. D, Rempel, R. E, Gilboa, E, Sullenger, B. A, & Giangrande, P. H. (2006) Cell type-specific delivery of siRNAs with aptamer-siRNA chimeras. *Nature Biotechnology* **24**, 1005–1015.

[51] Wullner, U, Neef, I, Eller, A, Kleines, M, Tur, M. K, & Barth, S. (2008) Cell-specific induction of apoptosis by rationally designed bivalent aptamer-siRNA transcripts silencing Eukaryotic Elongation Factor 2. *Current Cancer Drug Targets* **8**, 554–565.

[52] Zhou, J, Li, H, Li, S, Zaia, J, & Rossi, J. J. (2008) Novel dual inhibitory function aptamer-siRNA delivery system for HIV-1 therapy. *Molecular Therapy* **16**, 1481–1489.

[53] Zhou, J, Swiderski, P, Li, H, Zhang, J, Neff, C. P, Akkina, R, & Rossi, J. J. (2009) Selection, characterization and application of new RNA HIV gp 120 aptamers for facile delivery of Dicer substrate siRNAs into HIV infected cells. *Nucleic Acids Research* **37**, 3094–3109.

[54] Dassie, J. P, Liu, X.-Y, Thomas, G. S, Whitaker, R. M, Thiel, K. W, Stockdale, K. R, Meyerholz, D. K, McCaffrey, A. P, McNamara, J. O, & Giangrande, P. H. (2009) Systemic administration of optimized aptamer-siRNA chimeras promotes regression of PSMA-expressing tumors. *Nature Biotechnology* **27**, 839–849.

[55] Esposito, C. L, Cerchia, L, Catuogno, S, De Vita, G, Dassie, J. P, Santamaria, G, Swiderski, P, Condorelli, G, Giangrande, P. H, & de Franciscis, V. (2014) Multifunctional aptamer-miRNA conjugates for targeted cancer therapy. *Molecular Therapy : The Journal of the American Society of Gene Therapy* **22**, 1151–1163.

[56] Cerchia, L, Esposito, C. L, Camorani, S, Rienzo, A, Stasio, L, Insabato, L, Affuso, A, & de Franciscis, V. (2012) Targeting Axl with an high-affinity inhibitory aptamer. *Molecular Therapy : The Journal of the American Society of Gene Therapy* **20**, 2291–2303.

[57] Li, Y, Ye, X, Tan, C, Hongo, J. A, Zha, J, Liu, J, Kallop, D, Ludlam, M. J. C, & Pei, L. (2009) Axl as a potential therapeutic target in cancer: Role of Axl in tumor growth, metastasis and angiogenesis. *Oncogene* **28**, 3442–3455.

[58] Lee, Y. S & Dutta, A. (2007) The tumor suppressor microRNA let-7 represses the HMGA2 oncogene. *Genes & Development* **21**, 1025–1030.

[59] Johnson, S. M, Grosshans, H, Shingara, J, Byrom, M, Jarvis, R, Cheng, A, Labourier, E, Reinert, K. L, Brown, D, & Slack, F. J. (2005) RAS is regulated by the let-7 microRNA family. *Cell* **120**, 635–647.

[60] Kim, Y. S, Niazi, J. H, Chae, Y. J, Ko, U.-R, & Gu, M. B. (2011) Aptamers-in-liposomes for selective and multiplexed capture of small organic compounds. *Macromolecular Rapid Communications* **32**, 1169–1173.

[61] Willis, M. C, Collins, B. D, Zhang, T, Green, L. S, Sebesta, D. P, Bell, C, Kellogg, E, Gill, S. C, Magallanez, A, Knauer, S, Bendele, R. A, Gill, P. S, Janjić, N, & Collins, B. (1998) Liposome-anchored vascular endothelial growth factor aptamers. *Bioconjugate Chemistry* **9**, 573–582.

[62] Miyamoto, D, Tang, Z, Takarada, T, & Maeda, M. (2007) Turbidimetric detection of ATP using polymeric micelles and DNA aptamers. *Chemical Communications (Cambridge, England)* pp. 4743–4745.

[63] Wu, Y, Sefah, K, Liu, H, Wang, R, & Tan, W. (2010) DNA aptamer-micelle as an efficient detection/delivery vehicle toward cancer cells. *Proceedings of the National Academy of Sciences of the United States of America* **107**, 5–10.

[64] Guo, Z, Ren, J, Wang, J, & Wang, E. (2011) Single-walled carbon nanotubes based quenching of free FAM-aptamer for selective determination of ochratoxin A. *Talanta* **85**, 2517–2521.

[65] So, H.-M, Park, D.-W, Jeon, E.-K, Kim, Y.-H, Kim, B. S, Lee, C.-K, Choi, S. Y, Kim, S. C, Chang, H, & Lee, J.-O. (2008) Detection and titer estimation of Escherichia coli using aptamer-functionalized single-walled carbon-nanotube field-effect transistors. *Small (Weinheim an der Bergstrasse, Germany)* **4**, 197–201.

[66] Kang, W. J, Chae, J. R, Cho, Y. L, Lee, J. D, & Kim, S. (2009) Multiplex imaging of single tumor cells using quantum-dot-conjugated aptamers. *Small (Weinheim an der Bergstrasse, Germany)* **5**, 2519–2522.

[67] Zhang, C.-Y & Johnson, L. W. (2009) Single quantum-dot-based aptameric nanosensor for cocaine. *Analytical Chemistry* **81**, 3051–3055.

[68] Farokhzad, O. C, Cheng, J, Teply, B. A, Sherifi, I, Jon, S, Kantoff, P. W, Richie, J. P, & Langer, R. (2006) Targeted nanoparticle-aptamer bioconjugates for cancer chemotherapy in vivo. *Proceedings of the National Academy of Sciences of the United States of America* **103**, 6315–6320.

[69] Pilapong, C, Sitthichai, S, Thongtem, S, & Thongtem, T. (2014) Smart magnetic nanoparticle-aptamer probe for targeted imaging and treatment of hepatocellular carcinoma. *International Journal of Pharmaceutics* **473**, 469–474.

[70] Farokhzad, O. C, Karp, J. M, & Langer, R. (2006) Nanoparticle-aptamer bioconjugates for cancer targeting. *Expert Opinion on Drug Delivery* **3**, 311–324.

[71] Zhang, L, Radovic-Moreno, A. F, Alexis, F, Gu, F. X, Basto, P. A, Bagalkot, V, Jon, S, Langer, R. S, & Farokhzad, O. C. (2007) Co-delivery of hydrophobic and hydrophilic drugs from nanoparticle-aptamer bioconjugates. *ChemMedChem* **2**, 1268–1271.

[72] Ashworth, T. R. (2010) A case of cancer in which cells similar to those in th etumours were seen in the blood after death. *The Australian Medical Journal* **11**, 146–147.

[73] Wong, M. P. (2012) Circulating tumor cells as lung cancer biomarkers. *Journal of Thoracic Disease* **4**, 631–634.

[74] Kling, J. (2012) Beyond counting tumor cells. *Nature Biotechnology* **30**, 578–580.

[75] Sheng, W, Chen, T, Tan, W, & Fan, Z. H. (2013) Multivalent DNA nanospheres for enhanced capture of cancer cells in microfluidic devices. *ACS Nano* **7**, 7067–7076.

[76] Russell, S. J & Peng, K.-W. (2007) Viruses as anticancer drugs. *Trends in Pharmacological Sciences* **28**, 326–333.

[77] D'Atri, V, Oliviero, G, Amato, J, Borbone, N, D'Errico, S, Mayol, L, Piccialli, V, Haider, S, Hoorelbeke, B, Balzarini, J, & Piccialli, G. (2012) New anti-HIV aptamers based on tetra-end-linked DNA G-quadruplexes: Effect of the base sequence on anti-HIV activity. *Chemical Communications (Cambridge, England)* **48**, 9516–9518.

[78] Liang, H.-R, Liu, Q, Zheng, X.-X, Gai, W.-W, Xue, X.-h, Hu, G.-Q, Wu, H.-X, Wang, H.-L, Yang, S.-T, & Xia, X.-Z. (2013) Aptamers targeting rabies virus-infected cells inhibit viral replication both in vitro and in vivo. *Virus Research* **173**, 398–403.

[79] Shi, S, Yu, X, Gao, Y, Xue, B, Wu, X, Wang, X, Yang, D, & Zhu, H. (2014) Inhibition of hepatitis C virus production by aptamers against the core protein. *Journal of Virology* **88**, 1990–1999.

[80] Labib, M, Zamay, A. S, Muharemagic, D, Chechik, A. V, Bell, J. C, & Berezovski, M. V. (2012) Electrochemical differentiation of epitope-specific aptamers. *Analytical Chemistry* **84**, 2548–2556.

[81] Binning, J. M, Wang, T, Luthra, P, Shabman, R. S, Borek, D. M, Liu, G, Xu, W, Leung, D. W, Basler, C. F, & Amarasinghe, G. K. (2013) Development of RNA aptamers targeting Ebola virus VP35. *Biochemistry* **52**, 8406–8419.

[82] Jeon, S. H, Kayhan, B, Ben-Yedidia, T, & Arnon, R. (2004) A DNA aptamer prevents influenza infection by blocking the receptor binding region of the viral hemagglutinin. *Journal of Biological Chemistry* **279**, 48410–48419.

[83] Bruno, J. G, Carrillo, M. P, Phillips, T, & Andrews, C. J. (2010) A novel screening method for competitive FRET-aptamers applied to E. coli assay development. *Journal of Fluorescence* **20**, 1211–1223.

[84] Cao, X, Li, S, Chen, L, Ding, H, Xu, H, Huang, Y, Li, J, Liu, N, Cao, W, Zhu, Y, Shen, B, & Shao, N. (2009) Combining use of a panel of ssDNA aptamers in the detection of Staphylococcus aureus. *Nucleic Acids Research* **37**, 4621–4628.

[85] Yang, M, Peng, Z, Ning, Y, Chen, Y, Zhou, Q, & Deng, L. (2013) Highly specific and cost-efficient detection of Salmonella Paratyphi A combining aptamers with single-walled carbon nanotubes. *Sensors (Basel, Switzerland)* **13**, 6865–6881.

[86] Kolovskaya, O. S, Savitskaya, A. G, Zamay, T. N, Reshetneva, I. T, Zamay, G. S, Erkaev, E. N, Wang, X, Wehbe, M, Salmina, A. B, Perianova, O. V, Zubkova, O. A, Spivak, E. A, Mezko, V. S, Glazyrin, Y. E, Titova, N. M, Berezovski, M. V, & Zamay,

A. S. (2013) Development of bacteriostatic DNA aptamers for salmonella. *Journal of Medicinal Chemistry* **56**, 1564–1572.

[87] Dock, G & Wakthin, A. S. (1904) A clinical and pathological study of two cases of splenic anaemia, with early and late stages of cirrhosis. *The American Journal of the Medical Sciences* **127**, 24.

[88] Parato, K. A, Senger, D, Forsyth, P. A. J, & Bell, J. C. (2005) Recent progress in the battle between oncolytic viruses and tumours. *Nature Reviews - Cancer* **5**, 965–976.

[89] Russell, S. J, Peng, K.-W, & Bell, J. C. (2012) Oncolytic virotherapy. *Nature Biotechnology* **30**, 658–670.

[90] Goodbourn, S, Didcock, L, & Randall, R. E. (2000) Interferons: cell signalling, immune modulation, antiviral response and virus countermeasures. *Journal of General Virology* **81**, 2341–2364.

[91] Knipe, D. M. (2013) *Fields virology*, Fields Virology. (Wolters Kluwer Health).

[92] Diallo, J.-S, Vähä-Koskela, M, Le Boeuf, F, & Bell, J. (2012) Propagation, purification, and in vivo testing of oncolytic vesicular stomatitis virus strains. *Methods in Molecular Biology (Clifton, N.J.)* **797**, 127–140.

[93] Breitbach, C. J, Burke, J, Jonker, D, Stephenson, J, Haas, A. R, Chow, L. Q. M, Nieva, J, Hwang, T.-H, Moon, A, Patt, R, Pelusio, A, Le Boeuf, F, Burns, J, Evgin, L, De Silva, N, Cvancic, S, Robertson, T, Je, J.-E, Lee, Y.-S, Parato, K, Diallo, J.-S, Fenster, A, Daneshmand, M, Bell, J. C, & Kirn, D. H. (2011) Intravenous delivery of a multi-mechanistic cancer-targeted oncolytic poxvirus in humans. *Nature* **477**, 99–102.

[94] Cobleigh, M. A, Buonocore, L, Uprichard, S. L, Rose, J. K, & Robek, M. D. (2010) A vesicular stomatitis virus-based hepatitis B virus vaccine vector provides protection against challenge in a single dose. *Journal of Virology* **84**, 7513–7522.

[95] Stojdl, D. F, Lichty, B, Knowles, S, Marius, R, Atkins, H, Sonenberg, N, & Bell, J. C. (2000) Exploiting tumor-specific defects in the interferon pathway with a previously unknown oncolytic virus. *Nature Medicine* **6**, 821–825.

[96] Stojdl, D. F, Lichty, B. D, tenOever, B. R, Paterson, J. M, Power, A. T, Knowles, S, Marius, R, Reynard, J, Poliquin, L, Atkins, H, Brown, E. G, Durbin, R. K, Durbin, J. E, Hiscott, J, & Bell, J. C. (2003) VSV strains with defects in their ability to shutdown innate immunity are potent systemic anti-cancer agents. *Cancer Cell* **4**, 263–275.

[97] Lemay, C. G, Rintoul, J. L, Kus, A, Paterson, J. M, Garcia, V, Falls, T. J, Ferreira, L, Bridle, B. W, Conrad, D. P, Tang, V. A, Diallo, J. S, Arulanandam, R, Le Boeuf, F, Garson, K, Vanderhyden, B. C, Stojdl, D. F, Lichty, B. D, Atkins, H. L, Parato, K. A, Bell, J. C, & Auer, R. C. (2012) Harnessing oncolytic virus-mediated antitumor immunity in an infected cell vaccine. *Molecular Therapy* **20**, 1791–1799.

[98] Breitbach, C. J, De Silva, N. S, Falls, T. J, Aladl, U, Evgin, L, Paterson, J, Sun, Y. Y, Roy, D. G, Rintoul, J. L, Daneshmand, M, Parato, K, Stanford, M. M, Lichty, B. D, Fenster, A, Kirn, D, Atkins, H, & Bell, J. C. (2011) Targeting tumor vasculature with an oncolytic virus. *Molecular Therapy* **19**, 886–894.

[99] Wollmann, G, Rogulin, V, Simon, I, Rose, J. K, & van den Pol, A. N. (2010) Some attenuated variants of vesicular stomatitis virus show enhanced oncolytic activity against human glioblastoma cells relative to normal brain cells. *Journal of Virology* **84**, 1563–1573.

[100] Russell, S. J. (2002) RNA viruses as virotherapy agents. *Cancer Gene Therapy* **9**, 961–966.

[101] Russell, S. J. (2001) *RNA viral vectors in gene therapy.* (John Wiley & Sons, Ltd, Chichester).

[102] Conti, C, Mastromarino, P, & Orsi, N. (1991) Role of membrane phospholipids and glycolipids in cell-to-cell fusion by VSV. *Comparative Immunology, Microbiology and Infectious Diseases* **14**, 303–313.

[103] Coil, D. A & Miller, A. D. (2004) Phosphatidylserine is not the cell surface receptor for vesicular stomatitis virus. *Journal of Virology* **78**, 10920–10926.

[104] Finkelshtein, D, Werman, A, Novick, D, Barak, S, & Rubinstein, M. (2013) LDL receptor and its family members serve as the cellular receptors for vesicular stomatitis virus. *Proceedings of the National Academy of Sciences of the United States of America* **110**, 7306–7311.

[105] Amirache, F, Lévy, C, Costa, C, Mangeot, P.-E, Torbett, B. E, Wang, C. X, Nègre, D, Cosset, F.-L, & Verhoeyen, E. (2014) Mystery solved: VSV-G-LVs do not allow efficient gene transfer into unstimulated T cells, B cells, and HSCs because they lack the LDL receptor. *Blood* **123**, 1422–1424.

[106] Li, J & Zhang, Y. (2012) in *Methylation - From DNA, RNA and Histones to Diseases and Treatment*, ed. Dricu, A. (InTech).

[107] Schneider, M, Graham, F. L, & Prevec, L. (1989) Expression of the glycoprotein of vesicular stomatitis virus by infectious adenovirus vectors. *The Journal of general virology* **70 (Pt 2)**, 417–427.

[108] Murphy, K. M. (2011) *Janeway's Immunobiology.* (Garland Science).

[109] Loureiro, J & Ploegh, H. L. (2006) Antigen presentation and the ubiquitin-proteasome system in host-pathogen interactions. *Advances in Immunology* **92**, 225–305.

[110] Yokosuka, T, Takamatsu, M, Kobayashi-Imanishi, W, Hashimoto-Tane, A, Azuma, M, & Saito, T. (2012) Programmed cell death 1 forms negative costimulatory microclusters that directly inhibit T cell receptor signaling by recruiting phosphatase SHP2. *Journal of Experimental Medicine* **209**, 1201–1217.

[111] Moser, M & Leo, O. (2010) Key concepts in immunology. *Vaccine* **28**, C2–C13.

[112] Prechtel, A. T & Steinkasserer, A. (2007) CD83: An update on functions and prospects of the maturation marker of dendritic cells. *Archives of Dermatological Research* **299**, 59–69.

[113] Berezovski, M. V, Lechmann, M, Musheev, M. U, Mak, T. W, & Krylov, S. N. (2008) Aptamer-facilitated biomarker discovery (AptaBiD). *Journal of the American Chemical Society* **130**, 9137–9143.

[114] Zhou, L. J & Tedder, T. F. (1995) Human blood dendritic cells selectively express CD83, a member of the immunoglobulin superfamily. *Journal of Immunology (Baltimore, Md. : 1950)* **154**, 3821–3835.

[115] Lechmann, M, Berchtold, S, Hauber, J, & Steinkasserer, A. (2002) CD83 on dendritic cells: more than just a marker for maturation. *Trends in Immunology* **23**, 273–275.

[116] Lin, H, Liang, S, Zhong, Z, Wen, J, Li, W, Wang, L, Xu, J, Zhong, F, & Li, X. (2014) Soluble CD83 inhibits human monocyte differentiation into dendritic cells in vitro. *Cell Immunology* **292**, 25–31.

[117] Osipovich, O & Oltz, E. M. (2010) Regulation of antigen receptor gene assembly by genetic-epigenetic crosstalk. *Seminars in Immunology* **22**, 313–322.

[118] Gourley, T. S, Wherry, E. J, Masopust, D, & Ahmed, R. (2004) Generation and maintenance of immunological memory. *Seminars in Immunology* **16**, 323–333.

[119] Hammarlund, E, Lewis, M. W, Hansen, S. G, Strelow, L. I, Nelson, J. A, Sexton, G. J, Hanifin, J. M, & Slifka, M. K. (2003) Duration of antiviral immunity after smallpox vaccination. *Nature Medicine* **9**, 1131–1137.

[120] Amzel, L. M & Poljak, R. J. (1979) Three-dimensional structure of immunoglobulins. *Annual Review of Biochemistry* **48**, 961–997.

[121] Tsai, V. (2004) Impact of human neutralizing antibodies on antitumor efficacy of an oncolytic adenovirus in a murine model. *Clinical Cancer Research* **10**, 7199–7206.

[122] Ikeda, K, Ichikawa, T, Wakimoto, H, Silver, J. S, Deisboeck, T. S, Finkelstein, D, Harsh, IV, G. R, Louis, D. N, Bartus, R. T, Hochberg, F. H, & Antonio Chiocca, E. (1999) Oncolytic virus therapy of multiple tumors in the brain requires suppression of innate and elicited antiviral responses. *Nature Medicine* **5**, 881–887.

[123] Wakimoto, H, Ikeda, K, Abe, T, Ichikawa, T, Hochberg, F. H, Ezekowitz, R. A, Pasternack, M. S, & Chiocca, E. A. (2002) The complement response against an oncolytic virus is species-specific in its activation pathways. *Molecular Therapy* **5**, 275–282.

[124] Worgall, S, Wolff, G, Falck-Pedersen, E, & Crystal, R. G. (1997) Innate immune mechanisms dominate elimination of adenoviral vectors following in vivo administration. *Human Gene Therapy* **8**, 37–44.

[125] Ye, X, Jerebtsova, M, & Ray, P. E. (2000) Liver bypass significantly increases the transduction efficiency of recombinant adenoviral vectors in the lung, intestine, and kidney. *Human Gene Therapy* **11**, 621–627.

[126] Chen, Y, Yu, D. C, Charlton, D, & Henderson, D. R. (2000) Pre-existent adenovirus antibody inhibits systemic toxicity and antitumor activity of CN706 in the nude mouse LNCaP xenograft model: Implications and proposals for human therapy. *Human Gene Therapy* **11**, 1553–1567.

[127] Power, A. T, Wang, J, Falls, T. J, Paterson, J. M, Parato, K. A, Lichty, B. D, Stojdl, D. F, Forsyth, P. A. J, Atkins, H, & Bell, J. C. (2007) Carrier cell-based delivery of an oncolytic virus circumvents antiviral immunity. *Molecular Therapy : The Journal of the American Society of Gene Therapy* **15**, 123–130.

[128] Abuchowski, A, Van Es, T, Palczuk, N. C, & Davis, F. F. (1977) Alteration of immunological properties of bovine serum albumin by covalent attachment of polyethylene glycol. *Journal of Biological Chemistry* **252**, 3578–3581.

[129] Duncan, R. (2006) Polymer conjugates as anticancer nanomedicines. *Nature Reviews - Cancer* **6**, 688–701.

[130] Green, N. K, Herbert, C. W, Hale, S. J, Hale, A. B, Mautner, V, Harkins, R, Hermiston, T, Ulbrich, K, Fisher, K. D, & Seymour, L. W. (2004) Extended plasma circulation time and decreased toxicity of polymer-coated adenovirus. *Gene Therapy* **11**, 1256–1263.

[131] Doronin, K, Shashkova, E. V, May, S. M, Hofherr, S. E, & Barry, M. A. (2009) Chemical modification with high molecular weight polyethylene glycol reduces transduction of hepatocytes and increases efficacy of intravenously delivered oncolytic adenovirus. *Human Gene Therapy* **20**, 975–988.

[132] Croyle, M. A, Callahan, S. M, Auricchio, A, Schumer, G, Linse, K. D, Wilson, J. M, Brunner, L. J, & Kobinger, G. P. (2004) PEGylation of a vesicular stomatitis virus G pseudotyped lentivirus vector prevents inactivation in serum. *Journal of Virology* **78**, 912–921.

[133] Young, B. A, Spencer, J. F, Ying, B, Tollefson, A. E, Toth, K, & Wold, W. S. M. (2013) The role of cyclophosphamide in enhancing antitumor efficacy of an adenovirus oncolytic vector in subcutaneous Syrian hamster tumors. *Cancer Gene Therapy* **20**, 521–530.

[134] Peng, K.-W, Myers, R, Greenslade, A, Mader, E, Greiner, S, Federspiel, M. J, Dispenzieri, A, & Russell, S. J. (2012) Using clinically approved cyclophosphamide regimens to control the humoral immune response to oncolytic viruses. *Gene Therapy* **20**, 255–261.

[135] Coukos, G, Makrigiannakis, A, Kang, E. H, Caparelli, D, Benjamin, I, Kaiser, L. R, Rubin, S. C, Albelda, S. M, & Molnar-Kimber, K. L. (1999) Use of carrier cells to deliver a replication-selective herpes simplex virus-1 mutant for the intraperitoneal therapy of epithelial ovarian cancer. *Clinical Cancer Research: An Official Journal of the American Association for Cancer Research* **5**, 1523–1537.

[136] Qiao, J, Wang, H, Kottke, T, Diaz, R. M, Willmon, C, Hudacek, A, Thompson, J, Parato, K, Bell, J, Naik, J, Chester, J, Selby, P, Harrington, K, Melcher, A, & Vile, R. G. (2008) Loading of oncolytic vesicular stomatitis virus onto antigen-specific T cells enhances the efficacy of adoptive T-cell therapy of tumors. *Gene Therapy* **15**, 604–616.

[137] Ong, H. T, Hasegawa, K, Dietz, A. B, Russell, S. J, & Peng, K.-W. (2007) Evaluation of T cells as carriers for systemic measles virotherapy in the presence of antiviral antibodies. *Gene Therapy* **14**, 324–333.

[138] Muharemagic, D, Labib, M, Ghobadloo, S. M, Zamay, A. S, Bell, J. C, & Berezovski, M. V. (2012) Anti-Fab aptamers for shielding virus from neutralizing antibodies. *Journal of the American Chemical Society* **134**, 17168–17177.

[139] Muharemagic, D, Zamay, A, Ghobadloo, S. M, Evgin, L, Savitskaya, A, Bell, J. C, & Berezovski, M. V. (2014) Aptamer-facilitated protection of oncolytic virus from neutralizing antibodies. *Molecular therapy - Nucleic acids* **3**, e167.

[140] High, K. (2012) *Approaches to blocking the immune response to gene Transfer with viral vectors.* (Frontiers in Microbiology).

[141] Kronvall, G. (1973) A surface component in group A, C, and G streptococci with non-immune reactivity for immunoglobulin G. *Journal of Immunology (Baltimore, Md. : 1950)* **111**, 1401–1406.

[142] Björck, L & Blomberg, J. (1987) Streptococcal protein G: A sensitive tool for detection of antibodies to human immunodeficiency virus proteins in Western blot analysis - Springer. *European Journal of Clinical Microbiology.*

[143] Labib, M, Zamay, A. S, Muharemagic, D, Chechik, A, Bell, J. C, & Berezovski, M. V. (2012) Electrochemical sensing of aptamer-facilitated virus immunoshielding. *Analytical Chemistry* **84**, 1677–1686.

[144] Bennett, R. M, Gabor, G. T, & Merritt, M. M. (1985) DNA binding to human leukocytes. Evidence for a receptor-mediated association, internalization, and degradation of DNA. *Journal of Clinical Investigation* **76**, 2182–2190.

[145] Chan, T. M, Frampton, G, & Cameron, J. S. (2008) Identification of DNA-binding proteins on human umbilical vein endothelial cell plasma membrane. *Clinical & Experimental Immunology* **91**, 110–114.

[146] Belotserkovskii, B. P, Johnston, B. H, Gaillard, C, & Strauss, F. (1996) Polypropylene tube surfaces may induce denaturation and multimerization of DNA. *Science* **271**, 222–222.

[147] Heider, S & Metzner, C. (2014) Quantitative real-time single particle analysis of virions. *Virology* **462-463**, 199–206.

[148] Mironov, G. G, Chechik, A. V, Ozer, R, Bell, J. C, & Berezovski, M. V. (2011) Viral quantitative capillary electrophoresis for counting intact viruses. *Analytical Chemistry* **83**, 5431–5435.

[149] Azizi, A, Mironov, G. G, Muharemagic, D, Wehbe, M, Bell, J. C, & Berezovski, M. V. (2012) Viral quantitative capillary electrophoresis for counting and quality control of RNA viruses. *Analytical Chemistry* **84**, 9585–9591.

[150] Grigorov, B, Rabilloud, J, Lawrence, P, & Gerlier, D. (2011) Rapid titration of measles and other viruses: optimization with determination of replication cycle length. *PLoS ONE* **6**, e24135.

[151] Fukushima, K, Takahashi, T, Takaguchi, M, Ueyama, H, Ito, S, Kurebayashi, Y, Kawanishi, T, Mckimm-Breschkin, J. L, Takimoto, T, Minami, A, & Suzuki, T. (2011) Plaque formation assay for human parainfluenza virus type 1. *Biological and Pharmaceutical Bulletin* **34**, 996–1000.

[152] Camorani, S, Esposito, C. L, Rienzo, A, Catuogno, S, Iaboni, M, Condorelli, G, de Franciscis, V, & Cerchia, L. (2014) Inhibition of receptor signaling and of glioblastoma-derived tumor growth by a novel PDGFRβ aptamer. *Molecular Therapy : The Journal of the American Society of Gene Therapy* **22**, 828–841.

[153] Zhou, J, Neff, C. P, Swiderski, P, Li, H, Smith, D. D, Aboellail, T, Remling-Mulder, L, Akkina, R, & Rossi, J. J. (2013) Functional in vivo delivery of multiplexed anti-HIV-1 siRNAs via a chemically synthesized aptamer with a sticky bridge. *Molecular Therapy* **21**, 192–200.

[154] An, Z. (2009) Therapeutic monoclonal antibodies: From bench to clinic.

[155] Mallikaratchy, P. R, Ruggiero, A, Gardner, J. R, Kuryavyi, V, Maguire, W. F, Heaney, M. L, McDevitt, M. R, Patel, D. J, & Scheinberg, D. A. (2011) A multivalent DNA aptamer specific for the B-cell receptor on human lymphoma and leukemia. *Nucleic Acids Research* **39**, 2458–2469.

[156] Galasso, G. J. (1967) Quantitative studies on the quality, effects of aggregation and thermal inactivation of vesicular stomatitis virus. *Archiv Für Die Gesamte Virusforschung* **21**, 437–446.

[157] Kim, J. B, Urban, K, Cochran, E, Lee, S, Ang, E, Rice, B, Bata, A, Campbell, K, Coffee, R, Gorodinsky, A, Lu, Z, Zhou, H, Kishimoto, T. K, & Lassota, P. (2010) Non-invasive detection of a small number of bioluminescent cancer cells in vivo. *PLoS ONE* **5**.

[158] Craft, N, Bruhn, K. W, Nguyen, B. D, Prins, R, Liau, L. M, Collisson, E. A, De, A, Kolodney, M. S, Gambhir, S. S, & Milleri, J. F. (2005) Bioluminescent imaging of melanoma in live mice. *Journal of Investigative Dermatology* **125**, 159–165.

[159] Kang, H, O'Donoghue, M. B, Liu, H, & Tan, W. (2010) A liposome-based nanostructure for aptamer directed delivery. *Chemical Communications (Cambridge, England)* **46**, 249–251.

[160] Zhao, Y, Duan, S, Zeng, X, Liu, C, Davies, N. M, Li, B, & Forrest, M. L. (2012) Prodrug strategy for PSMA-targeted delivery of TGX-221 to prostate cancer cells. *Molecular Pharmaceutics* **9**, 1705–1716.

[161] Yang, L, Meng, L, Zhang, X, Chen, Y, Zhu, G, Liu, H, Xiong, X, Sefah, K, & Tan, W. (2011) Engineering polymeric aptamers for selective cytotoxicity. *Journal of the American Chemical Society* **133**, 13380–13386.

[162] Bailey, T. L & Elkan, C. (1994) Fitting a mixture model by expectation maximization to discover motifs in biopolymers. *Proceedings International Conference on Intelligent Systems for Molecular Biology* **2**, 28–36.

[163] Zhang, J, McCabe, K. A, & Bell, C. E. (2011) Crystal structures of lambda exonuclease in complex with DNA suggest an electrostatic ratchet mechanism for processivity. *Proceedings of the National Academy of Sciences of the United States of America* **108**, 11872–11877.

[164] Rusk, N. (2009) Focus on next-generation sequencing data analysis. Forward. *Nature Methods* **6**, S1.

[165] Blankenberg, D, Von Kuster, G, Coraor, N, Ananda, G, Lazarus, R, Mangan, M, Nekrutenko, A, & Taylor, J. (2010) Galaxy: a web-based genome analysis tool for experimentalists. *Current Protocols in Molecular Biology* **Chapter 19**, Unit 19.10.1–21.

[166] Goecks, J, Nekrutenko, A, Taylor, J, & Galaxy Team. (2010) Galaxy: a comprehensive approach for supporting accessible, reproducible, and transparent computational research in the life sciences. *Genome Biology* **11**, R86.

[167] Giardine, B, Riemer, C, Hardison, R. C, Burhans, R, Elnitski, L, Shah, P, Zhang, Y, Blankenberg, D, Albert, I, Taylor, J, Miller, W, Kent, W. J, & Nekrutenko, A. (2005) Galaxy: a platform for interactive large-scale genome analysis. *Genome Research* **15**, 1451–1455.

[168] Beinoravičiūtė-Kellner, R, Lipps, G, & Krauss, G. (2005) In vitro selection of DNA binding sites for ABF1 protein from Saccharomyces cerevisiae. *FEBS Letters* **579**, 4535–4540.

[169] Ghobadloo, S. M, Gargaun, A, Casselman, R, Muharemagic, D, & Berezovski, M. V. (2014) Aptamer-facilitated cryoprotection of viruses. *ACS Medicinal Chemistry Letters*.

[170] Berezovski, M, Drabovich, A, Krylova, S. M, Musheev, M, Okhonin, V, Petrov, A, & Krylov, S. N. (2005) Nonequilibrium capillary electrophoresis of equilibrium mixtures: a universal tool for development of aptamers. *Journal of the American Chemical Society* **127**, 3165–3171.

[171] Krylov, S. N. (2006) Nonequilibrium capillary electrophoresis of equilibrium mixtures (NECEEM): A novel method for biomolecular screening. *Journal of Biomolecular Screening* **11**, 115–122.

[172] Berezovski, M. V, Musheev, M. U, Drabovich, A. P, Jitkova, J. V, & Krylov, S. N. (2006) Non-SELEX: selection of aptamers without intermediate amplification of candidate oligonucleotides. *Nature Protocols* **1**, 1359–1369.

[173] Sauter, B, Albert, M. L, Francisco, L, Larsson, M, Somersan, S, & Bhardwaj, N. (2000) Consequences of cell death: Exposure to necrotic tumor cells, but not primary tissue cells or apoptotic cells, induces the maturation of immunostimulatory dendritic cells. *Journal of Experimental Medicine* **191**, 423–433.

[174] Lechmann, M, Kremmer, E, Sticht, H, & Steinkasserer, A. (2002) Overexpression, purification, and biochemical characterization of the extracellular human CD83 domain and generation of monoclonal antibodies. *Protein Expression and Purification* **24**, 445–452.

[175] Fugier-Vivier, I, Servet-Delprat, C, Rivailler, P, Rissoan, M. C, Liu, Y. J, & Rabourdin-Combe, C. (1997) Measles virus suppresses cell-mediated immunity by interfering with the survival and functions of dendritic and T cells. *Journal of Experimental Medicine* **186**, 813–823.

[176] Engelmayer, J, Larsson, M, Subklewe, M, Chahroudi, A, Cox, W. I, Steinman, R. M, & Bhardwaj, N. (1999) Vaccinia virus inhibits the maturation of human dendritic cells: a novel mechanism of immune evasion. *Journal of Immunology (Baltimore, Md. : 1950)* **163**, 6762–6768.

[177] Kruse, M, Rosorius, O, Krätzer, F, Stelz, G, Kuhnt, C, Schuler, G, Hauber, J, & Steinkasserer, A. (2000) Mature dendritic cells infected with herpes simplex virus type 1 exhibit inhibited T-cell stimulatory capacity. *Journal of Virology* **74**, 7127–7136.

[178] Kummer, M, Turza, N. M, Muhl-Zurbes, P, Lechmann, M, Boutell, C, Coffin, R. S, Everett, R. D, Steinkasserer, A, & Prechtel, A. T. (2007) Herpes simplex virus type 1 induces CD83 degradation in mature dendritic cells with immediate-early kinetics via the cellular proteasome. *Journal of Virology* **81**, 6326–6338.

[179] Hart, D. N. J. (1997) Dendritic cells: Unique leukocyte populations which control the primary immune response. *Blood* **90**, 3245–3287.

[180] Wilson, R, Bourne, C, Chaudhuri, R. R, Gregory, R, Kenny, J, & Cossins, A. (2014) Single-step selection of bivalent aptamers validated by comparison with SELEX using high-throughput sequencing. *PLoS ONE* **9**, e100572.

[181] Beier, R, Boschke, E, & Labudde, D. (2014) New strategies for evaluation and analysis of SELEX experiments. *BioMed research international* **2014**, 849743.

[182] Hünniger, T, Wessels, H, Fischer, C, Paschke-Kratzin, A, & Fischer, M. (2014) Just in time-selection: A rapid semiautomated SELEX of DNA aptamers using magnetic separation and BEAMing. *Analytical Chemistry* **86**, 10940–10947.

[183] Toporkiewicz, M, Meissner, J, Matusewicz, L, Czogalla, A, & Sikorski, A. F. (2015) Toward a magic or imaginary bullet? Ligands for drug targeting to cancer cells:

principles, hopes, and challenges. *International journal of nanomedicine* **10**, 1399–1414.

[184] Van Simaeys, D, Turek, D, Champanhac, C, Vaizer, J, Sefah, K, Zhen, J, Sutphen, R, & Tan, W. (2014) Identification of cell membrane protein stress-induced phosphoprotein 1 as a potential ovarian cancer biomarker using aptamers selected by cell systematic evolution of ligands by exponential enrichment. *Analytical Chemistry* **86**, 4521–4527.